Characterization of Major Structural Proteins of the Infectious Salmon Anemia Virus (ISAV)

Vidar Teis Aspehaug

Doctoral Thesis

Department of Biology
University of Bergen
2005

ISBN XX-XXXX-XXX-X
Bergen, Norway 2005

Acknowledgements

This work has been carried out in 2001-2005 at the University of Bergen, Department of Biology where I have been a research fellow during these years, and received financial support from the Norwegian Research Council and from Intervet Norbio. I thank these institutions for enabling me to perform this work.

I express my sincere gratitude to my supervisor, Professor Curt Endresen for encouraging me to start a research career, and for his support and participation during these years.

Also, I thank my co-supervisors: Dr. Eirik Biering (Intervet Norbio, currently at the Institute of Marine Research, Bergen) has contributed greatly to my contentment with being a scientist, and have provided interesting and productive discussions throughout this study. Dr. Knut Falk (National Veterinarian Institute, Oslo) introduced me to the field of virus protein characterization, and inspired me to discover many interesting aspects of this field. I am deeply grateful to you both!

Furthermore, I would like to thank my other co-authors, Bjørn Krossøy, Aase B. Mikalsen, Lindsey Moore, Lisette Sanders, Mike Snow, Jegatheswaran Thevarajan, Stephane Villoing and Reinhard Vlasak.

Special thanks to friends and colleagues in the Fish Disease group for inspiring discussions and for providing a socially unique place of work.

I am deeply grateful to my family for believing in me and encouraging me through the years. Especially, thanks to my daughter Marta Grethe who made me realize that there are more important things to life than science and to my better half - Audny - love you!! You have contributed significantly to this thesis by taking care of things at home and by your input on the manuscripts.

Contents

List of Original Papers

This thesis is based on the following original articles, which will be referred to by their Roman numerals:

Paper I Falk, K., **V. Aspehaug**, R. Vlasak, and C. Endresen. 2004. Identification and partial characterisation of viral structural proteins of infectious salmon anaemia (ISA) virus. J Virol 78:3063-71.

Paper II **Aspehaug, V.**, K. Falk, B. Krossøy, J. Thevarajan, L. Sanders, L. Moore, C. Endresen, and E. Biering. 2004. Infectious salmon anemia virus (ISAV) genomic segment 3 encodes the viral nucleoprotein (NP), an RNA-binding protein with two monopartite nuclear localization signals (NLS). Virus Res 106:51-60.

Paper III **Aspehaug, V.**, A. B. Mikalsen, M. Snow, E. Biering, and S. Villoing. First Characterization of the Infectious Salmon Anemia Virus Fusion Protein. (Submitted to J Virol).

INTRODUCTION

During the last thirty years the Norwegian aquaculture industry has grown from close to nothing into a high-tech industry with major growth potential. Today, Norway is the world leading producer of Atlantic salmon (*Salmo salar* L.), exporting half a million tons yearly representing values of about 1.8 billion USD (2003). For a small country like Norway this represents a substantial value, and fish is one of the main export articles, after oil and gas (Source: The Norwegian Seafood Export Council).

The salmon industry is operating in a highly competitive international market, forcing the producer to reduce production costs and risk factors to a minimum. After experiencing major losses in the eighties and in the beginning of the nineties due to vibrosis, cold water vibriosis, furunculosis, infectious pancreas necrosis (IPN), and infectious salmon anaemia (ISA), the industry became increasingly aware of the significance and profitability of preventive healthcare. The introduction of effective bacterial vaccines and improved health management rescued the industry from total collapse and reduced the total use of antibacterial drugs in farmed fish by 99%. However, viral vaccines have so far not proved as efficacious as the bacterial vaccines, and fairly well characterized diseases like IPN, ISA, and pancreas disease (PD), are still causing major losses in the industry. In addition, some less characterized diseases such as haemorrhagic smolt syndrome (HSS), heart and skeletal muscle inflammation (HSMI), and cardiac myopathy syndrome (CMS), all suspected to be of viral etiology, are of increasing concern. Thus, good health monitoring and efficient diagnostics are of vital importance to prevent viral diseases, and continued research on aquatic diseases is essential to fully exploit the potential of the Norwegian aquaculture industry.

The focus of this thesis will be on ISA with particular focus on the characterization of the ISA-virus (ISAV) major structural proteins. This knowledge can contribute to establish potential determinants of pathogenicity of the ISAV, and provide key information for the development of improved diagnostics and recombinant subunit vaccines.

Twenty Years of ISA

Since the first officially recorded outbreak of ISA in Norway in November 1984 (111), several outbreaks have been reported yearly, with a peak of nearly 100 new cases in 1990 (52). Control measures including regulations on transportation, fish movement restrictions, disinfection of wastewater, and introduction of combat zones, contributed to reduce the number of outbreaks, and in 1994 only two outbreaks were registered (52). In addition the unspecific protection provided by the oil-adjuvant bacterial vaccines might have contributed to this end. Since then, the number of outbreaks in Norway has been stable, with 15 to 20 new cases each year.

The first incidence of ISA was a chronically proceeding disease among Atlantic salmon parr in a hatchery on the West Coast of Norway (Bremnes). The disease was characterized by severe anemia and high cumulative mortality. Affected fish were lethargic with pale gills, fin rot, exophthalmia, and hemorrhages in the anterior eye chamber and abdominal skin. Pathological changes included dark, pale or yellowish liver, a dark and swollen spleen, congested intestinal walls, petechia in periviceral fat, acites fluid, edemas, hemorrhages in the swim bladder wall, and muscular hemorrhages (111).

For more than a decade ISA was considered to be an exclusively Norwegian problem, but as of today ISA have affected fish farms in Scotland, Canada, the Faeroe Islands, and the United

States (6, 69, 77, 91, 98, 111), and the virus has been isolated from Coho salmon (*Oncorhynchus kisutch*) in Chile (54). The annual costs of ISA outbreaks has been substantial, and in 1999 reported losses were 11 million USD in Norway, 14 million USD in Canada, and the 1998 - 1999 epidemics in Scotland were estimated to cost 32 million USD (43). In North-America ISA vaccination programs were initiated some years ago, and recently vaccination was initiated in the Faeroe Islands. However, ISA is classified as a list I disease according to the OIE (Office International des Epizooties), and in principle vaccination is forbidden, but it might be authorized under certain circumstances. In Norway, the general policy when dealing with ISA outbreaks is stamping-out and fallowing. Nevertheless, vaccination may become important in future strategies to control ISA and much effort has been aimed at the development of ISA vaccines. However, efficacious and cost-effective inactivated/killed viral vaccines have proven difficult to develop, and increasing focus is being put into subunit vaccines (104).

ISAV an Orthomyxovirus?

The first outbreak of ISA started an epizootic suggestive of a transmissible disease, and the following years new cases of the disease emerged (111). Antibacterial treatment and nutritional additives failed to reduce mortalities. Infection trials verified that the disease was caused by a transmissible agent, and the agent was recovered after filtration through 100 nm pores, suggesting a viral nature of the disease (110). The first purification of virus from infectious plasma using sucrose gradients revealed that the virus had a buoyant density in the range 1.184 to 1.262 g/ml (15), and later this have been specified to 1.18 g/ml using both sucrose and CsCl gradients (32). Exposure to lipid solvents indicated that the virus was enveloped (15, 110), and in 1994 electron microscopy studies presenting pictures of enveloped spherical virus particles suggested to be the ISAV was published (49). ISAV was

reported to have a diameter of approximately 100 nm, and was budding from endothelial cells lining blood vessels in tissue samples from infected salmon (49). The following year, a cell culture supporting the propagation of the ISAV was reported, enabling the isolation and a final confirmation of the causative agent of ISA (23, 33).

In vitro cultivation of ISAV laid the foundation for more detailed studies of the virus, and several succeeding papers have focused on virus characterization. The first report substantiating that the ISAV resembled the orthomyxoviruses presented a genomic characterization (73). It was demonstrated that the virus has a genome consisting of eight negative strand RNA segments that range from 1.0 to 2.3 kb, with a total size of approximately 14.5 kb. Also, the first ISAV-specific molecular clone corresponding to segment eight was sequenced, but no homology to other sequences was found (73). However, cumulative data on the morphological and replicational properties suggested that the virus resembled the orthomyxoviruses. Supportive biochemical, physicochemical, and morphological properties of the virus were published shortly after, including hemagglutination, receptor-destroying enzyme activity, and a nuclear replication strategy sensitive to actinomycin D (32). Another important piece in the puzzle of the ISAV classification was the sequencing of the basic polymerase 1 (PB1) gene, showing core polymerase motifs characteristic to all RNA-dependent RNA polymerases (60). The conserved motifs showed similarities to other negative strand, segmented RNA viruses, especially to the members of the *Orthomyxoviridae*, substantiating the classification of the ISAV as an orthomyxovirus. According to the International Committee of Taxonomy of Viruses (ICTV), the ISAV is now the type species of the fifth genera amongst the orthomyxoviruses, namely the Isaviruses.

ISAV Replication

Infection of a cell by a virus involves a number of steps. The virus must attach to the cell surface, penetrate, and subsequently become uncoated to make its genome accessible to the viral or host machinery for transcription and translation. Enveloped viruses (such as the orthomyxoviruses, paramyxoviruses, and retroviruses) rely on fusion of their envelopes with the cell membrane during penetration, and have separate coat proteins which are involved in the activities of virus attachment, entry, and penetration. Generally, two different entry strategies are used by various viruses. Influenza A is the prototype of a virus that requires a low pH environment in the endosomal compartment to trigger membrane fusion (100). In contrast, other viruses, such as paramyxoviruses and retroviruses, use a pH-independent mechanism (18). For these viruses, fusion occurs at the plasma membrane, but may occur in the endosomes as well. Unlike other RNA viruses, influenza virus mRNA synthesis has a unique dependence on host cell nuclear function, and in response to acidification and penetration, internal viral proteins facilitate the release and transport of the viral genome to the nucleus. Following genome amplification, the newly formed viral genomes leave the nucleus and incorporate into virus particles that are budding off the plasma membrane. The infectious cycle is completed when new virions are released from the cell by a receptor-destroying enzyme (51).

ISAV replication seems to share general characteristics with other orthomyxoviruses except that ISAV has an optimal replication at 15°C, and is accordingly slower (32). In the following, documented characteristics of the ISAV “life cycle” are summarized. Figure 1 provides an overview of each step in the ISAV replication.

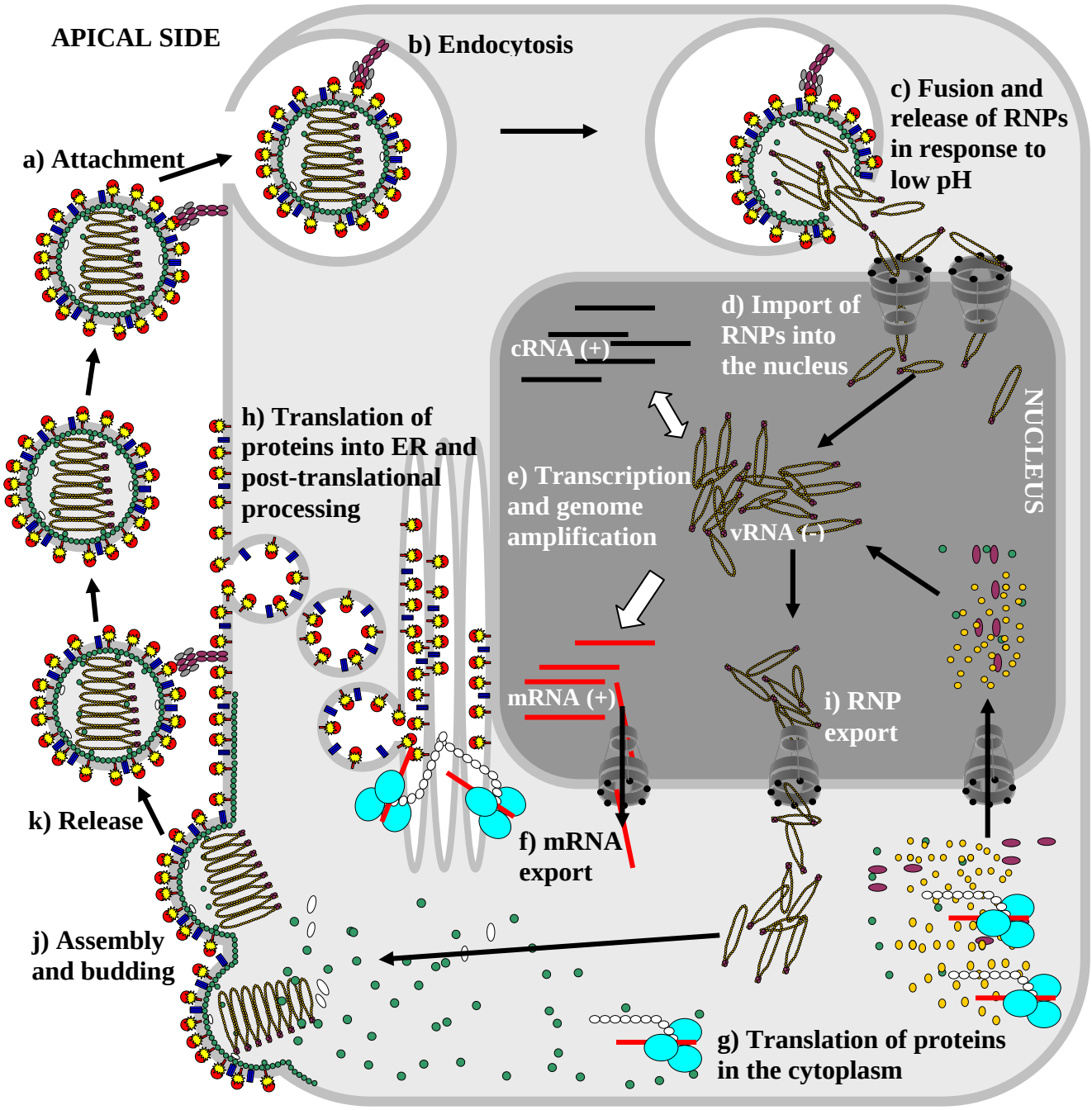

FIGURE 1. A simplified model of the ISAV replication. See main text for more details of the model. The virus first binds to sialic-acid-containing receptors (lilac and grey) on the cell surface via the hemagglutinin-esterase (HE) protein (red and yellow) (a). It then enters the cell by endocytosis (b) and in response to a lowering of the pH in the endosomes the viral fusion protein (blue) mediates the fusion of the viral and endosomal membranes, and the ribonucleoprotein (RNP) complexes are released into the cytoplasm (c). The viral genome segments are transported into the nucleus (d) where transcription and genome amplification takes place (e). Viral mRNA transcripts are exported to the cytoplasm (f), and translation of viral proteins is initiated (g). Surface proteins are translated into the endoplasmatic reticulum (ER) (h) where they enter the secretory pathway, going through posttranslational modifications prior to exposure in the plasma membrane. Proteins that will be components of new RNPs are transported into the nucleus, and late in the infection cycle newly synthesized viral genomes are transported out of the nucleus in the form of RNPs (i). RNPs are packaged into progeny virions that bud off from the plasma membrane, most frequently at the apical side of polarized cells (j). Mature virions are released from the cell surface by the receptor cleavage activity mediated by the HE (k).

ISAV attachment, entry, and penetration have been elucidated in some detail. ISAV is an enveloped virus (15, 110) and enters the cells by fusion in acidic vesicles (24). Virus characterization studies revealed that the ISAV has hemagglutinating and receptor-destroying enzyme activities, the latter suggested to be an acetylesterase of a different specificity than the influenza C virus (32). The beneficial effect of trypsin on the *in vitro* replication of ISAV indicated proteolytic activation of a fusion protein as part of the fusion process (32).

More recent studies have demonstrated that ISAV attach to the surface of a susceptible cell by binding to sialic acid receptors (Fig. 1), and this binding is pH-dependent, with increasing binding at decreasing pH (28). Studies with specific hydrolase inhibitors have revealed that the receptor-destroying activity of the ISAV is inhibited by both diisopropyl fluorophosphates and 3,4-dichloroisocoumarin, indicating that the viral enzyme represents a serine esterase (58, Paper I). Morphologically, the mushroom-shaped hemagglutinin spikes observed in ISAV using electron microscopy seemed different from the rod-shaped hemagglutinin projections of the influenza A viruses (31, 32). Recent studies have revealed that these spikes are hemagglutinin-esterases (HE) that specifically hydrolyze Neu4,5Ac_2 sialic acids (44, Paper I), and under the assumption that the receptor-destroying enzyme specificity reflects receptor usage, Neu4,5Ac_2 was suggested to represent a major ISAV receptor determinant (44).

Bound viral particles are internalized by receptor-mediated endocytosis and transported to endosomes and lysosomes, where the fusion of virus and endosomal/lysosomal membranes takes place in a pH-dependent manner (28, 49, Fig. 1). Compared to the fusion rate at pH 7.4, the fusion rate at pH 5.6 and 4.0 increased nearly 3 and 6 fold, respectively. Inhibitors of the endosomal acidification prevented the fusion process, further demonstrating the dependence on a lowering of the pH for fusion (28), and recent studies have demonstrated that the fusion

process is initiated at pH 5.4-5.6 (Paper III). However, amantadine did not inhibit ISAV replication, and attempts to demonstrate a pH-dependent association of the nucleoprotein (NP) and matrix proteins have not been successful (32, 65, Paper I). This could indicate that the mechanism for the release of ribonucleoprotein (RNP) complexes during ISAV entry is dissimilar from influenza A, questioning whether an ion channel contributes to lower the intra-viral pH to facilitate the release of RNP complexes.

Key characteristics in the proceeding steps in the ISAV replication is similar to the influenza virus replication, indicating that the general mechanisms involved are comparable. ISAV pursue a nuclear replication strategy (32, 74, Paper II), and subsequent to membrane fusion, the RNP complexes must be released into the cytoplasm and transported to the nucleus for transcription (Fig. 1). The replication of both ISAV and influenza viruses is sensitive to inhibitors of mRNA synthesis such as actinomycin D and α-amanitin which block the activity of the RNA polymerase II by binding to double-stranded DNA (32, 51, 63, 96). Thus, these viruses steal the 5' cap from host cellular mRNA to generate appropriate primers for the initiation of viral mRNA transcription (96). This is reflected by the heterogeneous sequences representing the cellular 5` cap in the 5`-end of ISAV mRNA nucleotide sequences (96). The viral segments 7 and 8 have been shown to contain conserved nucleotides at both ends, and computer based secondary structure modeling suggested that the terminal 21 to 24 nucleotides are able to form self-complementary panhandle structures (96). These are structures assumed to be important for the transcriptional regulation of the viral RNA (vRNA), since both 3`- and 5`-end terminal sequences are believed to be involved in the initiation of transcription (35). As genome sequences of all ISAV segments have been published, corresponding conserved regions with minor modifications has also been identified from 5`-end mRNA transcripts representing gene segments 1, 2, 3, 4, and 6 (4, 16, 59, 60, 88, 90, 103).

Several viruses that transcribe their genome in the cell nucleus have evolved mechanisms that promote the selective export of their mRNA transcripts, and in some cases, inhibit the export of cellular transcripts. To what extent the ISAV utilizes its potential to inhibit the expression of cellular proteins is unknown, but the general mechanisms of mRNA processing is similar to that of the influenza viruses (96), implying that the same regulatory mechanisms can be involved (14). These include the above mentioned cap-stealing, which contribute to reduce the export of cellular mRNA, but more importantly, the polyadenylation of influenza viral mRNAs is accomplished by the viral polymerase itself, which repeatedly copies a short stretch of U residues in the template genome RNA during transcription (14, 65). Indications that all ISAV vRNAs contain similar stretches of conserved polyadenlyation signals have been published (16, 59, 96, 103). This enables the virus to block the adenylation of cellular mRNA, inhibiting the expression of cellular proteins. In influenza, it is the non-structural protein 1 (NS1) that inhibits the cellular polyadenylation of mRNAs by reacting with the cleavage and polyadenylation specificity factor and the poly(A) binding protein II (14, 65).

The ISAV NP has been found to be produced early in the infection cycle, and the export to the cytoplasm coincides with the detection of the late proteins, indicating that the replication control system is similar to that of the influenza viruses (Papers I, II, III). In influenza A, the NP is synthesized early, presumably because it is needed for the synthesis of template RNAs and vRNAs. The synthesis of the matrix 1 (M1) is delayed, probably because this protein stops the transcription of vRNA into viral mRNA, and because it is a major regulator of nuclear export of vRNP (11, 65, 70).

Following transcription and translation, the synthesized proteins seem to follow the same path as in influenza. Briefly, the ISAV NP is transported to the nucleus where it is assumed to encapsidate vRNA and assembles into RNP complexes containing vRNA, NP, and the polymerases. These are exported to the cytoplasm and transported towards the cellular membrane to be incorporated into budding viral particles (Fig. 1, Papers I, II). The glycoproteins contain N-terminal signal sequences to be synthesized on membrane-bound ribosomes and are thought to be translocated across the membrane of the endoplasmatic reticulum (ER) (16, 41, Paper II). N-terminal signal sequences are cleaved off (16, 41), most likely in the ER. Subsequently, these proteins are transported along the classical intracellular route for glycoproteins, through the secretory pathway, going through posttranslational modifications prior to exposure in the plasma membrane (51, Papers II, III).

For most enveloped viruses, targeting of viral glycoproteins in polarized epithelial cells defines the site of budding (3, 51, 78). Polarized virus assembly and release may be important in determining the pathogenesis of viral infections because it can influence in a major fashion the pattern of virus spread in the infected host (65, 78). Because the glycoproteins define the site of virus budding, specific interactions between the viral NP and the glycoproteins, sometimes mediated by a matrix protein, must take place to ensure that the genome of the virus is incorporated (51). ISAV has been found budding from endothelial cells lining blood vessels and from endocardial cells and leucocytes, and the apical side of polarized epithelial cells seem to be the preferential site of budding (49, 81, 82). The polarized targeting of the ISAV HE often observed in infected cells grown *in vitro* indicate that the ISAV HE is involved in mediating this polarized ISAV budding (Fig. 2, unpublished results), as does the tight association between the RNPs and the matrix protein (Paper I). The infectious cycle is completed by the cleavage of sialic acids bound to HE in the budding particles, and this

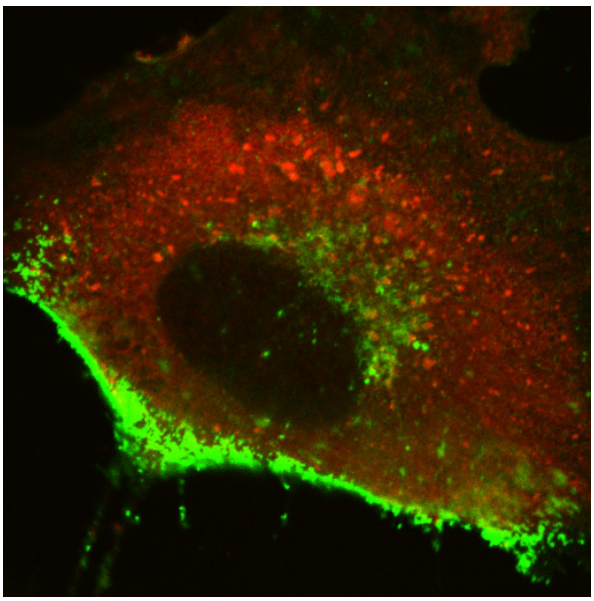

FIGURE 2. Cellular localization of the NP (red) and HE (green) in ISAV infected ASK cells 48 h post infection (p.i.). The NP is distributed in the cytoplasm, while the HE is localized perinuclearly, probably to the ER or golgi. Also, the HE locates to the plasma membrane at one side of the cell, indicating a polarized distribution correlating to the apical budding observed in electron microscopy (49, 81, 82).

cleavage is mediated by the viral receptor-destroying enzyme activity located to the HE, as described above (Fig. 1).

ISAV Genome Organization and Encoded Proteins

The ISAV genome is composed of eight negative-sense, single-strand RNA segments, and nucleotide sequences of all segments have been published (16, 59, 60, 73, 87, 88, 90, 101, 103). Segment 1 through 6 has one open reading frame (ORF), while segment 7 and 8 has two ORFs, as in other orthomyxoviruses. Segment 7 has an arrangement of un-spliced and spliced mRNAs analogous to that of influenza A virus segments 7 and 8, while ISAV segment 8 contains two overlapping ORFs (4, 73).

A total of 12 proteins have been detected by immunoprecipitation of lysates from radiolabeled infected cells (54), while four major structural proteins, and two minor proteins suggested to be precursor proteins, breakdown products, dimeric forms of one of the structural proteins, or minor viral proteins, have been recognized in purified ISAV particles (32, Paper I). Interestingly, a protein band corresponding to one of the major structural proteins observed in purified viruses (50-53 kDa protein) was not included amongst the 12 detected by immunoprecipitation (32, 54, Paper I), but three new viral proteins of 19-20, 29-30, and 33.5-36 was demonstrated. This is discussed further in the: “ISAV Protein Profile” section in the general discussion.

Initial suggestions on gene assignments in the ISAV have primarily been based on indications obtained by computer analysis, and have usually not been supported by experimental data. Naturally, after the establishment that the ISAV is an orthomyxovirus, gene assignments have been influenced by the assumption that it would have an organization similar to other orthomyxoviruses, and this is reflected by the confusion in the literature. Although protein

TABLE 1. ISAV segments and coding assignments as compared to other relevant viral proteins as indicated. Boldface information is considered as accepted for the ISAV.

Influenza A and other comparable viral proteins		Segment # and size		ISAV			
Comparable protein	**Important protein features[a]**	**Flu A**	**ISAV[d]**	**Suggested coding assignment**	**ORF #bp**	**MW[c] (kDa)**	**References**
Flu A Basic polymerase 2	Cap recognition of host cell RNA; component of RNPs and RNA transcriptase complex; **nuclear localization; positive charge[f];**	1 (2.3 kb)	**1 (2.3 kb)**	Basic polymerase 2	**722**	**79.5**	(16, 65, 103)
Flu A Basic polymerase 1	Endonuclease activity; catalyzes nucleotide addition; **positive charge[f];** component of RNPs and RNA transcriptase and replication complex; **conserved polymerase motifs characteristic to all RDRP[b]**	2 (2.3 kb)	**2 (2.3 kb)**	**Basic polymerase 1**	**708**	**80.5**	(60, 65)
Flu A Nucleoprotein	**Monomer binds to RNA** to **form RNPs**; involved in switch from mRNA to template RNA synthesis and in virion RNA synthesis; **nuclear localization; early protein;**	5 (1.6 kb)	**3 (2.2 kb)**	**Nucleoprotein**	**617**	**68.0**	(16, 65, 90, 101, Papers I, II)
Flu A Acidic polymerase	**Component of RNPs** and RNA transcriptase and replication complex; function unknown; **negative charge[f]**	3 (2.2 kb)	**4 (2.0 kb)**	Acidic polymerase	**579**	**65.3**	(16, 65, 90, unpublished results)
Type I viral membrane fusion protein	**Surface glycoprotein**; antigenic determinant**: proteolytic cleavage activation: low pH induced conformational change and fusion activity; fusion peptide; post fusion stable trimer; coiled-coil; late protein**	4 (HA) (1.8 kb)	**5 (1.7 kb)**	**Fusion protein**	**445**	**48.8**	(16, 65, Papers I, III)
Viral hemagglutinin -esterase	**Major surface glycoprotein; dimer; receptor binding: esterase activity; major antigenic determinant; late protein**	4 (HA) 6 (NA[g]) (1.4 kb)	**6 (1.5 kb)**	**Hemagglutinin - esterase**	**392**	**42.2**	(59, 62, 65, 87, Papers I, III)
Flu A (seg 8 ORF 1) Non-structural protein 1	High abundance in cells, not present in virion; **localize to cytoplasm and nucleus**; inhibits cellular pre-mRNA 3`end cleavage and polyadenylation; inhibits pre-mRNA splicing, sequesters dsRNA[h] from PKR kinase **reducing interferon response**	8 (0.9 kb)	**7[e] (1.3 kb)**	Non-structural protein 1	**ORF 1 300**	**34.2**	(4, 65, 102)
Flu A (seg 8 ORF 2) Nuclear Export Protein (NEP (NS2))	Minor component of virions; cytoplasmic and nuclear location; interacts with matrix 1 and involved in nuclear export of RNPs; **originate from spliced mRNA**	8	**7[e]**	Unknown **(Spliced mRNA)**	**ORF 2 159**	**17.5**	(65)
Flu A (seg 7 ORF 1) Matrix 1	**Major protein of virion**, **underlies lipid bilayer; interacts with RNPs** and NEP; **nuclear localization; late protein**	7 (1.0 kb)	**8 (1.0 kb)**	**Matrix**	**ORF 1 185**	**22**	(4, 65, 73, Paper I)
Flu A (seg 7 ORF 2) Matrix 2	Integral membrane protein; ion channel activity essential for virus uncoating; channel inhibited by amantadine; originate from spliced mRNA	7	**8**	Unknown **(Non-spliced mRNA)**	**ORF 2 234**	**27.4**	(65)

a) Accepted features for the tentatively corresponding ISAV protein are marked in bold. b) RNA-dependent RNA polymerases. c) Estimated from amino acid sequence of first published sequence. Isolate variations are not considered. d) (16, 73). e) A third ORF tentatively encoding a protein of 11 kDa has been suggested in ISAV segment 7 (57). f) Charge has been estimated from the protein sequence. g) Neuraminidase. h) Double-stranded RNA.

assignments have not been settled for all gene segments, the disorders resolved so far has involved the two smallest segments and the receptor-destroying enzyme and fusion protein in particular. This illustrates the value of functional characterization of proteins when they have limited or no sequence similarity to other characterized proteins. Table 1 summarizes what is known about the features of ISAV proteins as compared to other seemingly similar viral proteins, with an emphasis on the relevant influenza A proteins. The cumulative knowledge on the gene assignments of the ISAV is summarized in the following:

ISAV RNA segment 1 has been suggested to encode the basic polymerase 2 (PB2), as indicated by its similarity in size and amino acid composition to the influenza PB2, its level of conservation amongst isolates, and its intrinsic properties of nuclear localization (103). The intrinsic nuclear localization has been verified by transfection studies, but beyond that the experimental data is limited.

ISAV RNA segment 2 encodes the polymerase basic protein 1 (PB1) as evident by the presence of polymerase motifs characteristic to all RNA-dependent RNA polymerases (60). PB1 is the most conserved protein amongst orthomyxoviruses (66), and ISAV segment 2 show 20.8-24.1% amino acid identity to other orthomyxoviruses (60). The presence of the conserved polymerase motifs has been considered sufficient to conclude on its coding assignment relative to the influenza viruses.

ISAV RNA segment 3 has been suggested to encode the ISAV NP as supported by sequence analysis, although no significant sequence similarity to other proteins were identified (16, 90, 101). Supportive data were based on similarities to the influenza A NP, including amino acid composition, putative phosphorylation sites in two regions of the protein, and a hydrophobic

C-terminal end. Additionally, an RNA-binding site was predicted by comparison of the physicochemical characteristics of amino acids within the putative RNA-binding site of influenza NP (16). One study proposed that this protein is one of the major tissue antigens, but supportive experimental data are not clear (90). Experimental data supporting that segment 3 encodes the ISAV NP have been published, and is discussed in detail in papers I and II.

ISAV RNA segment 4 has been proposed to encode the acidic polymerase (PA) (90). The knowledge about the function of this protein in influenza is limited, and it is termed the acidic polymerase simply because it is part of the polymerase complex, and has a negative charge. Thus, the basis for characterizing this protein is limited, and so is the experimental data supporting this gene assignment in the ISAV (Table 1). Indicative data were based on sequence comparison to the influenza A PA, and included a slightly negative charge, the size, putative sites of phosphorylation, lack of predicted transmembrane regions, and a predicted cytoplasmic localization of the protein (90). However, even though proteins are synthesized in the cytoplasm, all influenza polymerases have intrinsic properties to be transported to the nucleus (51), thus at this point, the presumptive supportive data is conflicting with the influenza literature. However, indication that segment 4 encodes an integral protein of the RNP complex has been obtained by radioimmunoprecipitation studies using an antibody towards recombinant protein encoded by segment 4 (unpublished results). Two proteins thought to represent the NP and the matrix were detected, indicating that the antibody was reactive to the RNP complex. Attempts to disrupt the complex by SDS and boiling prior to precipitation was not successful, further substantiating that the targeted protein is part of the RNP complex (51).

ISAV RNA segment 5 has been suggested to encode a glycoprotein corresponding to the 53 kDa protein detected in purified virus (16). This was supported by N-terminal sequencing, which also demonstrated that the initial 17 N-terminal residues constitute a signal sequence. Functional studies have established that the encoded protein is a glycoprotein with the general properties of a type I viral membrane fusion protein, and this is discussed in detail in papers I and III.

ISAV RNA segment 6 has been shown to encode a 43 kDa HE (59, 87, Paper I), which is glycosylated (41, Paper I) and responsible for eliciting virus neutralizing antibodies (31), hemagglutination activity (31, 59, 87), and esterase activity (Paper I). This is discussed in further detail in paper I, and in the: “ISAV Replication” section above. Segment 6 has been found to hold the highest genomic variation amongst ISAV isolates, including a highly variable region very close to the predicted transmembrane region of the encoded protein, and phenotypic variation has been observed (25, 55, 56, 59, 72).

The coding assignments for the two smallest ISAV segments, have been, and are still causing discussion. In influenza viruses, the smallest of these genome segments uses an arrangement of unspliced and spliced mRNA transcripts to encode one non-structural (NS1) protein and one protein termed the nuclear export protein (NEP, previously termed NS2) (65). The coding strategies used by the second smallest segment on the other hand, vary, even though the proteins encoded are believed to have similar functionality (65, 76). In the influenza A virus, they are encoded by a colinear and a spliced transcript, while in influenza B M1 is encoded by a colinear transcript, and BM2 is transcribed by utilizing a tandem cistron translational stop-start mechanism (48). In influenza C virus CM1 derives from a spliced mRNA, whereas CM2

is the proteolytic product of a precursor protein that also produces a rapidly degraded membrane-bound polypeptide of unknown function (65).

ISAV RNA segment 7 has been shown to produce two partly overlapping mRNA species by splicing, and encode two proteins of 34.2 and 17.5 kDa (4, 88). The largest protein has been suggested to encode a non-structural protein as indicated by the lack of reactivity of recombinant protein to a polyclonal antibody prepared against purified virus (4). Additionally, indication that this protein is an interferon antagonist support that it corresponds to the influenza A NS1 (4, 102). This suggests that the orthomyxovirus genome segments encoding the NS proteins generally use the same coding strategy.

ISAV RNA segment 8 contains two overlapping ORFs. The first and smallest ORF encodes a protein with expected molecular weight of 22 kDa, and the second encodes a protein of 27.4 kDa. Experimental studies have demonstrated that the first of these proteins is a major structural protein corresponding to the virus matrix protein (4, Paper I), suggesting that the ISAV has a fourth coding strategy amongst the orthomyxoviruses for the segment encoding the matrix protein.

Segment 8 was the first ISAV gene sequence published (73), but the original paper did not suggest a coding assignment. Still, several authors have proposed, with reference to the original paper and to similarities between ISAV and the influenza viruses, that segment 8 encodes NS1 and NS2 (5, 21, 53, 89, 90, 101). Even recently, long after the publication of experimental data showing that the first ORF in segment 8 encodes the matrix protein (4, Paper I), scientists disagree on whether the encoded protein is structural or not (57).

AIMS OF THE PRESENT STUDY

The goal of this project was to identify and characterize the major structural proteins of the ISAV, and to determine the localization of the most important activities expected to be associated to these proteins based on the knowledge from the influenza literature. Specific aims were to:

1. Confirm the major structural proteins of the virus.
2. Establish the glycosylation and phosphorylation status of the ISAV major structural proteins, and determine the localization of these proteins in the virus particle.
3. Determine the localization of the most important biological activities associated to the major structural proteins.
4. Provide further characterization of the proteins to contribute to the identification of potential determinants of pathogenicity, and to support the development of improved diagnostics and recombinant subunit vaccines.

OVERVIEW OF PAPERS I-III

Paper I in this thesis describes an initial identification and characterization of the four major structural proteins of ISAV. Metabolic labeling experiments demonstrated that the ISAV has two glycosylated proteins with molecular masses of 42 (gp42) and 50 kDa (gp50), one 66 kDa phosphoprotein (vp66) and one 22 kDa protein (vp22). The localization of these proteins in the virus particle was further resolved by solubilizing the viral membrane of purified virus using a detergent and separating the soluble and the non-soluble proteins into two fractions by ultracentrifugation. The two glycoproteins and vp22 were detected in the soluble fraction, reflecting a membrane association of these proteins, while vp66 and a minor part of vp22 were found in the pelleted fraction, indicating that these are located to the internal side of the viral envelope. Additionally, vp22 was found to be the most abundant protein in the virion, and immunofluorescence studies demonstrated that it is a late protein accumulating in the cell nucleus. Based on these results we concluded that the vp66 is the nucleoprotein, vp22 is the matrix protein, and gp42 and gp50 are surface proteins. Additionally it was demonstrated that the viral esterase is located to gp42, previously shown to represent the ISAV hemagglutinin, and this protein was demonstrated to form dimers, and possibly trimers. Finally, the active site serine residue could be tentatively identified at position 32 within the amino acid sequence of the hemagglutinin of ISAV strain Glesvaer/2/90. We proposed that the ISAV vp66 protein should be termed nucleoprotein (NP), the gp42 should be termed hemagglutinin-esterase (HE) protein, and the vp22 should be termed matrix protein.

Paper II presents the expression of the ISAV genome segment 3, demonstrating that it encodes vp66, and provides further data confirming that this protein is the viral NP. It was demonstrated that it is an RNA-binding protein, expressed as an early protein during viral replication, initially detected in the cell nucleus. Two monopartite nuclear localization signals

(NLS) at amino acids ^{230}RPKR^{233} and ^{473}KPKK^{476} were identified by computer analysis, and validated by site-directed mutagenesis. Both NLSs had to be present for the ISAV NP protein to be transported into the nucleus, indicating that these motifs cooperate to target the protein to the nucleus. This is in contrast to other orthomyxovirus NPs that have several NLSs that function independently of each other.

Paper III presents the characterization of the ISAV gp50 as the viral membrane fusion protein (F). Cloned sequences showed identity to previously published segment 5 sequences, and computational analysis of the protein sequence revealed a potential coiled-coil and a tentative viral fusion peptide (FP). The F protein was found to be synthesized as a precursor termed F_0, cleavable by trypsin to the disulfide linked fragments F_1 and F_2. Size estimates of F_1 and F_2 and the localization of the FP and theoretical trypsin cleavage sites suggested a proteolytic cleavage site after residue K^{277} in the protein sequence. Cell-cell fusion assays demonstrated the requirement for trypsin and low pH to induce fusion. Treatment of purified virus with trypsin and low pH induced a conformational change in the protein, revealing a band suggestive of a trimer in WB, indicating a trimerization as part of the fusion process, or more likely, a stabilization of the trimer. This conformational change was coincident with induction of membrane-fusion activity, providing strong evidence that it represents the formation of the fusogenic structure. The same conformational change could be induced by high temperature and by urea, suggesting that the cleaved form of the protein is in a metastable state, all in accordance with characteristics of type I viral membrane fusion proteins. Sequence data indicated that the cleavage site structure is not a major determinant of pathogenicity in the ISAV.

GENERAL DISCUSSION

Although the overall morphological and physicochemical properties of the ISAV are similar to those of the other orthomyxoviruses, ISAV is distinct from the influenza viruses in a number of ways. ISAV infects fish, and have an optimal replication at 15°C (32). It is structurally unique in having several homologous proteins that bear no significant similarity in primary sequence to those of the other orthomyxoviruses, and its genomic organization differs in several ways. Particularly, the organization of the activities associated to the ISAV surface proteins is different from that of the other orthomyxoviruses.

With regard to genome structure, the major difference among influenza A, B, and C viruses pertains to the surface glycoproteins, and as demonstrated, the ISAV represents an additional variant (Fig. 3). Influenza A and B viruses have eight gene segments and contain separate attachment and receptor-destroying envelope glycoproteins (HA and neuraminidase (NA)), whereas ISAV contains one glycoprotein providing both of these functions (HE) and a separate F protein (Papers I, III). In influenza A and B viruses the fusion activity is located to the attachment protein (HA). Influenza C viruses contain only a single glycoprotein providing all of these functions (hemagglutinin-esterase-fusion, HEF), as reflected in the genome by the concomitant loss of one RNA segment (65) (Fig. 3).

Despite these differences, the structures of influenza A HA and influenza C HEF have been demonstrated to be largely comparable, having structurally similar receptor-binding domains as well as comparable stem domains thought to form independent fusion domains (92). The segregation of the three functions in HEF into structurally distinct domains led to the speculation that the trimeric fusion domain may have been an ancestral membrane-fusion protein (92). It was suggested that the HEF has evolved by recombination events resulting in

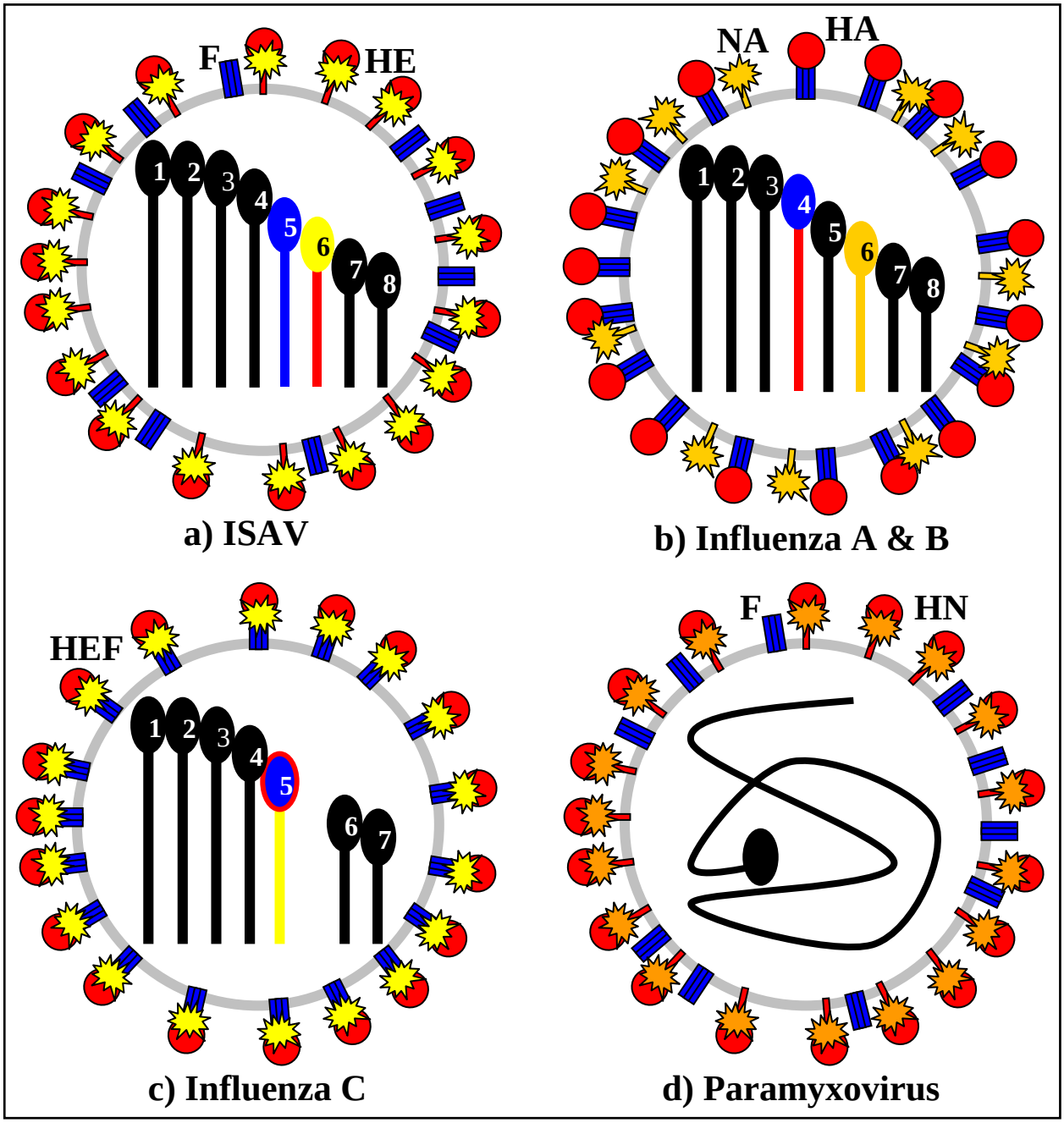

FIGURE 3. Organization of the activities associated to the surface proteins of the ISAV, Influenza A, B, and C viruses, and one paramyxovirus, as indicated. The localization of the receptor-binding activity is illustrated as red balls, the receptor-destroying activity as stars in yellow (esterase) or orange (neuraminidase), and the fusion activity as blue triple-bars. ISAV has a receptor-binding and -destroying protein termed the HE, and a separate F protein (a). Influenza A and B has a receptor-binding and fusion protein termed the HA, and a separate receptor-destroying protein termed the NA. Influenza C has all activities associated to a single protein termed the hemagglutinin-esterase-fusion protein (HEF) (c), while paramyxoviruses (d) has a similar organization as the ISAV except their receptor-destroying activity is a neuraminidase and not an esterase as in the ISAV. Thus paramyxoviruses have a hemagglutinin-neuraminidase (HN). Enumerated bars with head in a), b), and c) illustrate the viral genome segments, and the same colors that were used to indicate activities above, have been used to indicate the coding assignment of segments encoding the surface proteins. Paramyxoviruses have a non-segmented genome as illustrated in d).

the insertion of a receptor-binding domain and an esterase domain into an ancestral fusion protein analogous to the single-function fusion proteins of paramyxoviruses (92). Paramyxovirus fusion proteins (F) are different from the orthomyxovirus fusion proteins, particularly because of its pH-independence (51), and since the ISAV fusion protein is the first single function orthomyxovirus fusion protein described (Paper III), it may be more closely related to such an ancestral fusion protein.

Another distinguishable difference amongst the orthomyxovirus genera involves the coding strategy for the gene segment encoding the matrix proteins. The ISAV matrix protein has been linked to the first and smallest ORF in segment 8 (4) (Table 1), as opposed to the other genera in which the second smallest segment encode the M1. In Paper I we demonstrated that this protein is the most abundant protein in the virus particle, and that it is associated to both the membrane fraction and to the RNPs. It is a late protein, detected at 23 h post infection and it is accumulating in the nucleus (Paper I). However, as opposed to the matrix proteins in the influenza A, B, and C viruses, we were not able to demonstrate phosphorylation of this protein (65, Paper I). The phosphorylation of these proteins is thought to be associated to the active transport of these proteins in and out of the nucleus during the infection cycle (11, 79), and the unphosphorylated nature of the ISAV matrix could indicate a novel mechanism mediating this transport. However, transfection studies have established that the ISAV matrix has intrinsic ability to be transported to the nucleus, and it has a theoretical NLS (personal observation and personal communication Snow, M.). Thus, the importance of phosphorylation for this nuclear transport is questionable. Alternatively, the protein is phosphorylated, but the sensitivity of our immunoprecipitation assays was too low. This could be explained by the relatively low affinity of the antibody used towards the matrix (Paper I).

ISAV Protein Profile

ISAV contains eight RNA segments encoding at least ten proteins, and so far a total of 13 ISAV protein bands have been detected (Table 2). These include four major structural proteins of 22, 42, 50, and 66 kDa, and two minor proteins of 30 and 82 kDa which all have been recognized in purified ISAV particles (32, Paper I). The present study has established that these major structural proteins represent the matrix, HE, the F protein precursor (F_0) and the NP respectively, and the 82 kDa protein is a dimer of the HE (Papers I, II, III). A total of 7 protein bands have been associated to the F protein by Western blot analysis after various treatments, including the F_0 monomer, the cleaved fragments F_1 and F_2, F dimer, F trimer, and possible intermediates of these F polymers (cleaved and uncleaved) (Paper III, table 2). The 30 kDa protein detected in purified virus probably corresponds to F_1 (Paper I). Kibenge et al. (54) identified three additional viral proteins of 19-20, 29-30, and 33.5-36 kDa by

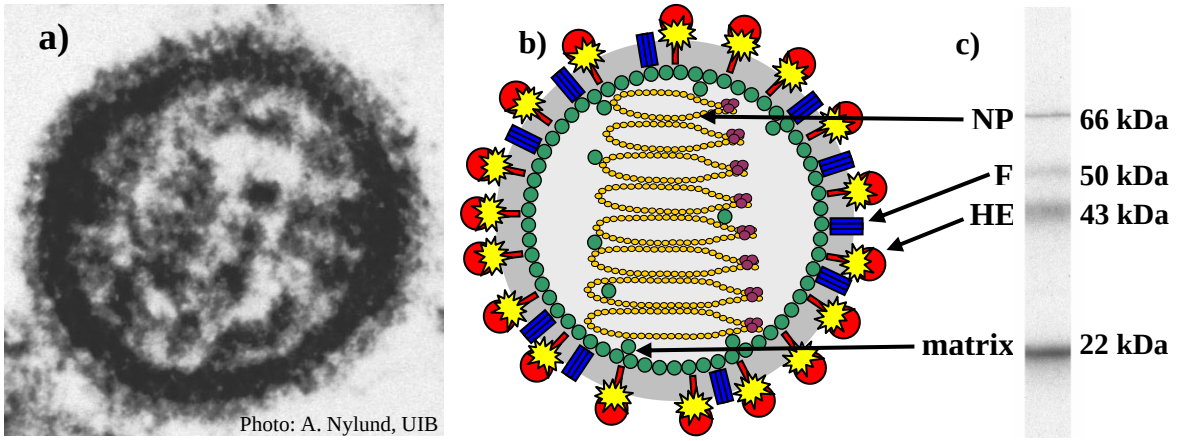

FIGURE 4. The ISAV particle. (a) Electron micrograph showing an ISAV particle. The particle is approximately 100 nm wide. (b) A schematic reproduction of the ISAV particle, showing the location of the different structural viral proteins. The NP (orange) associates with each of the eight vRNA segments to form RNP complexes. The subunits of the viral RNA-dependent RNA polymerase complex PB1, PB2, and PA (lilac) are also associated with the RNPs. ISAV has a receptor-binding and -destroying protein termed the HE, and a separate F protein. The localization of the receptor-binding activity is illustrated as red balls, the receptor-destroying activity as yellow stars (esterase), and the fusion activity as blue triple-bars. The matrix protein (green) is derived from a colinear mRNA of segment 8 and interacts both with the membrane and with the RNPs inside the virion. No attempt has been made to reconstruct the relative size proportions of proteins or number of copies of each protein in the virus particle. Also, proteins of unknown status have not been included. (c) Radioactively labeled purified virus run in SDS-PAGE is demonstrated on the right, reflecting the migration and relative quantity of the four major structural ISAV proteins (see also paper I).

radioimmunoprecipitation, but in their study the protein band corresponding to F_0 (50 kDa) was not detected. The absence of F_0 may indicate that the samples analyzed contained non-inactivated proteolytic enzymes, and that the 19-20 and 29-30 kDa protein bands represent the cleaved products of the fusion protein, namely F_1 and F_2 (54, Paper III). Also, previous studies have demonstrated that the ISAV HE is cleavable by trypsin, producing a cleaved fragment of 34 kDa (59, Paper I), suggesting that the 33.5-36 kDa protein may represent a cleaved form of the HE. This is supported by the size difference of this protein band amongst isolates which might be due to different numbers of glycosylation sites in the HE (16, 32, 41, 54, 56, 59, 87, Papers I, III). It is also suggested that the protein bands in the range 80-94 kDa represents dimers of HE and not the polymerases as suggested by Kibenge et al. (54), and also this is supported by the size variability amongst isolates. Thus, the present study suggests an alternative explanation to the protein profile observed by Kibenge et al (54), and this is summarized in table 2.

TABLE 2. Suggested assignments to protein bands observed in the ISAV protein profile, generated by summarizing observations from immunoprecipitation studies, SDS-PAGE, and WB from several publications as indicated.

SDS-PAGE			
Protein bands observed in present study (kDa)	Size-range of corresponding protein bands from other studies (kDa)	**Suggested protein**	**References**
170[a]		HE trimer or tetramer?	Paper I, unpublished results
150[a, c]		F trimer	Paper III
125[a, c]		F intermediate	Paper III
100[a]		F dimer	Paper III
82[a]	80-94	HE dimer	(54, Paper I)
75[a, c]		F intermediate	Paper III
66	66-74	NP	(32, 54, 56, Papers I, II)
50	47-53	F	(16, 32, 56, Paper III)
42	38-46	HE	(16, 32, 54, 56, 59, 87, Paper I)
34[b?]	33.5-36	Cleaved HE?	(54, Paper I)
30[b]	29-30	F_1	(54, Paper III)
22	22-26.5	Matrix	(4, 32, 54, 56, Paper I)
20[b]	19-20	F_2	(54, Paper III)

a) non-reducing SDS-PAGE. b) trypsin treated virus. c) trypsin and low pH treated virus.

The association of the viral membrane fusion activity to the second ISAV glycoprotein (gp50) verifies that the ISAV has a HE and not a HEF (59, Paper I and III). Additionally, it has been established that the ISAV HE has substantial sequence similarities to the regions around the active-site serine residue of other HEs, including the influenza C HEF (Paper I), and an enzyme activity comparable to that of certain coronaviruses (44). In coronaviruses, the HE is not absolutely necessary for virus infection in culture (62), while the presence of the HE in all isolates analyzed so far suggests that this is not the case in ISAV (25, 59, 72). In Paper I we suggested the ISAV HE to exist as dimers and probably trimers, as indicated by the presence of a second and third protein band in Western blots of non-reduced, non-heat-treated samples of precipitated HE. However, HE proteins of coronaviruses are found as dimers (86), and the trimeric nature of the HA, HEF, and F proteins are primarily related to the fusogenic activity of these proteins (18, 29, 75, 84, 92, 119). Additionally, the receptor binding domains of HEF, which is a trimer, has been suggested to have structural relationship to the HE of coronaviruses (92), suggesting that the polymerization status of these proteins is of secondary importance to the receptor-binding domains. Thus it is suspected that the ISAV HE is a dimer, and that the third protein band observed in WB which was suggested to represent a trimer (Paper I), may be a tetramer. This is supported by recent size estimates on this protein indicating that it is approximately 170 kDa (unpublished results), which is in agreement with it being a tetramer.

Potential Determinants of Pathogenicity

Increased virulence is consistently associated with a change in the function of one or several viral proteins, resulting in a more efficient completion of the infectious cycle, and/or altered tissue tropism. Thus, identifying and characterizing proteins involved in each step of the viral replication is crucial for the understanding of ISAV pathogenicity. Additionally, studies of the

intrinsic properties of these proteins can gain valuable information on the mechanisms involved in modulating viral pathogenicity, and combined with genome sequence information from several isolates, this can provide an important foundation to understand the genetic basis for virulence in ISAV.

The majority of the ISAV isolates isolated so far are pathogenic as they originate from outbreaks of ISA in fish farms, and a system of classifying isolates as virulent or avirulent is not yet established. Still, speculations that a full length archetype variant of the HE highly polymorphic region (HPR) represents an avirulent phenotype of the virus has been presented (20, 80). The avirulent nature of these strains were indicated by the lack of disease in the host fish, and by their poor replication in cell culture (19, 20). The model suggests that virulent variants of the full length archetype arise by deletion of several nucleotides in the HPR, suggesting that the HPR is a major determinant of pathogenicity in the ISAV (19, 20, 72, 80). The HPR is located to the stalk of the HE, and deletions in the HPR may affect several properties of the HE, including flexibility and receptor-binding specificity and affinity, antigenicity, esterase activity, interaction with other proteins, and possibly the polymerization of the protein, potentially affecting all the previously mentioned properties (see for instance 2, 115). Additionally, the variable glycosylation of the HE can potentially contribute to modulate pathogenicity, as it does in other orthomyxoviruses (9, 65). Thus the ISAV HE is a prime candidate in modulating the pathogenicity of the ISAV.

The most notable determinant of pathogenicity in other orthomyxoviruses and in paramyxoviruses is the cleavage properties displayed by the fusion promoting proteins (see for instance 13, 17, 37, 38, 40, 85, 106-109, 112). Virulent isolates generally have an F protein which is cleavable by ubiquitous intracellular proteases due to multiple basic residues

at the cleavage site, enabling a systemic spread of the virus, thereby increasing virulence. Still, it is also clear that several gene segments can contribute to the pathogenic phenotype of these viruses, depending on considerations such as the genetic background of the virus, the host, and the route of infection (7-10, 65). Also, it seems that when gene segments harbor traits that are known to influence pathogenicity, the genetic background provided by other segments can play a significant role in modulating this phenotype (107). Thus in the following, I will focus on other potential modulators of ISAV pathogenicity than that of the HE directly, particularly on the roles of the F and NP.

The apparent lack of multiple basic residues in the F protein cleavage site sequence of the distantly related virulent ISAV isolates published so far suggests that the cleavage site structure is not as important in determining the pathogenicity of the ISAV as in other orthomyxoviruses (Paper III). Nevertheless, the ISAV fusion activity, including the cleavability of the F protein, might still be a target of pathogenicity altering mechanisms. In our experiments, cell-cell fusion were observed in cells co-transfected with the HE and F genes, excluding the requirement of other viral proteins for fusion. Yet, conclusive data on whether the F protein could induce fusion independently of the HE was not obtained due to the generally low transfection efficacy obtained in fish cells. Nevertheless, an interaction between these two proteins, in which the HE affects the fusion activity, cannot be excluded. Several studies confirm the importance of the hemagglutinin-neuraminidase in influencing the fusion activity in paramyxoviruses (1, 45, 50, 64, 83), and residues in the paramyxovirus FP found to influence this regulatory effect seem conserved in the ISAV (95, Paper III). Also, the fusion activity of the Influenza A HA has been suggested to be modulated by other viral genes (9). Although a an interaction between the ISAV HE-F might simply serve to bring the target membranes and the F protein close enough to undergo fusion, attempts to induce

trimerization, or even to induce trypsin cleavage of recombinant F protein expressed alone in either Sf9 cells, *Escherichia coli*, or fish cells have so far been unsuccessful (unpublished results). This suggests that the ISAV HE might have a role in regulating the availability of the F protein cleavage site. As mentioned, the natural variation in the ISAV HE HPR has already attracted the attention of researchers interested in viral evolution and determinants of host range and virulence (25, 55, 59, 72, 80). However, the concept that HE might affect the F protein phenotype is new, and further research is required to determine its significance.

Papers I and II established that the NP is a phosphoprotein encoded by segment 3 which accumulate in the nucleus until the export is initiated at the onset of the detection of the late proteins. The ability of the NP to be transported to the cell nucleus is an intrinsic property of the protein, regulated by two NLSs which was identified and verified by site-directed mutagenesis (Paper II). Both ISAV NLSs are required to transport the NP to the nucleoplasma in transfected cells, and this is in contrast to other orthomyxovirus-NPs that have independent NLSs (79, 114). Mutations in virulent variants of Influenza A have been shown to repeatedly involve NLSs and sites of protein and RNA interaction, implicating them as potential modulators of virulence (9). However, NP genome sequences from only three isolates have been published so far, and supplementary sequence analyses and functional studies are needed to establish the importance of these findings.

In the absence of other viral proteins, the NP appear in the nucleolus and in structures resembling Cajal bodies before it is detectable in the nucleoplasma (Paper II). Initially, this led us to speculate whether phenotypic differences existed between Bremnes/98 (used for transfections) and Glesvaer/2/90 (used for infections). However, the ISAV NP was only rarely observed in the nucleolus of immunostained infected cells using either isolate, and we

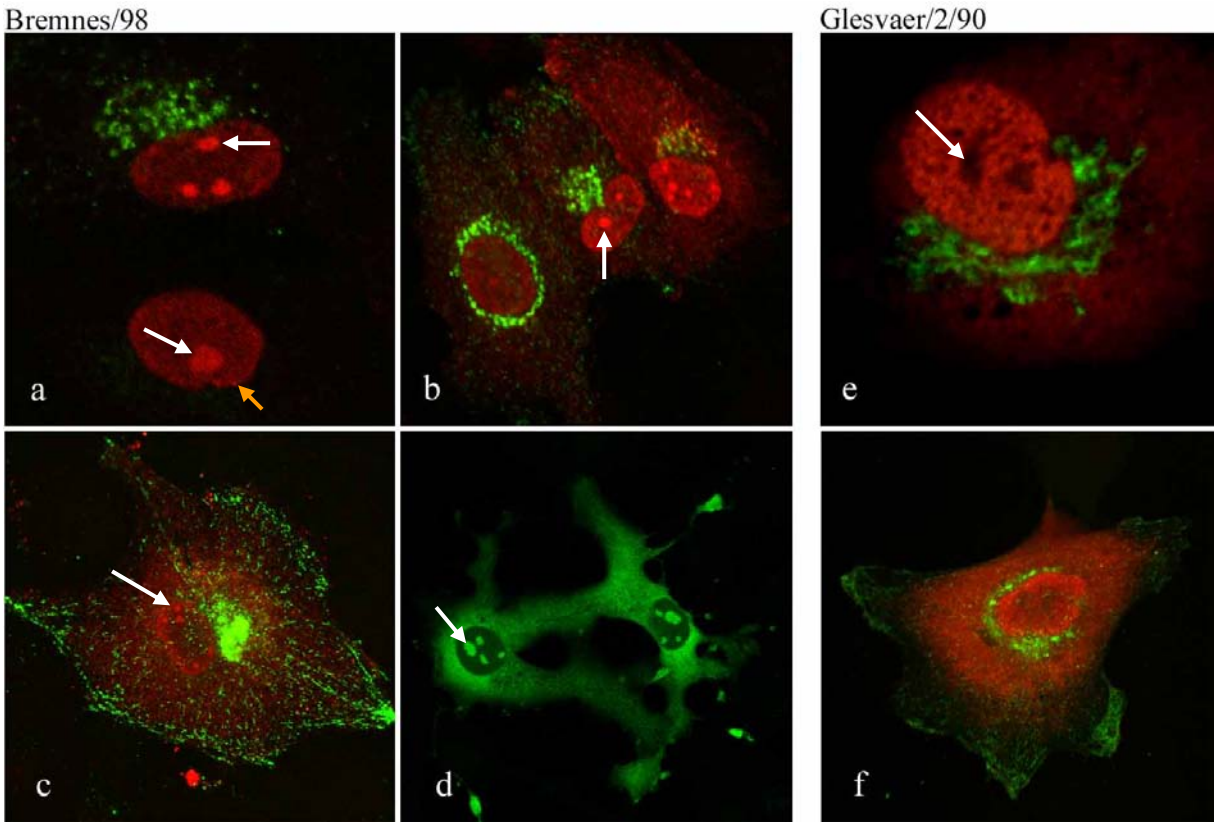

FIGURE 5. Cellular localization of NP (red) and HA (green) in ASK cells infected with two isolates of ISAV (a-c, e, and f), and localization of the NP in transfected COS cells (d) (NB: in (d) NP is shown in green). Immunofluorescence analysis are shown from 20 (a), 24(b), and 36 (c) h p.i. using the Bremnes/98 isolate, and 24 (e) and 36 (f) h p.i. using Glesvaer/2/90 (method of staining is as described in paper II). As described in paper II, the NP can be detected in the nucleus at 8 h p.i., while the HA appears at about 20 h p.i. (c). Using the Bremnes/98 isolate, the NP seem to accumulate in the nucleolus as indicated by arrows (a, b and, c). An orange arrow indicates a structure possibly representing a Cajal body (a). When expressed in COS cells, the NP located to the nucleolus and the cytoplasm. Conversely, the NP of the Glesvaer/2/90 isolate was only sporadically observed in the nucleolus, seemingly very early after the onset of NP detection (paper II), while the nucleolus appeared devoid of NP during the remaining of the infectious cycle (e, f).

suggested that the NP might require another viral protein to facilitate the transport from the nucleolus (Paper II). However, recent studies have shown that cells infected with the Bremnes/98 isolate give a significantly higher number of cells with NP localized to the nucleolus than the Glesvaer/2/90 isolate does, substantiating a phenotypic difference between the two isolates (Fig. 5 a, b, c, e, f, unpublished results). Also, these results suggest that localization to the nucleolus may be of functional significance to the ISAV. Several viruses and viral proteins including the Influenza A NP, have been shown to interact with the nucleolus and its components, and evidence suggests that viruses may target these structures

to favor viral transcription, translation, and perhaps alter the cell cycle in order to promote virus replication (12, 42, 47, 93, 94, 116, 118). In addition, cellular and viral proteins that localize to the nucleolus have been found to be involved in apoptosis events (42, 46, 97, 105). Nucleolus targeting is mediated by nucleolus localization signals (NoLS) which consist of clustered basic Arg/Lys residues. These are separate from, but in many cases overlapping, NLSs (39, 61, 99, 117) (Table 3). Our studies using mutants of segment 3 to identify the NLSs indicated that NLS1 was implicated in the transport of the NP to the nucleolus in transfected cells (Paper II), and by comparing this region with NoLSs identified in other viral proteins, a tentative NoLS spanning NLS1 can be suggested (Table 3).

TABLE 3. NoLSs in viral and cellular proteins. NoLSs consist of clustered basic Arg/Lys residues, and are separate from, but in many cases overlapping, NLSs. The basic residues are shown in bold, and NLSs are underlined. The ISAV NP NLS1-region has residues comparable to other NoLS, and experimental data has indicated that this region may be implicated in the nucleolus targeting of the NP (Paper II), while the ISAV NP NLS2-region is less similar to NoLSs.

Proteins	Sequences	References
GGNNV Protein α	**RRR**ANN**RRR**	(42)
MDV MEQ	**RRRKR**N**R**DAA**RRRRRK**Q	(67)
HIV-1 Tat	GR**KKRR**Q**RR**AP	(22)
HIV-1 Rev	**R**QA**RR**N**RRRR**WE**R**Q**R**	(61)
HTLV-I Rex	P**K**T**RRRPRR**SQ**RKR**P	(99)
Semliki capsid protein NoLS-1	**K**P**KKKK**TT**K**P**K**P**K**TQP	(34)
Semliki capsid protein NoLS-2	**RRRK****R**NRDAA**RRRRK**WQ	(34)
PRRSV nucleocapsid	PG**KK**N**KKK**NPE**K**PHFPLATEDDV**R**HHFTPPSE**R**	(94)
PTHrP	G**KKKK**G**K**PG**KRR**EQE**KKKRR**T	(46)
DEDD	**KR**PA**R**G**R**ATLGSQP**KRRK**SV	(42, 97, 105)
ISAV NP NLS1-region	**K**AAF**R**QS**RPKR**SDY**RK**GQGS**K**AT	Paper II
ISAV NP NLS2-region	SNI**K**ANTT**KPKK**DSTYTIQGL**R**LSN	Paper II

Abbreviations: GGNNV - greasy grouper nervous necrosis virus (fish betanodavirus), MDV - Marek's disease virus (avian alphaherpesvirus), HIV - human immunodeficiency virus (retrovirus), HTLV-I - Human T cell leukemia virus type I (retrovirus), PRRSV- porcine reproductive and respiratory syndrome virus (arterivirus), PTHrP - Parathyroid hormone-related peptide, DEDD - death effector domain-containing DNA-binding protein.

Recent studies have also revealed that when expressed in mammalian cells (COS cells) the ISAV NP (Bremnes/98) is transported to the nucleolus but not to the nucleoplasma, indicating

that there is conserved mechanisms for the nucleolus localization in these cells (Fig. 4d, unpublished results). These results are in agreement with observations on protein α in fish betanodaviruses which also contains a NoLS that is functional in mammalian cells, while the NLSs are not (42). However, in this context, the phenotypic variation with respect to nucleolus localization is surprising, and further studies are needed to verify the ISAV NoLS to determine whether the phenotypic difference observed is intrinsic to the NP, or affected by other viral proteins.

The localization of the NP to structures resembling Cajal bodies in transfected cells may also be of importance for viral pathogenicity as other viruses have been shown to modulate downstream antiviral effects by targeting such structures (47). Cajal bodies are nuclear organelles whose morphology and composition have been highly conserved from plants to animals (71). They contain the three eukaryotic RNA polymerases and a variety of factors involved in transcription and processing of all types of RNA (36). Thus, even though the NP localization to Cajal bodies was less prominent and only rarely observed in infected cells (Fig. 5 a), the prominent localization of the NP to these structures in transfected cells could imply that they are involved in ISAV replication.

CONCLUDING REMARKS AND FUTURE PERSPECTIVES

The present study has characterized the major structural proteins of the ISAV, including their localization in the virus particle and their key characteristics as compared to other viral proteins. Thus, this thesis contributes to the general understanding of the structure and replication of the ISAV, and provides decisive information for the development of subunit vaccines, and valuable information in the improvement of diagnostics. Also, potential therapeutic targets have been identified, and the organization of the activities associated to the surface proteins has been resolved, providing important information for the understanding of mechanisms controlling virulence.

In future studies, the isolation and characterization of avirulent ISAV isolates will be of major importance to establish mechanism used to induce increased ISAV virulence. However, this seems very complicated, and until then the verification of the F protein cleavage site and the importance of this structure should be of special interest. Although the pathogenicity of the ISAV probably is polygenic as in other viruses, this may contribute to substantiate the importance of the HE HPR as a determinant of pathogenicity in the ISAV. Either way, the surface proteins should be investigated in concert, particularly since the F protein phenotype might be influenced by the HE. Also, the phenotypic variation observed between the Bremnes/98 and Glesvaer/2/90 NP suggests that the nucleolus may be of functional significance to the ISAV replication. In the following, supplementary sequence data will be of great importance to understand the genetic basis for virulence in ISAV variants, with the hope that specific mutations will be indicators and thus predictors of virulence. Also, continued research to establish the coding assignment of the remaining ISAV genes, and to identify active sites, will be important to further understand the mechanisms utilized by this virus to generate virulent variants.

In recent years, F protein coiled-coils and fusion peptides have been the target for development of new anti-viral drugs, suggesting that F proteins might be important candidates both for vaccination and as therapeutic targets (27, 68, 113). In the present study, both peptides and antibodies were produced, but not tested due to the lack of a quantitative fusion assay. Thus, future studies will aim to establish such an assay to exploit the anti-viral effect of targeting these structures.

The diagnosis of ISA include pathological and haematological examinations as well as isolation of the pathogen in cell culture, ISAV-specific immunofluorescent antibody test (IFAT) and/or reverse transcriptase polymerase chain reaction (RT-PCR) (23, 24, 26, 30, 31, 73). So far, the ISA IFAT has been based on the use of a monoclonal antibody towards the HE (31), but the specificity of this antibody in diagnostics have been questioned, and special skills are required for interpretation (43). The present study draw attention to the potential of the NP as a diagnostic target using antibody based methods, as it is expressed in vast amounts in infected cells, and localize to the cell nucleus (Paper II). These are characteristics that could contribute to simplify the interpretation of the results by providing an additional means of verifying the specificity of the reaction, namely the nuclear localization, potentially improving both the specificity and sensitivity. Additionally, the NP is an internal protein in the virion, and should be expected to have less antigenic variation than the surface proteins that are exposed to the immune system of the host. Indeed, segment 6 encoding the HE, is one of the most variable genome segments in the ISAV (25, 59, 72, 80), and phenotypic variation, including antigenicity, has been related to this protein (41, 55, 56). In paper III we used a monoclonal antibody towards the NP which is commercially available (Aquatic Diagnostics Ltd.). Although a mix of different monoclonal antibodies towards the NP would be optimal to

avoid false negative results due to phenotypic variation, this antibody probably represents a good alternative for use in antibody based diagnostics of the ISAV.

REFERENCES

1. **Bagai, S., and R. A. Lamb.** 1995. Quantitative measurement of paramyxovirus fusion: differences in requirements of glycoproteins between simian virus 5 and human parainfluenza virus 3 or Newcastle disease virus. J Virol **69:**6712-9.
2. **Baigent, S. J., and J. W. McCauley.** 2003. Influenza type A in humans, mammals and birds: determinants of virus virulence, host-range and interspecies transmission. Bioessays **25:**657-71.
3. **Barman, S., A. Ali, E. K. Hui, L. Adhikary, and D. P. Nayak.** 2001. Transport of viral proteins to the apical membranes and interaction of matrix protein with glycoproteins in the assembly of influenza viruses. Virus Res **77:**61-9.
4. **Biering, E., K. Falk, E. Hoel, J. Thevarajan, M. Joerink, A. Nylund, C. Endresen, and B. Krossøy.** 2002. Segment 8 encodes a structural protein of infectious salmon anaemia virus (ISAV); the co-linear transcript from Segment 7 probably encodes a non-structural or minor structural protein. Dis Aquat Organ **49:**117-22.
5. **Blake, S., D. Bouchard, W. Keleher, M. Opitz, and B. L. Nicholson.** 1999. Genomic relationships of the North American isolate of infectious salmon anemia virus (ISAV) to the Norwegian strain of ISAV. Dis Aquat Organ **35:**139-44.
6. **Bouchard, D. A., K. Brockway, C. Giray, W. Keleher, and P. L. Merrill.** 2001. First report of infectious salmon anemia (ISA) in the United States. Bull Eur Assoc Fish Pathol **21:**86-88.
7. **Brown, E. G.** 1990. Increased virulence of a mouse-adapted variant of influenza A/FM/1/47 virus is controlled by mutations in genome segments 4, 5, 7, and 8. J Virol **64:**4523-33.
8. **Brown, E. G.** 2000. Influenza virus genetics. Biomed Pharmacother **54:**196-209.
9. **Brown, E. G., H. Liu, L. C. Kit, S. Baird, and M. Nesrallah.** 2001. Pattern of mutation in the genome of influenza A virus on adaptation to increased virulence in the mouse lung: identification of functional themes. Proc Natl Acad Sci U S A **98:**6883-8.
10. **Brown, I. H., S. Ludwig, C. W. Olsen, C. Hannoun, C. Scholtissek, V. S. Hinshaw, P. A. Harris, J. W. McCauley, I. Strong, and D. J. Alexander.** 1997. Antigenic and genetic analyses of H1N1 influenza A viruses from European pigs. J Gen Virol **78:**553-62.
11. **Bui, M., E. G. Wills, A. Helenius, and G. R. Whittaker.** 2000. Role of the influenza virus M1 protein in nuclear export of viral ribonucleoproteins. J Virol **74:**1781-1786.
12. **Chen, H., T. Wurm, P. Britton, G. Brooks, and J. A. Hiscox.** 2002. Interaction of the coronavirus nucleoprotein with nucleolar antigens and the host cell. J Virol **76:**5233-50.
13. **Chen, J., K. H. Lee, D. A. Steinhauer, D. J. Stevens, J. J. Skehel, and D. C. Wiley.** 1998. Structure of the hemagglutinin precursor cleavage site, a determinant of influenza pathogenicity and the origin of the labile conformation. Cell **95:**409-17.
14. **Chen, Z., and R. M. Krug.** 2000. Selective nuclear export of viral mRNAs in influenza-virus-infected cells. Trends Microbiol **8:**376-83.
15. **Christie, K. E., B. Hjeltnes, I. Uglenes, and J. R. Winton.** 1993. Determination of buoyant density and sensitivity to chloroform and freon for the etiologic agent of infectious salmon anaemia. Dis Aquat Org **15:**225-228.
16. **Clouthier, S. C., T. Rector, N. E. Brown, and E. D. Anderson.** 2002. Genomic organization of infectious salmon anaemia virus. J Gen Virol **83:**421-8.
17. **Collins, M. S., J. B. Bashiruddin, and D. J. Alexander.** 1993. Deduced amino acid sequences at the fusion protein cleavage site of Newcastle disease viruses showing variation in antigenicity and pathogenicity. Arch Virol **128:**363-70.
18. **Colman, P. M., and M. C. Lawrence.** 2003. The structural biology of type I viral membrane fusion. Nat Rev Mol Cell Biol **4:**309-19.
19. **Cook-Versloot, M., S. Griffiths, R. Cusack, S. McGeachy, and R. Ritchie.** 2004. Identification and characterisation of infectious salmon anaemia virus (ISAV) haemagglutinin gene highly polymorphic region (HPR) type 0 in North America. Bulletin of the European Association of Fish Pathologists **24:**203-208.

20. **Cunningham, C. O., A. Gregory, J. Black, I. Simpson, and R. Raynard.** 2002. A novel variant of the infectious salmon anaemia virus (ISAV) haemagglutinin gene suggests mechanisms for virus diversity. Bull Eur Assic Fish Pathol **22:**366-374.
21. **Cunningham, C. O., and M. Snow.** 2000. Genetic analysis of infectious salmon anaemia virus (ISAV) from Scotland. Dis Aquat Organ **41:**1-8.
22. **Dang, C. V., and W. M. Lee.** 1989. Nuclear and nucleolar targeting sequences of c-erb-A, c-myb, N-myc, p53, HSP70, and HIV tat proteins. J Biol Chem **264:**18019-23.
23. **Dannevig, B. H., K. Falk, and E. Namork.** 1995. Isolation of the causal virus of infectious salmon anemia (ISA) in a long-term cell-line from Atlantic salmon head kidney. J Gen Virol **76:**1353-1359.
24. **Dannevig, B. H., K. Falk, and C. M. Press.** 1995. Propagation of infectious salmon anemia (ISA) virus in cell culture. Vet Res **26:**438-442.
25. **Devold, M., K. Falk, B. Dale, B. Krossøy, E. Biering, V. Aspehaug, F. Nilsen, and A. Nylund.** 2001. Strain variation, based on the hemagglutinin gene, in Norwegian ISA virus isolates collected from 1987 to 2001: indications of recombination. Dis Aquat Organ **47:**119-28.
26. **Devold, M., B. Krossøy, V. Aspehaug, and A. Nylund.** 2000. Use of RT-PCR for diagnosis of infectious salmon anaemia virus (ISAV) in carrier sea trout (*Salmo trutta*) after experimental infection. Dis Aquat Organ **40:**9-18.
27. **Eckert, D. M., and P. S. Kim.** 2001. Mechanisms of viral membrane fusion and its inhibition. Annu Rev Biochem **70:**777-810.
28. **Eliassen, T. M., M. K. Frøystad, B. H. Dannevig, M. Jankowska, A. Brech, K. Falk, K. Romøren, and T. Gjøen.** 2000. Initial events in infectious salmon anemia virus infection: evidence for the requirement of a low-pH step. J Virol **74:**218-227.
29. **Epand, R. M.** 2003. Fusion peptides and the mechanism of viral fusion. Biochim Biophys Acta **1614:**116-21.
30. **Falk, K., and B. H. Dannevig.** 1995. Demonstration of infectious salmon anaemia (ISA) viral antigens in cell cultures and tissue sections. Vet Res **26:**499-504.
31. **Falk, K., E. Namork, and B. H. Dannevig.** 1998. Characterization and applications of a monoclonal antibody against infectious salmon anaemia virus. Dis Aquat Org **34:**77-85.
32. **Falk, K., E. Namork, E. Rimstad, S. Mjaaland, and B. H. Dannevig.** 1997. Characterization of infectious salmon anemia virus, an orthomyxo-like virus isolated from Atlantic salmon (*Salmo salar* L.). J Virol **Dec:**9016-9023.
33. **Falk, K., C. M. Press, T. Landsverk, and B. H. Dannevig.** 1995. Spleen and kidney of Atlantic salmon (*Salmo salar* L.) show histochemical changes early in the course of experimentally induced infectious salmon anaemia (ISA). Vet Immunol Immunopathol **49:**115-26.
34. **Favre, D., E. Studer, and M. R. Michel.** 1994. Two nucleolar targeting signals present in the N-terminal part of Semliki Forest virus capsid protein. Arch Virol **137:**149-55.
35. **Fodor, E., D. C. Pritlove, and G. G. Brownlee.** 1994. The influenza virus panhandle is involved in the initiation of transcription. J Virol **68:**4092-6.
36. **Gall, J. G.** 2001. A role for Cajal bodies in assembly of the nuclear transcription machinery. FEBS Lett **498:**164-7.
37. **Garten, W., F. X. Bosch, D. Linder, R. Rott, and H. D. Klenk.** 1981. Proteolytic activation of the influenza virus hemagglutinin: The structure of the cleavage site and the enzymes involved in cleavage. Virology **115:**361-74.
38. **Glickman, R. L., R. J. Syddall, R. M. Iorio, J. P. Sheehan, and M. A. Bratt.** 1988. Quantitative basic residue requirements in the cleavage-activation site of the fusion glycoprotein as a determinant of virulence for Newcastle disease virus. J Virol **62:**354-6.
39. **Goatley, L. C., M. B. Marron, S. C. Jacobs, J. M. Hammond, J. E. Miskin, C. C. Abrams, G. L. Smith, and L. K. Dixon.** 1999. Nuclear and nucleolar localization of an African swine fever virus protein, I14L, that is similar to the herpes simplex virus-encoded virulence factor ICP34.5. J Gen Virol **80 (Pt 3):**525-35.
40. **Goto, H., and Y. Kawaoka.** 1998. A novel mechanism for the acquisition of virulence by a human influenza A virus. Proc Natl Acad Sci U S A **95:**10224-10228.

41. **Griffiths, S., M. Cook, B. Mallory, and R. Ritchie.** 2001. Characterisation of ISAV proteins from cell culture. Dis Aquat Org **45:**19-24.
42. **Guo, Y. X., K. Dallmann, and J. Kwang.** 2003. Identification of nucleolus localization signal of betanodavirus GGNNV protein alpha. Virology **306:**225-35.
43. **Hastings, T., G. Olivier, R. Cusack, I. Bricknell, A. Nylund, and M. Binde.** 1999. Infectious Salmon Anaemia. Bull Eur Ass Fish Pathol **19:**286- 288.
44. **Hellebø, A., U. Vilas, K. Falk, and R. Vlasak.** 2004. Infectious salmon anemia virus specifically binds to and hydrolyzes 4-O-acetylated sialic acids. J Virol **78:**3055-62.
45. **Heminway, B. R., Y. Yu, and M. S. Galinski.** 1994. Paramyxovirus mediated cell fusion requires co-expression of both the fusion and hemagglutinin-neuraminidase glycoproteins. Virus Res **31:**1-16.
46. **Henderson, J. E., N. Amizuka, H. Warshawsky, D. Biasotto, B. M. Lanske, D. Goltzman, and A. C. Karaplis.** 1995. Nucleolar localization of parathyroid hormone-related peptide enhances survival of chondrocytes under conditions that promote apoptotic cell death. Mol Cell Biol **15:**4064-75.
47. **Hiscox, J. A.** 2002. The nucleolus - a gateway to viral infection? Arch Virol **147:**1077-89.
48. **Horvath, C. M., M. A. Williams, and R. A. Lamb.** 1990. Eukaryotic coupled translation of tandem cistrons: identification of the influenza B virus BM2 polypeptide. EMBO J **9:**2639-47.
49. **Hovland, T., A. Nylund, K. Watanabe, and C. Endresen.** 1994. Observation of infectious salmon anaemia virus in Atlantic salmon, *Salmo salar* L. J Fish Dis **17:**291-296.
50. **Hu, X. L., R. Ray, and R. W. Compans.** 1992. Functional interactions between the fusion protein and hemagglutinin-neuraminidase of human parainfluenza viruses. J Virol **66:**1528-1534.
51. **Hunter, E.** 2001. General virology: Virus assembly, p. 171-197. *In* D. M. Knipe, P. M. Howley, G. D. E., M. M. A., L. R. A., R. B., and S. E. Straus (ed.), Fields virology, 4th ed. ed. Lippincott-Raven, Philadelphia, Pa.
52. **Håstein, T., B. J. Hill, and J. R. Winton.** 1999. Successful aquatic animal disease emergency programmes. Rev sci tech Off int Epiz **18:**214-227.
53. **Inglis, J. A., J. Bruce, and C. O. Cunningham.** 2000. Nucleotide sequence variation in isolates of infectious salmon anaemia virus (ISAV) from Atlantic salmon (*Salmo salar*) in Scotland and Norway. Dis Aquat Organ **43:**71-6.
54. **Kibenge, F. S., O. N. Garate, G. Johnson, R. Arriagada, M. J. Kibenge, and D. Wadowska.** 2001. Isolation and identification of infectious salmon anaemia virus (ISAV) from Coho salmon in Chile. Dis Aquat Organ **45:**9-18.
55. **Kibenge, F. S., M. J. Kibenge, P. K. McKenna, P. Stothard, R. Marshall, R. R. Cusack, and S. McGeachy.** 2001. Antigenic variation among isolates of infectious salmon anaemia virus correlates with genetic variation of the viral haemagglutinin gene. J Gen Virol **82:**2869-79.
56. **Kibenge, F. S., J. R. Lyaku, D. Rainnie, and K. L. Hammell.** 2000. Growth of infectious salmon anaemia virus in CHSE-214 cells and evidence for phenotypic differences between virus strains. J Gen Virol **81:**143-150.
57. **Kibenge, F. S., K. Munir, M. J. Kibenge, T. Joseph, and E. Moneke.** 2004. Infectious salmon anemia virus: causative agent, pathogenesis and immunity. Anim Health Res Rev **5:**65-78.
58. **Kristiansen, M., M. K. Frøystad, A. L. Rishovd, and T. Gjøen.** 2002. Characterization of the receptor-destroying enzyme activity from infectious salmon anaemia virus. J Gen Virol **83:**2693-7.
59. **Krossøy, B., M. Devold, L. Sanders, P. M. Knappskog, V. Aspehaug, K. Falk, A. Nylund, S. Koumans, C. Endresen, and E. Biering.** 2001. Cloning and identification of the infectious salmon anaemia virus haemagglutinin. J Gen Virol **82:**1757-65.
60. **Krossøy, B., I. Hordvik, F. Nilsen, A. Nylund, and C. Endresen.** 1999. The putative polymerase sequence of infectious salmon anemia virus suggests a new genus within the *Orthomyxoviridae*. J Virol **73:**2136-42.

61. **Kubota, S., H. Siomi, T. Satoh, S. Endo, M. Maki, and M. Hatanaka.** 1989. Functional similarity of HIV-I rev and HTLV-I rex proteins: identification of a new nucleolar-targeting signal in rev protein. Biochem Biophys Res Commun **162:**963-70.
62. **Lai, M. M. C., and K. V. Holmes.** 2001. *Coronaviridae*: The viruses and their replication, p. 1163-1185. *In* D. M. Knipe, P. M. Howley, G. D. E., M. M. A., L. R. A., R. B., and S. E. Straus (ed.), Fields virology, 4th ed. Lippincott-Raven, Philadelphia, Pa.
63. **Lamb, R. A., and P. W. Choppin.** 1977. Synthesis of influenza virus polypeptides in cells resistant to alpha-amanitin: evidence for the involvement of cellular RNA polymerase II in virus replication. J Virol **23:**816-819.
64. **Lamb, R. A., and D. Kolakofsky.** 2001. *Paramyxoviridae*: The viruses and their replication, p. 1305-1340. *In* D. M. Knipe, P. M. Howley, G. D. E., M. M. A., L. R. A., R. B., and S. E. Straus (ed.), Fields virology, 4th ed. Lippincott-Raven, Philadelphia, Pa.
65. **Lamb, R. A., and R. M. Krug.** 2001. *Orthomyxoviridae*: The viruses and their replication, p. 1487-1579. *In* D. M. Knipe, P. M. Howley, G. D. E., M. M. A., L. R. A., R. B., and S. E. Straus (ed.), Fields virology, 4th ed. Lippincott-Raven, Philadelphia, Pa.
66. **Lin, D. A., S. Roychoudhury, P. Palese, W. C. Clay, and F. J. Fuller.** 1991. Evolutionary relatedness of the predicted gene product of RNA segment 2 of the tick-borne Dhori virus and the PB1 polymerase gene of influenza viruses. Virology **182:**1-7.
67. **Liu, J. L., L. F. Lee, Y. Ye, Z. Qian, and H. J. Kung.** 1997. Nucleolar and nuclear localization properties of a herpesvirus bZIP oncoprotein, MEQ. J Virol **71:**3188-96.
68. **Louis, J. M., I. Nesheiwat, L. Chang, G. M. Clore, and C. A. Bewley.** 2003. Covalent trimers of the internal N-terminal trimeric coiled-coil of gp41 and antibodies directed against them are potent inhibitors of HIV envelope-mediated cell fusion. J Biol Chem **278:**20278-85.
69. **Lovely, J. E., B. H. Dannevig, K. Falk, L. Hutchin, A. M. MacKinnon, K. J. Melville, E. Rimstad, and S. G. Griffiths.** 1999. First identification of infectious salmon anaemia virus in North America with haemorrhagic kidney syndrome. Dis Aquat Organ **35:**145-8.
70. **Martin, K., and A. Helenius.** 1991. Nuclear transport of influenza virus ribonucleoproteins: the viral matrix protein (M1) promotes export and inhibits import. Cell **67:**117-30.
71. **Matera, A. G.** 1998. Of coiled bodies, gems, and salmon. J Cell Biochem **70:**181-92.
72. **Mjaaland, S., O. Hungnes, A. Teig, B. H. Dannevig, K. Thorud, and E. Rimstad.** 2002. Polymorphism in the infectious salmon anemia virus hemagglutinin gene: importance and possible implications for evolution and ecology of infectious salmon anemia disease. Virology **304:**379-91.
73. **Mjaaland, S., E. Rimstad, K. Falk, and B. H. Dannevig.** 1997. Genomic characterization of the virus causing infectious salmon anemia in Atlantic salmon (*Salmo salar* L.): an orthomyxo-like virus in a teleost. J Virol **71:**7681-7686.
74. **Moneke, E. E., M. J. Kibenge, D. Groman, G. R. Johnson, B. O. Ikede, and F. S. Kibenge.** 2003. Infectious salmon anemia virus RNA in fish cell cultures and in tissue sections of Atlantic salmon experimentally infected with infectious salmon anemia virus. J Vet Diagn Invest **15:**407-17.
75. **Morrison, T. G.** 2003. Structure and function of a paramyxovirus fusion protein. Biochim Biophys Acta **1614:**73-84.
76. **Mould, J. A., R. G. Paterson, M. Takeda, Y. Ohigashi, P. Venkataraman, R. A. Lamb, and L. H. Pinto.** 2003. Influenza B virus BM2 protein has ion channel activity that conducts protons across membranes. Dev Cell **5:**175-84.
77. **Mullins, J. E., D. Groman, and D. Wadowska.** 1998. Infectious salmon anaemia in salt water Atlantic salmon (*Salmo salar* L.) in New Brunswick, Canada. Bull Eur Assic Fish Pathol **18:**110-114.
78. **Nayak, D. P., E. K. Hui, and S. Barman.** 2004. Assembly and budding of influenza virus. Virus Res **106:**147-65.
79. **Neumann, G., M. R. Castrucci, and Y. Kawaoka.** 1997. Nuclear import and export of influenza virus nucleoprotein. J Virol **71:**9690-700.
80. **Nylund, A., M. Devold, H. Plarre, E. Isdal, and M. Aarseth.** 2003. Emergence and maintenance of infectious salmon anaemia virus (ISAV) in Europe: a new hypothesis. Dis Aquat Organ **56:**11-24.

81. **Nylund, A., T. Hovland, K. Watanabe, and C. Endresen.** 1995. Presence of infectious salmon anemia virus (ISAV) in tissues of Atlantic salmon, *Salmo salar* L, collected during 3 separate outbreaks of the disease. J Fish Dis **18:**135-145.
82. **Nylund, A., B. Krossøy, K. Watanabe, and J. A. Holm.** 1996. Target cells for the ISA virus in Atlantic salmon, *Salmo salar* L. Bulletin of the European Association of Fish Pathology **16:**68-72.
83. **Paterson, R. G., M. A. Shaughnessy, and R. A. Lamb.** 1989. Analysis of the relationship between cleavability of a paramyxovirus fusion protein and length of the connecting peptide. J Virol **63:**1293-301.
84. **Peisajovich, S. G., and Y. Shai.** 2003. Viral fusion proteins: multiple regions contribute to membrane fusion. Biochim Biophys Acta **1614:**122-9.
85. **Perdue, M. L., and D. L. Suarez.** 2000. Structural features of the avian influenza virus hemagglutinin that influence virulence. Vet Microbiol **74:**77-86.
86. **Regl, G., A. Kaser, M. Iwersen, H. Schmid, G. Kohla, B. Strobl, U. Vilas, R. Schauer, and R. Vlasak.** 1999. The hemagglutinin-esterase of mouse hepatitis virus strain S is a sialate-4-O-acetylesterase. J Virol **73:**4721-7.
87. **Rimstad, E., S. Mjaaland, M. Snow, A. B. Mikalsen, and C. O. Cunningham.** 2001. Characterization of the infectious salmon anemia virus genomic segment that encodes the putative hemagglutinin. J Virol **75:**5352-6.
88. **Ritchie, R. J., A. Bardiot, K. Melville, S. Griffiths, C. O. Cunningham, and M. Snow.** 2002. Identification and characterisation of the genomic segment 7 of the infectious salmon anaemia virus genome. Virus Res **84:**161-70.
89. **Ritchie, R. J., M. Cook, K. Melville, N. Simard, R. Cusack, and S. Griffith.** 2001. Identification of infectious salmon anaemia virus in Atlantic salmon from Nova Scotia (Canada): evidence for functional strain differences. Dis Aquat Organ **44:**171-8.
90. **Ritchie, R. J., J. Heppell, M. B. Cook, S. Jones, and S. G. Griffiths.** 2001. Identification and characterization of segments 3 and 4 of the ISAV genome. Virus Genes **22:**289-97.
91. **Rodger, H. D., and R. H. Richards.** 1998. Haemorrhagic smolt syndrome: a severe anaemic condition in farmed salmon in Scotland. The Veterinary Record**:**538-541.
92. **Rosenthal, P. B., X. Zhang, F. Formanowski, W. Fitz, C. H. Wong, H. Meier-Ewert, J. J. Skehel, and D. C. Wiley.** 1998. Structure of the haemagglutinin-esterase-fusion glycoprotein of influenza C virus. Nature **396:**92-96.
93. **Rowland, R. R., P. Schneider, Y. Fang, S. Wootton, D. Yoo, and D. A. Benfield.** 2003. Peptide domains involved in the localization of the porcine reproductive and respiratory syndrome virus nucleocapsid protein to the nucleolus. Virology **316:**135-45.
94. **Rowland, R. R., and D. Yoo.** 2003. Nucleolar-cytoplasmic shuttling of PRRSV nucleocapsid protein: a simple case of molecular mimicry or the complex regulation by nuclear import, nucleolar localization and nuclear export signal sequences. Virus Res **95:**23-33.
95. **Russell, C. J., T. S. Jardetzky, and R. A. Lamb.** 2004. Conserved glycine residues in the fusion peptide of the paramyxovirus fusion protein regulate activation of the native state. J Virol **78:**13727-42.
96. **Sandvik, T., E. Rimstad, and S. Mjaaland.** 2000. The viral RNA 3'- and 5'-end structure and mRNA transcription of infectious salmon anaemia virus resemble those of influenza viruses. Arch Virol **145:**1659-1669.
97. **Schickling, O., A. H. Stegh, J. Byrd, and M. E. Peter.** 2001. Nuclear localization of DEDD leads to caspase-6 activation through its death effector domain and inhibition of RNA polymerase I dependent transcription. Cell Death Differ **8:**1157-68.
98. **Schyth, B. D., N. J. Olesen, P. Østergård, and K. Falk.** 2003. Presented at the Diseases of Fish and Shellfish, 11 th International Conference of the EAFP, Malta.
99. **Siomi, H., H. Shida, S. H. Nam, T. Nosaka, M. Maki, and M. Hatanaka.** 1988. Sequence requirements for nucleolar localization of human T cell leukemia virus type I pX protein, which regulates viral RNA processing. Cell **55:**197-209.
100. **Skehel, J. J., and D. C. Wiley.** 2000. Receptor binding and membrane fusion in virus entry: The influenza hemagglutinin. Annu Rev Biochem **69:**531-569.

101. **Snow, M., and C. O. Cunningham.** 2001. Characterisation of the putative nucleoprotein gene of infectious salmon anaemia virus (ISAV). Virus Res **74:**111-118.
102. **Snow, M., A. J. A. McBeath, R. Paley, S. Duraffour, V. Aspehaug, E. Biering, C. J. Secombes, and B. Collet.** (manuscript in prep). Identification of an interferon antagonist protein encoded by segment 7 of infectious salmon anaemia virus.
103. **Snow, M., R. Ritchie, O. Arnaud, S. Villoing, V. Aspehaug, and C. O. Cunningham.** 2003. Isolation and characterisation of segment 1 of the infectious salmon anaemia virus genome. Virus Res **92:**99-105.
104. **Sommerset, I., B. Krossøy, E. Biering, and P. Frost.** 2005. Vaccines for fish in aquaculture. Expert Rev Vaccines **4:**89-101.
105. **Stegh, A. H., O. Schickling, A. Ehret, C. Scaffidi, C. Peterhansel, T. G. Hofmann, I. Grummt, P. H. Krammer, and M. E. Peter.** 1998. DEDD, a novel death effector domain-containing protein, targeted to the nucleolus. EMBO J **17:**5974-86.
106. **Steinhauer, D. A.** 1999. Role of hemagglutinin cleavage for the pathogenicity of influenza virus. Virology **258:**1-20.
107. **Steinhauer, D. A., and J. J. Skehel.** 2002. Genetics of influenza viruses. Annu Rev Genet **36:**305-32.
108. **Suarez, D. L., D. A. Senne, J. Banks, I. H. Brown, S. C. Essen, C. W. Lee, R. J. Manvell, C. Mathieu-Benson, V. Moreno, J. C. Pedersen, B. Panigrahy, H. Rojas, E. Spackman, and D. J. Alexander.** 2004. Recombination resulting in virulence shift in avian influenza outbreak, Chile. Emerg Infect Dis **10:**693-9.
109. **Tashiro, M., N. L. McQueen, and J. T. Seto.** 1999. Determinants of organ tropism of sendai virus. Front Biosci **4:**D642-5.
110. **Thorud, K.** 1991. Infectious salmon anaemia: transmission trials, haematological, clinical chemical and morphological investigations. Ph.D. Norwegian College of Veterinary Medicine, Oslo, Norway.
111. **Thorud, K., and H. O. Djupvik.** 1988. Infectious salmon anaemia in Atlantic salmon (*Salmo salar* L.). Bull Eur Assoc Fish Pathol **8:**109-111.
112. **Toyoda, T., T. Sakaguchi, K. Imai, N. M. Inocencio, B. Gotoh, M. Hamaguchi, and Y. Nagai.** 1987. Structural comparison of the cleavage-activation site of the fusion glycoprotein between virulent and avirulent strains of Newcastle disease virus. Virology **158:**242-7.
113. **Vareckova, E., V. Mucha, S. A. Wharton, and F. Kostolansky.** 2003. Inhibition of fusion activity of influenza A haemagglutinin mediated by HA2-specific monoclonal antibodies. Arch Virol **148:**469-86.
114. **Weber, F., G. Kochs, S. Gruber, and O. Haller.** 1998. A classical bipartite nuclear localization signal on Thogoto and influenza A virus nucleoproteins. Virology **250:**9-18.
115. **Wu, E., and G. R. Nemerow.** 2004. Virus yoga: the role of flexibility in virus host cell recognition. Trends Microbiol **12:**162-9.
116. **Wurm, T., H. Chen, T. Hodgson, P. Britton, G. Brooks, and J. A. Hiscox.** 2001. Localization to the nucleolus is a common feature of coronavirus nucleoproteins, and the protein may disrupt host cell division. J Virol **75:**9345-56.
117. **Yamada, H., Y. M. Jiang, H. Y. Zhu, K. Inagaki-Ohara, and Y. Nishiyama.** 1999. Nucleolar localization of the UL3 protein of herpes simplex virus type 2. J Gen Virol **80 (Pt 8):**2157-64.
118. **Yoo, D., S. K. Wootton, G. Li, C. Song, and R. R. Rowland.** 2003. Colocalization and interaction of the porcine arterivirus nucleocapsid protein with the small nucleolar RNA-associated protein fibrillarin. J Virol **77:**12173-83.
119. **Zhu, J., C. W. Zhang, Y. Qi, P. Tien, and G. F. Gao.** 2002. The fusion protein core of measles virus forms stable coiled-coil trimer. Biochem Biophys Res Commun **299:**897-902.

Paper I

JOURNAL OF VIROLOGY, Mar. 2004, p. 3063–3071 Vol. 78, No. 6
0022-538X/04/$08.00+0 DOI: 10.1128/JVI.78.6.3063–3071.2004

Identification and Characterization of Viral Structural Proteins of Infectious Salmon Anemia Virus

Knut Falk,[1]* Vidar Aspehaug,[1,2] Reinhard Vlasak,[3] and Curt Endresen[2]

Section for Fish Health, National Veterinary Institute, Oslo,[1] and Department of Fisheries and Marine Biology, University of Bergen, Bergen,[2] Norway, and Institute of Molecular Biology, Austrian Academy of Sciences, Salzburg, Austria[3]

Received 21 September 2003/Accepted 24 November 2003

Infectious salmon anemia virus **(ISAV) is an unclassified *Orthomyxovirus* that has been shown to contain a segmented genome with eight single-stranded RNA species coding for 10 viral proteins. Four major structural proteins were characterized in the present study: two glycosylated proteins with estimated molecular masses of 42 and 50 kDa, one 66-kDa phosphoprotein, and one 22-kDa protein. Examination of lysed virions revealed the two glycoproteins and the 22-kDa protein in the soluble fraction, while the 66-kDa phosphoprotein and a minor part of the 22-kDa protein were found in the pelleted fraction. Immunofluorescence staining of infected cells demonstrated that the 22-kDa protein was a late protein accumulating in the nucleus. We conclude that the 66-kDa protein is the nucleoprotein, the 22-kDa protein is the matrix protein, and the 42- and 50-kDa proteins are the surface proteins. Radioimmunoprecipitation analysis of the 42-kDa glycoprotein, which was previously shown to represent the ISAV hemagglutinin, indicated that this protein exists at least as dimers. Further, by labeling of purified ISAV with [1,3-^{3}H]diisopropyl fluorophosphate, it was also demonstrated that the viral esterase is located with the hemagglutinin. This finding was confirmed by demonstration of acetylesterase activity in affinity-purified hemagglutinin preparations. Finally, the active-site serine residue could be tentatively identified at position 32 within the amino acid sequence of the hemagglutinin of ISAV strain Glesvaer/2/90. It is proposed that the ISAV vp66 protein be termed nucleoprotein, the gp42 protein be termed HE protein, and the vp22 protein be termed matrix protein.**

Infectious salmon anemia (ISA) is one of the most important viral diseases in farmed Atlantic salmon (*Salmo salar* L). The disease was first described for salmon parr in a hatchery on the southwest coast of Norway in 1984 (34), and later the disease was also observed in Canada, Scotland, the Faroe Islands, and the United States (2, 4, 26, 30). In addition, the ISA virus has been observed in Pacific coho salmon (*Oncorhyncus kisutch*) in Chile (1, 13) and in rainbow trout (*Oncorhyncus mykiss*) in Ireland.

The ISA virus has been shown to share several morphological, physiochemical, and biochemical characteristics with the influenza viruses, suggesting that it belongs to the *Orthomyxoviridae* (12, 18, 24). These characteristics include a single-stranded RNA genome that consists of eight segments with a tentative negative polarity (24), conservation of partially self-complementary terminal ends of the genomic segments (32), a replication strategy that both includes RNA production and protein accumulation in the nucleus (12, 32), morphological similarities, and the ability to hemagglutinate red blood cells (RBC) (12). The nucleotide sequences of all ISAV genome segments have now been published (3, 6, 18, 19, 24, 29, 33). In common with the influenza A and B viruses, segments 7 and 8 reveal two open reading frames (ORFs), while the others contain one ORF each. No significant sequence homology with the influenza viruses was found, although some sequence similarities suggesting coding assignment of the different genes have been reported.

* Corresponding author. Mailing address: Section for Fish Health, National Veterinary Institute, P.O. Box 8156 dep, N-0033 Oslo, Norway. Phone: 47 23 21 61 32. Fax: 47 23 21 61 01. E-mail: Knut.Falk@vetinst.no.

Influenza A and B viruses contain four major structural proteins and six minor proteins. The major proteins include the nucleoprotein (NP), which interacts with the viral RNA together with the polymerases (PB1, PB2, and PA) to form the viral ribonucleoprotein (vRNP) complex. The matrix protein (M1) is the most abundant structural protein and is believed to form a bridge between the vRNPs and the viral membrane. The two other major structural proteins of the virion are integral to the viral envelope. The hemagglutinin (HA) is a homotrimeric glycoprotein with receptor-binding and acid-activated membrane fusion activity, and the neuraminidase is a homotetramer with receptor-destroying enzyme (RDE) activity. Influenza C virus has only seven gene segments and has one surface glycoprotein, the HA-esterase (HE) protein. Further, while the RDEs of influenza A and B viruses are neuraminidases, the RDE of influenza C virus is an esterase (21).

ISAV has been shown to possess hemagglutinating, RDE, and fusion activities (9, 12). The RDE has been suggested to be an acetylesterase with specificity different from that of influenza C virus (12). Recently, it was found that 4-O-acetylated sialic acids serve both as a substrate for the RDE and as a receptor determinant for virus binding (12a). Four major structural proteins with estimated molecular masses of 71, 53, 43, and 24 kDa have been detected in purified ISAV particles (12, 14). Further, by immunoprecipitation of lysates from radiolabeled infected cells, Kibenge et al. (14) detected a total of 12 proteins. It is currently unknown whether these additional proteins represent minor structural proteins, precursor proteins, or breakdown products. Based on functional analysis and protein expression, the 43-kDa protein has been suggested to represent the HA and to be coded by genome segment 6 (6, 17, 28). The 71-kDa protein has been suggested to be encoded by

segment 3 and to represent the NP, though no experimental data supporting this assumption have been presented (6, 29). Recently the 24-kDa structural protein was linked to one of the two ORFs of segment 8 (3), and the 53-kDa was linked to segment 5 (6); however, no function or characterization of these two proteins has so far been presented.

In the present study we confirm the four major structural proteins and also document that the virus has one surface glycoprotein in addition to the earlier-described HA. We have also demonstrated, for the first time, that the HA is an HE protein. Furthermore, we provide both experimental data showing that the 22-kDa major structural protein is the matrix (M) protein and data indicating that the 66-kDa protein represents the NP.

MATERIALS AND METHODS

Virus and cells. The Norwegian ISA virus isolate Glesvaer/2/90 (7) was used throughout this study. Cultures of SHK cells (7) or ASK cells (8) were used for virus propagation. The cells were grown at 20°C in Leibovitz L-15 medium (L-15) supplemented with 5% (SHK cells) or 10% (ASK cells) fetal bovine serum, glutamine (4 mM), and gentamicin (50 μg ml^{-1}). Cells were incubated at 15°C after inoculation with virus. Unless otherwise stated, cells with the fluid overlay removed were inoculated with virus at a multiplicity of infection of 0.1 in serum free L-15. All assays were performed with the fourth or fifth passage of the virus. Infectivity titrations were done by end point titration in 96-well culture plates as previously described (11).

For preparation of radiolabeled whole virus, 25 μCi of [^{35}S]methionine (Pro-Mix; Amersham Biosciences) ml^{-1} was added to SHK cell cultures in 175-cm^2 tissue culture flasks at 1 day postinfection (p.i.), and incubation was continued for 3 days before harvest of the virus-containing cell culture medium. Radiolabeled cell lysates were prepared by infecting confluent monolayers of ASK cells in 25-cm^2 tissue culture flasks. Following a 4-h adsorption period, 350 μCi of [^{35}S]methionine, 350 μCi of [^{3}H]mannose (Amersham Biosciences), or 350 μCi pf [^{32}P]phosphate (Amersham Biosciences) ml^{-1} in 2.5 ml of methionine-, mannose-, or phosphate-free medium was added, and incubation was continued for 24 h. The cell cultures were then washed twice with PBS and lysed on ice for 15 min in lysis buffer (50 mM Tris [pH 7.6], 150 mM NaCl, 1% NP-40, 0.5% sodium deoxycholate), and insoluble debris were removed by centrifugation at 14,000 rpm (20,000 × *g*) for 20 min at 4°C. Lysates were stored at −80°C until used.

Antibodies. Antibodies used in the present study included a monoclonal antibody (MAb) directed at the ISAV HA (anti-HA MAb) (11), a rabbit antibody against purified whole virus (anti-ISAV polyclonal antibody [PAb]) (12), and a rabbit antibody against a recombinant protein based on the first ORF in ISAV genome segment 8 (anti-rVp22 PAb) (3). All polyclonal antisera were adsorbed by incubation on monolayers of acetone-fixed SHK or ASK cells prior to use.

Virus purification. Purified whole virus was prepared by sucrose gradient centrifugation of polyethylene glycol 8000-precipitated cell culture supernatant as described previously (12). Alternatively, virus was affinity purified directly from cell culture supernatants by using anti-mouse immunoglobulin G (IgG)-conjugated immunomagnetic beads (Dynabeads M-280; Dynal, Oslo, Norway) and the anti-HA MAb. Briefly, the beads were washed twice in PBS (10 mM phosphate [pH 7.4], 150 mM NaCl) with 0.1% bovine serum albumin (BSA) (PBS-BSA), incubated with the MAb in PBS for 1 h at room temperature (RT), and washed four times in PBS-BSA. Culture supernatant with [^{35}S]methionine-labeled virus was then incubated with the coated beads at 4°C for 3 h (0.1 mg of beads per 1 ml of supernatant). Finally, the beads were washed four times in PBS-BSA, resuspended in dissociation buffer, and analyzed by sodium dodecyl sulfate-polyacrylamide gel electrophoresis (SDS-PAGE) followed by autoradiography (see below).

RIPA of virus-specific proteins. Immune precipitation of radiolabeled viral antigen was performed on crude cytosol extracts. Antibody-coated magnetic beads (see above) were used for the precipitation. Radiolabeled cell lysates were first absorbed with uncoated beads for 1 h at RT, and then 250 μg of coated beads was incubated with 10 μl of cell lysate in 100 μl of PBS for 1 to 2 h at RT. Antibody-antigen complexes were washed two times with radioimmunoprecipitation assay (RIPA) buffer (PBS containing 1% Triton X-100, 0.1% BSA, 1% sodium deoxycholate, 0.5 M lithium chloride, and 0.1% SDS), once with PBS-BSA, and once with Tris-HCl (50 mM; pH 6.8). Finally, the beads were resuspended in dissociation buffer and analyzed by SDS-PAGE followed by autoradiography (see below). Noninfected, radiolabeled cell lysates were used as controls.

SDS-PAGE and Western blotting. Samples were treated with dissociation buffer (50 mM Tris-HCl [pH 6.8], 1% SDS, 50 mM dithiothreitol, 8 mM EDTA, 0.01% bromophenol blue) and heated for 5 min at 95°C. In the nonreduced samples, dithiothreitol was omitted and incubation was for 30 min at RT. The proteins were then separated by SDS-PAGE with the discontinuous system devised by Laemmli (20) and 0.5-mm-thick precast 12.5% polyacrylamide gels (ExcelGel SDS; Amersham Biosciences). ^{14}C-methylated marker proteins (Amersham Biosciences; range, 14.3 to 220 kDa) were run in adjacent lanes. For autoradiography, the gel was fixed in 10% acetic acid–40% ethanol in double-distilled water for 30 min, treated with Amplify (Amersham Biosciences) containing 3% glycerol for 30 min, dried, and exposed to X-ray film at −80°C.

For Western blotting, separated proteins were transferred to a nitrocellulose membrane in a semidry electroblotter (NovaBlot; Amersham Biosciences). The protein blot was then treated with blocking solution (PBS containing 1% Tween 20 and 5% nonfat dry milk) overnight at 4°C, followed by incubation for 2 h at RT with the primary rabbit immune serum diluted in blocking solution. The membrane was washed three times in blocking solution and reacted with a goat anti-rabbit–horseradish peroxidase (HRP) conjugate for 1 h at RT. Diaminobenzidine was used for detection of bound HRP conjugate.

For staining of glycosylated proteins with lectins, the protein blot was first treated with PBS with 0.1% Tween 20 and 5% BSA overnight at 4°C. The protein blot was then reacted with 15 mg of biotinylated concanavalin A (Sigma) ml^{-1} diluted in PBS with 0.1% Tween 20 and 1% BSA. The membrane was washed three times in PBS with 0.1% Tween 20 and reacted with HRP-conjugated streptavidin for 1 h at RT. Bound HRP-conjugate was detected as described above.

Labeling of ISAV protein with [1,3-^{3}H]diisopropyl fluorophosphate (DFP) (New England Nuclear; specific activity, 310.8 GBq/mmol) was done by incubating purified ISAV, containing 2 mU of esterase activity, with 74,000 Bq of [^{3}H]DFP for 1 h at RT, followed by an overnight incubation at 4°C. Reduced and nonreduced viral proteins were analyzed by electrophoresis on SDS–12 and 8% polyacrylamide gels, respectively. The gels were then incubated with Amplify, dried, and subjected to fluorography.

The autoradiographs and blots were scanned in a desktop scanner (Image Scanner; Amersham Biosciences) and subsequently analyzed and printed by using Gel-Pro gel scanning software (Media Cybernetics, Silver Spring, Md.).

Deglycosylation of viral glycoprotein. Immunoprecipitated [^{35}S]methionine-labeled viral proteins were heated at 95°C for 5 min in TNE buffer (10 mM Tris-HCl [pH 7.2], 100 mM NaCl, 1 mM EDTA) with 0.05% SDS. *N*-Octylglycoside (Roche) was added to 0.5%, and then the mixture was briefly heated again to 95°C and incubated overnight at 37°C with or without 2 U of *N*-glycosidase-F (Roche) ml^{-1}. Samples were subsequently prepared in dissociation buffer, followed by SDS-PAGE and autoradiography.

Trypsin treatment of virus-specific proteins. Immunoprecipitated [^{35}S]methionine-labeled viral proteins were treated with 20 μg of trypsin (Promega) ml^{-1} in TBS (50 mM Tris [pH 7.2], 100 mM NaCl) for 30 min at 37°C and immediately prepared in dissociation buffer, followed by SDS-PAGE and autoradiography.

Dissociation of virions. Virus metabolically labeled with [^{35}S]methionine was purified by sucrose gradient centrifugation. Purified virus was then diluted in lysis buffer (50 mM Tris [pH 7.6], 100 mM NaCl, 1% NP-40, 0.5% sodium deoxycholate, Complete Mini protease inhibition mix [Roche]) and incubated on ice for 15 min. The lysate was then pelleted through a cushion of 20% sucrose in lysis buffer at 50,000 rpm for 2 h at 4°C in a Beckman SW-60 rotor. The supernatant was collected and precipitated with trichloroacetic acid at a final concentration of 10% on ice for 30 min. The precipitate was washed three times with ethanol-ether (1:1), and both this precipitate and the pelleted fraction were resuspended in dissociation buffer and analyzed by SDS-PAGE, followed by autoradiography.

Hemagglutination and HI assays. Hemagglutination in microtiter plates was carried out as previously described (12). The hemagglutination inhibition (HI) test with the serine esterase inhibitors DFP (Sigma) and 3,4-dichloroisocoumarin (DCIC) (Sigma) was performed by first mixing 25 μl of inhibitor, diluted in PBS, with 25 μl of virus suspension containing 4 HA units, followed by incubation for 1 h. Fifty microliters of 0.5% Atlantic salmon RBC, 0.75% rabbit RBC, or 0.75% horse RBC was then added, and the agglutination end points were read following 1 and 6 h of incubation. All incubations were performed at RT. The hemagglutination activity (HA units) is expressed as the reciprocal value of the highest dilution showing complete agglutination of RBC.

Affinity purification of HA and detection of acetylesterase activity. The viral HA was affinity purified by using anti-HA MAb-coated immunomagnetic beads as described above for purification of whole virus. Briefly, 500 μg of coated beads was added to 300 μl of ISAV cell lysate and incubated for 30 min at RT. The

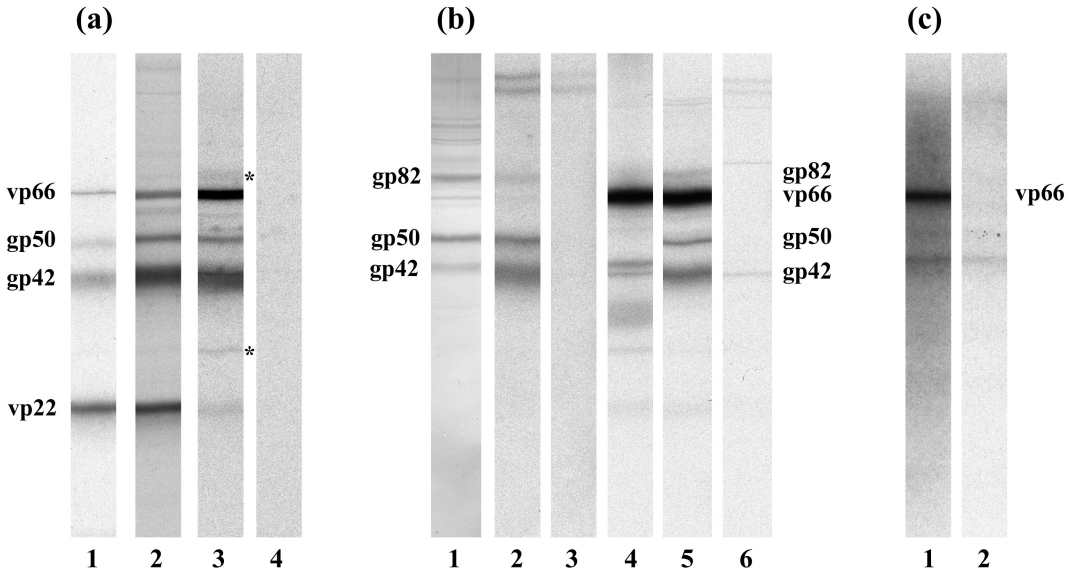

FIG. 1. (a) Autoradiograms of [^{35}S]methionine-labeled ISAV proteins resolved in SDS–12.5% polyacrylamide gels. Lanes: 1, whole virus purified by sucrose gradient centrifugation; 2, whole virus purified by affinity purification with immunomagnetic beads and an anti-HA MAb; 3, immunoprecipitation of cell lysates from virus-infected cell cultures with an anti-whole virus antibody (30- and 82-kDa proteins are indicated by asterisks); 4, control lysates of [^{35}S]methionine-labeled cells. (b) Detection of glycoproteins. Lanes: 1, Western blot of purified virus stained with biotinylated concanavalin A; 2, immunoprecipitation of cell lysates from virus-infected cells labeled with [^{3}H]mannose; 3, control lysates of [^{3}H]mannose-labeled cells; 4, [^{35}S]methionine-labeled ISAV proteins were immunoprecipitated, followed by deglycosylation; 5, nondeglycosylated control preparation; 6, control lysates of [^{35}S]methionine-labeled cells. (c) Detection of phosphoproteins. Lanes: 1, immunoprecipitation of cell lysates from virus-infected cells labeled with ^{32}P by using an anti-whole virus antibody; 2, control lysates of ^{32}P-labeled cells.

beads were then removed and washed, and both beads and cell lysate were assayed for esterase activity.

The acetylesterase activity was determined by incubating 25 μl of sample with 1 ml of 1 mM *p*-nitrophenyl acetate (pNPA) (Sigma) in double-distilled water. The release of acetate was monitored by determining the optical density at 400 nm. One unit of viral esterase was defined as the amount of enzymatic activity resulting in cleavage of 1 μmol of pNPA per min (16). Inhibition of acetylesterase activity was tested by incubating virus samples and inhibitors for 30 min at RT before testing for acetylesterase activity.

Immunofluorescence. Indirect immunofluorescence staining was performed on ISAV-infected ASK cells grown on coverslips. Following incubation, the cells were washed once in PBS, fixed in 10% buffered formalin for 10 min, rinsed in PBS, and subsequently permeabilized with 2% Triton X-100 in PBS for 30 min. After blocking with 5% nonfat dry milk in PBS for 30 min, the cells were incubated for 1 h with the primary antibody diluted in PBS with 2.5% nonfat dry milk. Alexa Fluor 546 goat anti-mouse IgG (Molecular Probes) and Alexa Fluor 488 goat anti-rabbit IgG (Molecular Probes) in PBS were used for the detection of bound antibodies. PBS was used for washing, and all incubations were performed at RT. The cell preparations were mounted with the SlowFade antifade kit (Molecular Probes) and examined in a confocal microscope (Leica TCS-SP).

Sequence alignments. For analysis we used the amino acid sequences of the European ISAV strain Glesvaer (accession number AAF32361) and the antigenically different Canadian isolate ISAV Bay of Fundy/97 (AAK30064) (15, 19). Accession numbers for the other HE sequences used for alignment are AAA43785 for influenza C virus, AAA46442 for mouse hepatitis virus strain JHM, P15776 for bovine coronavirus strain Mebus, and CAA71819 for Breda virus. The sequences were aligned by using the CLUSTAL method as described previously (38).

RESULTS

ISA virus structural proteins. Radioactively labeled virus preparations purified either by sucrose gradient centrifugation or by affinity purification with immunomagnetic beads coated with anti-HA MAb were analyzed by SDS-PAGE (Fig. 1a, lanes 1 and 2). Both purification methods gave essentially the same results, revealing four major structural proteins, as observed earlier by Falk et al. (12). The molecular masses were calculated based on the average of 10 different lanes, and the three most distinct bands were estimated to be approximately 22, 50, and 66 kDa, respectively, while the wide, less distinct band had a molecular mass peaking at 42 kDa (range, 40 to 43 kDa). By scanning the autoradiograms of the gels and performing a densiometric analysis, integrating the area under each peak, the relative amounts of the 22-, 42-, 50-, and 66-kDa bands were estimated to be approximately 40, 37, 11, and 12%, respectively.

By RIPA of [^{35}S]methionine-labeled cell lysates of infected cells with anti-ISAV PAb, we also found two minor proteins migrating at 30 and 82 kDa (Fig. 1a, lane 3), which probably represented precursor proteins, breakdown products, dimeric forms of one of the major proteins, or minor viral proteins. Comparing cell lysate RIPA protein profiles with those obtained with purified virus preparations, it was also evident that the relative amount of the 66-kDa protein had increased while the amount of the 22-kDa protein had decreased, probably reflecting differences in the immune response to these proteins in the rabbit. A relatively weak reaction to the 22-kDa protein was also seen on Western blots (see Fig. 3b, lane 3) supporting this observation.

Glycosylation of the major proteins was examined both by staining of Western blots with biotinylated concanavalin A (Fig. 1b, lane 1) and by RIPA of cell lysates labeled with [^{3}H]mannose (Fig. 1b, lane 2). The results revealed three bands comigrating with the 42-, 50-, and 82-kDa proteins, indicating the glycosylated nature of these proteins. This was further confirmed by deglycosylation experiments performed with [^{35}S]methionine-labeled viral proteins precipitated with

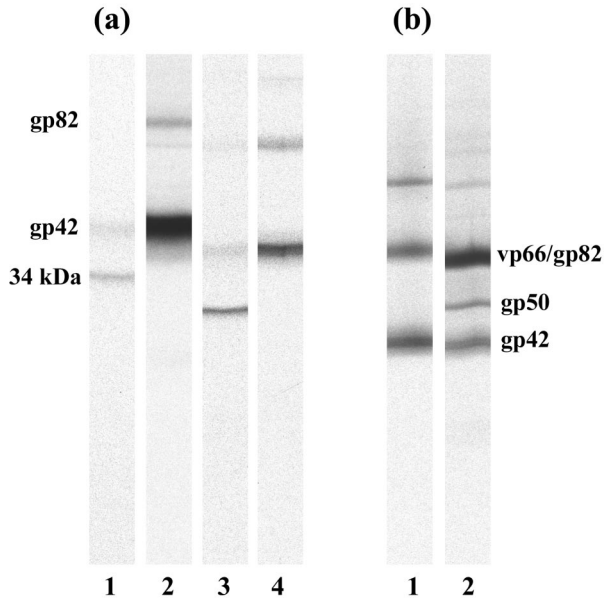

FIG. 2. (a) Effect of trypsin treatment of immunoprecipitated [^{35}S]methionine-labeled ISAV HA. Following treatment, proteins were resolved in SDS-12.5% polyacrylamide gels. Lanes: 1, trypsin treatment of proteins immunoprecipitated with an anti-HA MAb; 2, nontreated control of proteins in lane 1; 3, nonreduced sample of trypsin-treated proteins in lane 1; 4, nontreated control of proteins in lane 3. (b) SDS–8 to 18% polyacrylamide gels of nonreduced, non-heat-treated samples of the ISAV HA protein immunoprecipitated from [^{35}S]methionine-labeled ISAV cell lysate, demonstrating that the HA protein exists at least as dimers and probably as trimers (lane 1). Lane 2 is included for reference and contains proteins immunoprecipitated with a polyclonal anti-whole virus antibody.

the anti-ISAV PAb. The results of these experiments are shown in Fig. 1b, lane 4, and indicate that the deglycosylated gp50 has a molecular mass of 45 kDa while deglycosylated gp42 resulted in a wide band peaking at 35 kDa (range, 34 to 37 kDa). The protein band just below the 45-kDa band in Fig. 1b, lane 4, comigrated with a corresponding band in the control (Fig. 1b, lane 6) and was considered nonspecific.

Analysis of cell lysates labeled with inorganic ^{32}P revealed one major band comigrating with the 66-kDa major protein. (Fig. 1c, lane 1). Two minor bands were also found in the control preparations (Fig. 1c, lane 2), and thus the 66-kDa protein is the only major phosphorylated protein of the virion.

Trypsin treatment of proteins obtained by precipitation with the anti-HA MAb revealed that the gp42, as well as the gp82 also found by precipitation with this antibody, was almost completely digested, leaving one band at 34 kDa (Fig. 2a, lane 1), indicating that the HA could be subjected to proteolytic activation similar to that seen with influenza virus HA. However, when proteolytic activation of the influenza virus HA occurs, the two resulting proteins are bound together by S-S binding. To test whether this had happened during the trypsin digestion of the ISAV HA, nonreduced preparations were examined. The results revealed a digestion profile similar to that with reduced samples, indicating no S-S-binding (Fig. 2a, lane 3) and thus making the possibility of proteolytic activation of the HA less likely. The control in this experiment (Fig. 2a, lane 2) demonstrates, for the first time, that the anti-HA MAb binds to gp42.

Furthermore, in RIPA experiments with the anti-HA MAb examined in SDS–12% polyacrylamide gels, we also observed an 82-kDa glycoprotein. This protein was also seen, to a greater or less degree, in RIPA experiments with the anti-ISAV PAb. In addition, we also frequently observed a protein band in the interphase between the 5% stacking and 12% resolving gels. To find out whether these observations could be explained as a result of dimeric and trimeric HA, too tightly bound to be completely resolved by SDS-PAGE, we examined nonreduced, non-heat-treated samples of precipitated HA in an 8 to 18% gradient gel. The results are shown in Fig. 2b, lane 1, revealing three protein bands and thus suggesting that the ISAV HA exists at least as dimers and probably as trimers. It was also seen that the mass of gp82 relative to gp42 in these nonreduced samples had increased as measured by densitometry of scanned films, from approximately 1:5 to 1:2, further supporting this assumption.

Location of the proteins in the virion. Purified [^{35}S]methionine-labeled ISA virions were solubilized with 1% NP-40. Following ultracentrifugation of the detergent-treated virions through a sucrose layer, the supernatant and the pelleted fraction were recovered and analyzed by SDS-PAGE. The results are presented in Fig. 3a and show that this treatment solubilized gp42, gp50, and a major part of vp22 (Fig. 3a, lane 1), leaving a minor part of vp22 together with all of vp66 in the pelleted fraction (Fig. 3a, lane 2).

To demonstrate that the vp22 found in the pelleted fraction was similar to the vp22 found in the soluble fraction, the experiment was repeated and the two fractions were analyzed

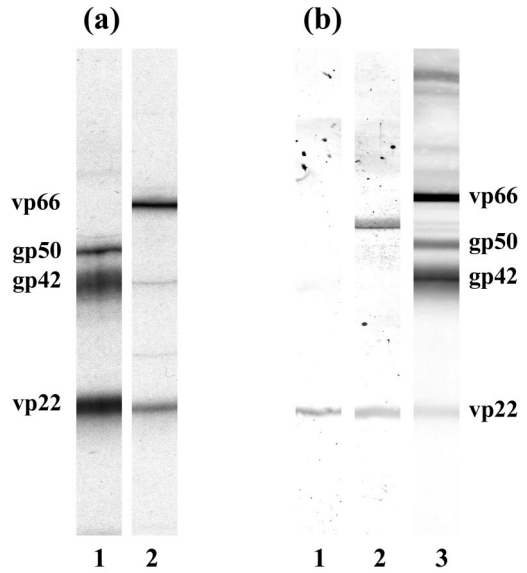

FIG. 3. Dissociation of ISAV with NP-40. [^{35}S]methionine-labeled virus was purified by sucrose gradient centrifugation, treated with 1% NP-40, loaded onto a 20% sucrose cushion, and centrifuged. The supernatant (lanes 1) and pellet (lanes 2) were then examined by SDS–12.5% PAGE. (a) Autoradiograms of the two fractions. (b) Western blot analysis of the two fractions stained with a PAb to recombinant vp22. Lane 3 is included for reference and contains purified virus stained with a polyclonal anti-whole virus antibody.

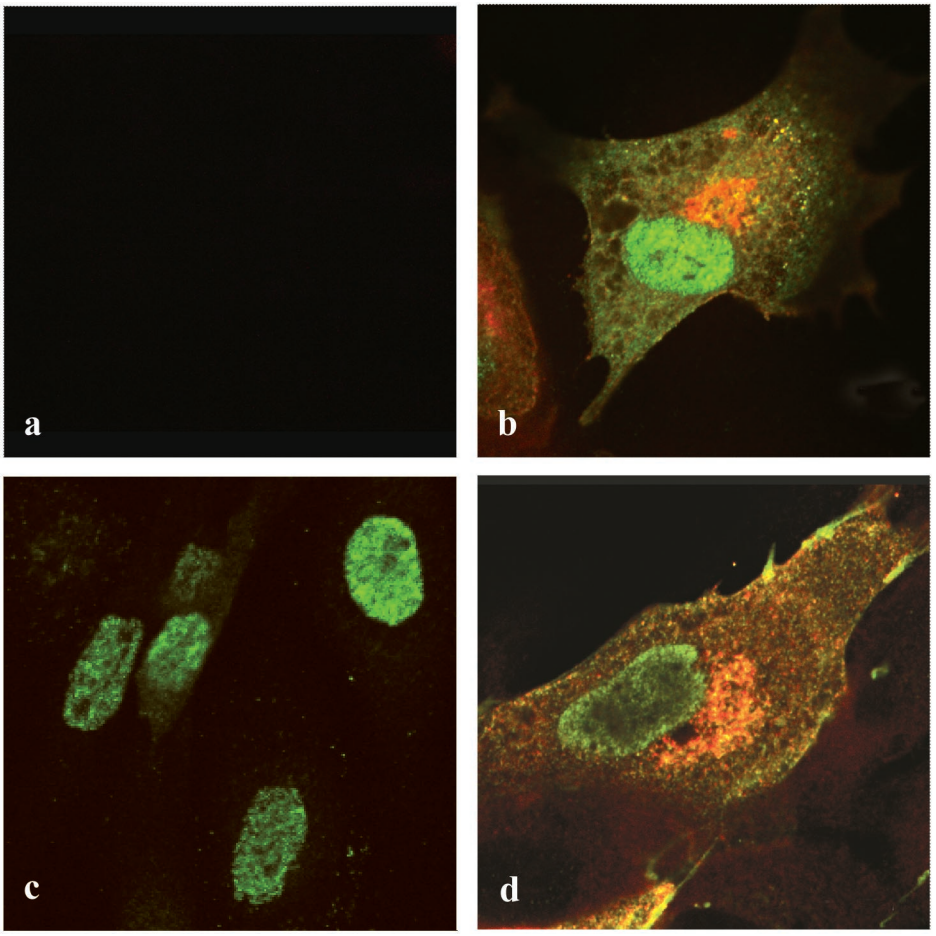

FIG. 4. Immunofluorescent staining of ISAV-infected ASK cells with PAbs to recombinant vp22 (green) (a and b) and whole virus (green) (c and d). All preparations were double stained with the anti-HA MAb (red). Neither vp22 nor HA was detected at 12 h p.i. (a and c), while virus protein was detected in the nucleus (c). At 24 h p.i., vp22 was detected in the nucleus (b), while HA was detected in the cytoplasm (b and d). The nuclear staining in panel d probably represents both the nucleoprotein and vp22.

by Western blotting with rabbit antibodies to a recombinant protein encoded by the first ORF of genome segment 8 (anti-rVp22 PAb), which was recently shown to be associated with vp22 (3). The results of this experiment are presented in Fig. 3b and show that this antibody detects vp22 both in the solubilized and in the pelleted fraction. An additional protein was detected in the pelleted fraction (Fig. 3b, lane 2); however, this protein did not colocalize with any of the ISAV proteins, as shown in the control preparation (Fig. 3b, lane 3). The most reasonable interpretation of these results is that the two glycoproteins in the soluble fraction are associated with the viral envelope; that the nonglycosylated vp22 found in both soluble and pelleted fractions is analogous to the M protein of influenza A, B, and C viruses; and that the vp66 found in the pelleted fraction is the NP.

To further confirm the identity of the suggested M protein, infected cell cultures on coverslips were fixed every 4 h and immunostained with the anti-rVp22 PAb. Parallel sections were stained with the anti-whole virus antibody (anti-ISAV PAb) in order to determine the relative time of appearance of the vp22. For reference purposes, the preparations were double stained with antibodies to the HA (anti-HA MAb). The results are presented in Fig. 4 and show that vp22 first appears in the nucleus as well as in the cytoplasm together with the HA at 24 h p.i. (Fig. 4b). In contrast, staining with the anti-whole virus antibody revealed an early protein in the nucleus, presumably the NP, at 12 h p.i. (Fig. 4c) The NP in other influenza viruses is known to be an early protein which initially accumulate in the nucleus (21). This demonstrates both that the vp22 accumulates in the nucleus during the infectious cycle and that vp22 and HA are late proteins.

Biological activities associated with the virus particle. To characterize hemagglutination and esterase activity, the two serine hydrolase inhibitors DFP and DCIC were tested both by HI, which showed an eventual lack of elution of the hemagglutination reaction, and by the pNPA test. The results of the HI experiments are presented in Fig. 5 and show that these inhibitors did not inhibit hemagglutination, while both DFP and DCIC inhibited elution from rabbit erythrocytes by the esterase at concentrations of as low as 0.1 mM and 12.5 μM, respectively. Similar results were obtained with horse and rainbow trout RBC. The inhibition experiments were further confirmed by testing the esterase inhibitors on purified virus and measuring esterase activity in solution by using the pNPA

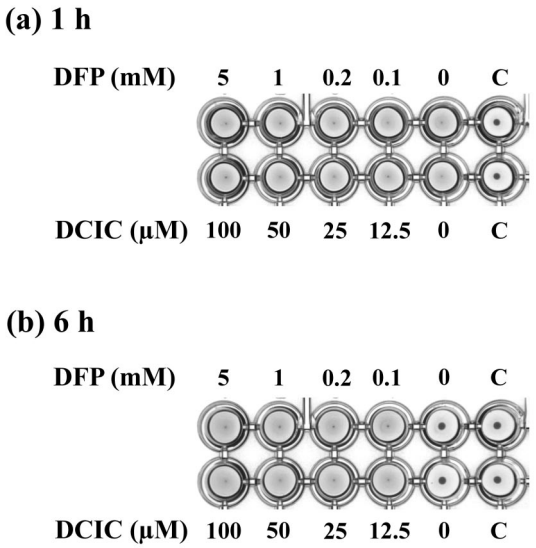

FIG. 5. Inhibition of virus elution by DFP and DCIC. Four HA units of virus was incubated with either 0.1 to 5 mM DFP or 12.5 to 100 μM DCIC, followed by addition of 0.75% rabbit RBC. Controls: 0, no inhibitor; C, no virus. (a) Incubation for 1 h, showing complete agglutination in all wells. (b) After 6 h of incubation, the agglutination had eluted in the control wells but not in wells containing esterase inhibitors.

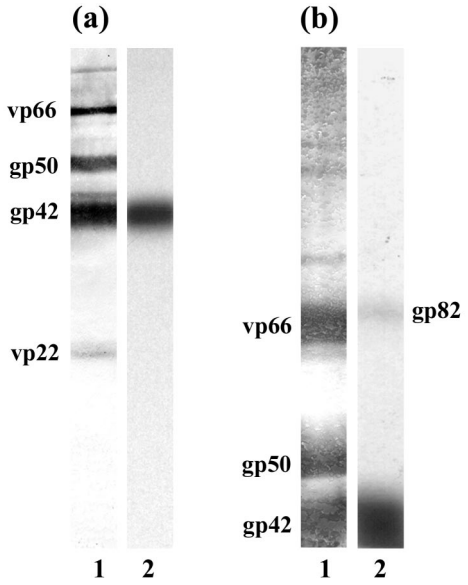

FIG. 6. Analysis of [1,3-^{3}H]DFP-labeled ISAV protein. Purified ISAV was incubated with [1,3-^{3}H]DFP for 1 h at room temperature, followed by an overnight incubation at 4°C. Viral proteins were analyzed by electrophoresis on a reducing SDS–12% polyacrylamide gel (a) or a nonreducing SDS–8% polyacrylamide gel (b). The gels were then cut into two pieces, and one part of each gel was blotted onto nitrocellulose and probed with ISAV-specific antiserum. The rest of the gel was incubated with Amplify (Amersham-Pharmacia), dried, and subjected to fluorography. Lanes: 1, Western blot; 2, [1,3-^{3}H]DFP.

esterase assay. The results revealed a similar inhibition of the esterase activity (data not shown).

To determine the location of the esterase activity, purified virus was incubated with [^{1,3}H]DFP, followed by SDS-PAGE analysis of reduced and nonreduced samples, followed by autoradiography. This approach was used earlier to identify the HE proteins of influenza C virus (25, 37) and of bovine coronavirus (36). When we incubated purified ISAV Glesvaer/2/90 with [1,3-^{3}H]DFP, we identified a single tritiated protein after SDS-PAGE and autoradiography. This protein comigrated with the 42-kDa HA protein, as shown by Western blot analysis (Fig. 6a). In nonreduced samples, an additional weak band was seen at 82 kDa, comigrating with the suggested dimeric HA (Fig. 6b). Since the viral esterase activity is inhibited by DFP, it appears likely that the labeled proteins represents the HA and the esterase.

In order to confirm these results, the ISAV HA protein was depleted from a Triton X-100 lysate of infected cells by using immunomagnetic beads coated with the anti-HA MAb. Following the first round of depletion, new antibody-coated beads were added to the original virus lysate in order to pick up any remaining HA protein. Altogether, three rounds were performed, and the lysate and beads were tested for esterase activity after each round by using the pNPA esterase assay. The results are presented in Table 1 and show that the esterase activity in the lysate decreased after each round, leaving the activity on the immunomagnetic beads, which confirms that the esterase activity is indeed located on the viral HA protein. Radioimmunoprecipitation of [^{35}S]methionine-labeled Triton X-100 cell lysates with the same coated beads was used to confirm that gp42, but not gp50, was precipitated by the beads, and the results were similar to those presented in Fig. 2a, lane 2.

These findings were also corroborated by a comparison of the amino acid sequence of the ISAV protein with the HEs of influenza C virus, group 2 coronaviruses, and Breda torovirus. As shown in Fig. 7A, substantial sequence similarities were observed with the E1 and E′ regions (31) of the influenza C virus esterase. Specifically the region around the active-site serine residue is conserved among all viral esterases. Amino acid sequences around the other residues of the catalytic triad are less well conserved. The putative active-site residues were detected at positions 32 (serine) (Fig. 7A) and 261 (aspartic acid) and 264 (histidine) (Fig. 7B) of the ISAV Glesvaer sequence. We found no substantial sequence similarities to the HAs of influenza A and B viruses. Our finding is consistent with the lack of esterase activity in those viruses. As demonstrated earlier by the structural analysis of the influenza C virus surface glycoprotein by Rosenthal et al. (31), the RDE domain is absent in the HA proteins of influenza A and B viruses.

TABLE 1. Repeated depletion of ISAV esterase from a cell lysate of ISAV-infected cells by using immunomagnetic beads coated with an anti-ISAV HA MAb

Precipitation	Esterase activity measured by pNPA assay in:	
	Lysate (mU)	Beads (absorbance[a])
Control	6.9	0
First round of depletion	2.3	0.52
Second round of depletion	1.2	0.33
Third round of depletion	0.3	0.03

[a] Only absorbance values were measured, as it was not possible to determine units in these samples.

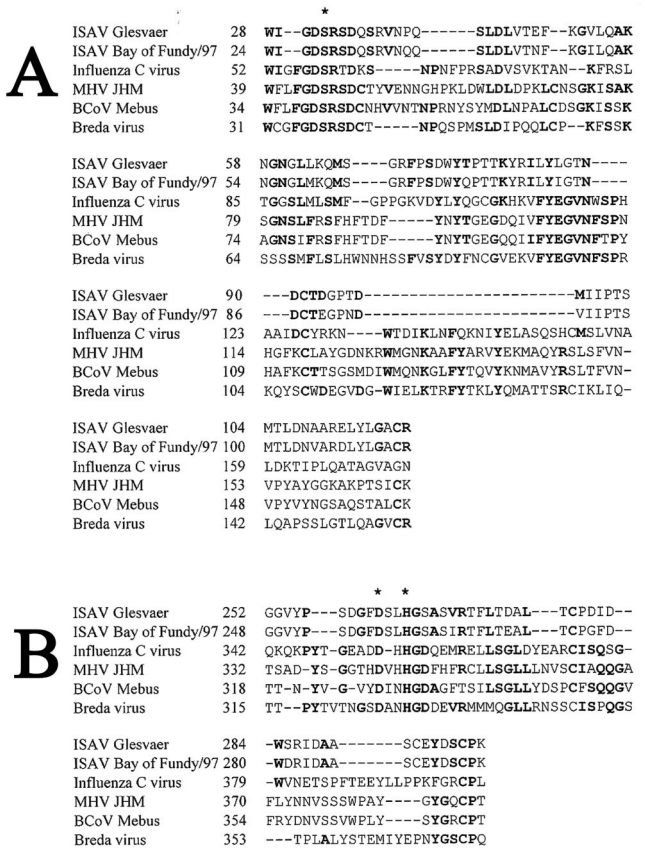

FIG. 7. Alignment of amino acid sequences around the active-site residues. The HA sequences of ISAV Glesvaer/2/90 and ISAV Bay of Fundy/97 were aligned by using the CLUSTAL algorithm with the sequences around the active-site serine residue (A) and Asp-352/His-355 (B) of the HE proteins of influenza C virus, mouse hepatitis virus strain JHM (MHV JHM), bovine coronavirus (BCoV) strain Mebus, and Breda torovirus. Amino acid residues identical to the consensus sequence are in boldface, and gaps are indicated by hyphens. Amino acid residues are numbered according to the GenBank entries. Active-site residues are marked by asterisks.

Instead of an esterase, those viruses possess a sialidase activity, which is encoded by the neuraminidase gene (21).

DISCUSSION

Virus purified by two independent methods revealed the same four major structural proteins that have been described earlier (12, 14). However, the estimated molecular masses, i.e., 22, 42, 50, and 66 kDa, differed slightly, probably due to the use of different molecular mass standards. Further, these new estimates are closer to the predicted molecular masses, which are 22.0, 42.4, 48.7, and 68.0 kDa, respectively (3, 6, 17). Metabolic labeling with tritiated mannose or with ^{32}P established that the 42- and 50-kDa proteins were glycosylated, while the 66-kDa protein was the only phosphorylated structural protein. The glycosylated nature of the gp42 and gp50 was further substantiated by lectin binding and deglycosylation experiments.

When purified virions were solubilized by NP-40 treatment followed by ultracentrifugation, the two glycoproteins and the nonglycosylated vp22 were recovered in the solubilized fraction. These results confirm that the two glycoproteins are surface proteins and also suggest that the nonglycosylated vp22 represents the ISAV M protein, analogous to the influenza virus M1 protein. The major protein in the pelleted fraction was the phosphorylated vp66, and there was also a minor fraction of vp22. Thus, vp66 represents the viral NP, which is the major part of the RNP complex, together with the viral RNA and the viral polymerases, in influenza viruses. Also, in influenza viruses this complex can be pelleted following solubilization. The finding of M protein in the pelleted fraction was not surprising, as complete separation of M1 from the RNP complex by using nonionic detergents is difficult to achieve and is dependent on NaCl concentration and pH in both orthomyxo- and paramyxoviruses (39). Attempts to demonstrate the effect of NaCl concentration and pH on solubilization were not successful, although indications that higher NaCl concentration promoted the separation of these proteins were observed (data not shown). The finding that vp66 represents the NP is supported by computer simulation studies of gene segment 3, which is thought to code for the vp66 (6, 29).

By immunofluorescence and confocal microscopy with an anti-vp22 immune serum, we were able to demonstrate that the putative ISAV M protein both accumulated in the nucleus and was a late protein. The M1 protein of the influenza viruses is the most abundant protein and has an important structural role in the influenza virus virion (21). It is located on the interior side of the lipid bilayer, forming a shell which surrounds the RNP complex. After entry of the virus through endosomal vesicles, the M1 protein undergoes a pH-dependent conformational change, resulting in release of the vRNPs into the cytoplasm. This is followed by vRNP import into the nucleus, where the viral genome is transcribed and replicated (21). In the course of the infection cycle, the M1 accumulates in the nucleus like the NP does, but in contrast to the NP, the M1 protein is a late protein, and it has been shown to inhibit viral transcription and may contribute to the shift of viral RNA synthesis towards replication in the late phase of infection (5, 21, 22). Furthermore, the nuclear accumulation of the M1 protein is a prerequisite for the nuclear export of newly synthesized vRNPs in the late phase of infection (23). Thus, based on the facts that the ISAV vp22 is the most abundant protein in the virion, that it is the only nonglycosylated soluble protein, and that it is a late protein that accumulates in the nucleus during the infectious cycle, we conclude that the vp22 is the ISAV M protein, analogous to the influenza virus M1 protein.

In ISAV we found only the NP protein to be phosphorylated. This was surprising, as previous studies have indicated major similarities between the ISAV and influenza virus structures and reproduction cycles (12, 32). In influenza A, B, and C viruses, both NP and M1 are phosphorylated, a property that it is thought to be associated with the active transport of these proteins in and out of the nucleus during the infection cycle (5, 27).

Previously, gp42 has been shown to hold the hemagglutinating activity and to be encoded by ISAV gene segment 6 (17, 28). Our findings further support this conclusion, showing the glycosylated nature of this protein, which it is solubilized by NP-40, and, by using RIPA, that the anti-ISAV HA MAb actually binds to gp42 (Fig. 2, lane 4). Both the RIPA using the anti-ISAV HA MAb with either [^{35}S]methionine-labeled or

[3H]mannose-labeled cell lysates and the [1,3-^{3}H]DFP-labeling experiment revealed a minor 82-kDa glycosylated protein. This 82-kDa glycoprotein had approximately twice the molecular mass of gp42, suggesting that it might be a dimer of gp42. When nonreduced, non-heat-treated samples were examined in an 8 to 18% gradient gel, the relative proportion of this protein increased and a third protein also was detected (Fig. 2b, lane 1). However, this possible trimeric form of gp42 was not detected in the [1,3-^{3}H]DFP-labeling experiment, which could be due to low sensitivity in this assay. Thus, the existence of a trimeric form of gp42 remains to be further documented.

In addition to the hemagglutinating activity, the surface glycoproteins of the influenza viruses exhibit RDE activity and fusion activity. Both of these activities have been detected in ISAV (9, 12); however, the localization of these activities has so far not been determined. Also, the RDE of ISAV has been suggested to be an acetylesterase different from that found in influenza C viruses (12). We demonstrated here that the ISAV RDE, but not hemagglutination, is inhibited by the serine hydrolase inhibitors DFP and DCIC, further supporting the idea that the ISAV RDE indeed is an acetylesterase. Both of these inhibitors have been shown to be potent inhibitors of the influenza C virus esterase (37).

In addition to influenza C viruses, several coronaviruses, including human and bovine coronavirus, hemagglutinating encephalomyelitis virus, mouse hepatitis virus, puffinosis coronavirus and sialodacryoadenitis virus, have also been shown to possess an esterase as the RDE (10, 35). All these viruses have a surface HE glycoprotein; i.e., both receptor binding and RDE activities are located on the same protein and they bind to cellular receptors, which contain O-acetylated sialic acids as the major receptor determinant. However, it should be noted that in coronaviruses the second surface glycoprotein, termed spike protein, is the major receptor-binding protein, whereas the coronavirus HE is a minor HA. On the other hand, both influenza A and B viruses, which also possess two surface structural glycoproteins, have hemagglutinating and fusion activities on one protein and RDE (a neuraminidase) activity on the other (21). We now present data showing that we have identified another HE protein in ISAV. By labeling purified ISAV with the serine hydrolase inhibitor [1,3-^{3}H]DFP, we detected one tritiated protein band on SDS-PAGE that comigrated with the viral HA. This finding was further confirmed by the demonstration of acetylesterase activity in preparations of affinity-purified viral HA. Finally, by comparing the amino acid sequence of the ISAV HA protein with those of the HEs of influenza C virus and several coronaviruses, substantial sequence similarities were observed. Studies of the three-dimensional structure of influenza C virus have revealed two different binding sites for O-acetylated sialic acids: the receptor-binding domain at the top of the trimeric molecule and the catalytic site, which is present at a position closer to the viral membrane. The active site is built by a catalytic triad composed of a serine residue, a histidine residue, and an aspartic acid residue, located at positions 57, 352, and 355, respectively (30). In ISAV strain Glesvaer/2/90, these residues were identified at positions 32, 261, and 264, respectively. Thus, in analogy to the HEs of influenza C virus and coronaviruses, it is proposed that the ISAV protein be renamed HE protein.

Data suggesting proteolytic activation of ISAV by trypsin treatment during replication in cell cultures have previously been presented (12). In the present work, trypsin treatment of immunoprecipitated gp42 followed by SDS-PAGE analysis revealed a 35-kDa breakdown product, suggesting that this protein could be subjected to proteolytic activation. However, examination of nonreduced samples revealed the same results, indicating no S-S binding of the cleaved products, and therefore it is not likely that gp42 is subjected to proteolytic activation. In the influenza viruses, HA or HE is synthesized as a precursor, which upon cleavage activation generates the two subunits, the HA_1 (or HE_1) and the N terminus of HA_2 (or HE_2) bound together by an S-S bridge. This cleavage primes the HA or HE for activation of its fusion activity and is required for the viruses to be infectious (21). The function of the gp50 surface glycoprotein is currently not known. Based on the fact that the hemagglutinating and esterase activities are associated with gp42, it is tempting to suggest that this protein holds the fusion activity. However, no documentation or indications supporting such an assumption have so far been presented, and hence this question remains to be resolved. In summary, we provide experimental evidence that the ISAV vp66 represents the phosphorylated NP, the gp42 is the viral HE, and the vp22 represents the analogue to the influenza virus M protein.

ACKNOWLEDGMENTS

We thank Hilde Welde and Ulrike Vilas for technical assistance, Ducan Colquhoun for proofreading, and Intervet Norbio for supplying recombinant proteins for immunization of rabbits.

This study was funded by grants 128044/103 and 146845/120 from the Norwegian Research Council, by project P 14104-Med from the Austrian Science Fund, and by Intervet International.

REFERENCES

1. **Anonymous.** 2003. Infectious salmon anaemia, p. 152–161. *In* OIE manual of diagnostic tests for aquatic animals. Office International des Epizooties, Paris, France.
2. **Anonymous.** 2003. Infectious salmon anaemia in the Faroe Islands. Dis. Infect. (O. I. E.) **14:**60.
3. **Biering, E., K. Falk, E. Hoel, J. Thevarajan, M. Joerink, A. Nylund, C. Endresen, and B. Krossoy.** 2002. Segment 8 encodes a structural protein of infectious salmon anaemia virus (ISAV); the colinear transcript from segment 7 probably encodes a non-structural or minor structural protein. Dis. Aquat. Org. **49:**117–122.
4. **Bouchard, D. A., K. Brockway, C. Giray, W. Keleher, and P. L. Merrill.** 2001. First report of infectious salmon anemia (ISA) in the United States. Bull. Eur. Assoc. Fish Pathol. **21:**86–88.
5. **Bui, M., E. G. Wills, A. Halenius, and G. R. Whittaker.** 2000. Role of the influenza virus M1 protein in nuclear export of viral ribonucleoproteins. J. Virol. **74:**1781–1786.
6. **Clouthier, S. C., T. Rector, N. E. C. Brown, and E. D. Anderson.** 2002. Genomic organization of infectious salmon anaemia virus. J. Gen. Virol. **83:**421–428.
7. **Dannevig, B. H., K. Falk, and E. Namork.** 1995. Isolation of the causal virus of infectious salmon anaemia (ISA) in a long-term cell line from Atlantic salmon head kidney. J. Gen. Virol. **76:**1353–1359.
8. **Devold, M., B. Krossoy, V. Aspehaug, and A. Nylund.** 2000. Use of RT-PCR for diagnosis of infectious salmon anaemia virus (ISAV) in carrier sea trout Salmo trutta after experimental infection. Dis. Aquat. Org. **40:**9–18.
9. **Eliassen, T. M., M. K. Froystad, B. H. Dannevig, M. Jankowska, A. Brech, K. Falk, K. Romoren, and T. Gjoen.** 2000. Initial events in infectious salmon anemia virus infection: evidence for the requirement of a low-pH step. J. Virol. **74:**218–227.
10. **Enjuanes, L., D. A. Brian, D. Cavanagh, K. V. Holmes, M. M. C. Lai, H. Laude, P. S. Masters, P. Rottier, S. Siddell, W. Spaan, F. Taguchi, and P. J. Talbot.** 2000. Nidovirales, p. 827–857. *In* M. H. V. van Regenmortel, C. M. Fauquet, and D. H. L. Bishop (ed.), Virus taxonomy. Classification and nomenclature of Viruses. Seventh report of the International Committee on Taxonomy of Viruses. Academic Press, San Diego, Calif.
11. **Falk, K., E. Namork, and B. H. Dannevig.** 1998. Characterization and ap-

plications of a monoclonal antibody against infectious salmon anaemia virus. Dis. Aquat. Org. **34:**77–85.
12. **Falk, K., E. Namork, E. Rimstad, S. Mjaaland, and B. H. Dannevig.** 1997. Characterization of infectious salmon anemia virus, an orthomyxo-like virus isolated from Atlantic salmon (*Salmo salar* L.). J. Virol. **71:**9016–9023.
12a. **Hellebø, A., U. Vilas, K. Falk, and R. Vlasak.** 2004. Infectious salmon anemia virus specifically binds to and hydrolyzes 4-O-acetylated sialic acids. J. Virol. **78:**3055–3062.
13. **Kibenge, F. S. B., O. N. Garate, G. Johnson, R. Arriagada, M. J. T. Kibenge, and D. Wadowska.** 2001. Isolation and identification of infectious salmon anaemia virus (ISAV) from Coho salmon in Chile. Dis. Aquat. Org. **45:**9–18.
14. **Kibenge, F. S. B., J. R. Lyaku, D. Rainnie, and K. L. Hammell.** 2000. Growth of infectious salmon anaemia virus in CHSE-214 cells and evidence for phenotypic differences between virus strains. J. Gen. Virol. **81:**143–150.
15. **Kibenge, F. S. B., S. K. Whyte, K. L. Hammell, D. Rainnie, M. T. Kibenge, and C. K. Martin.** 2000. A dual infection of infectious salmon anaemia (ISA) virus and a togavirus-like virus in ISA of Atlantic salmon Salmo salar in New Brunswick, Canada. Dis. Aquat. Org. **42:**11–15.
16. **Klausegger, A., B. Strobl, G. Regl, A. Kaser, W. Luytjes, and R. Vlasak.** 1999. Identification of a coronavirus hemagglutinin-esterase with a substrate specificity different from those of influenza C virus and bovine coronavirus. J. Virol. **73:**3737–3743.
17. **Krossoy, B., M. Devold, L. Sanders, P. M. Knappskog, V. Aspehaug, K. Falk, A. Nylund, S. Koumans, C. Endresen, and E. Biering.** 2001. Cloning and identification of the infectious salmon anaemia virus haemagglutinin. J. Gen. Virol. **82:**1757–1765.
18. **Krossoy, B., I. Hordvik, F. Nilsen, A. Nylund, and C. Endresen.** 1999. The putative polymerase sequence of infectious salmon anemia virus suggests a new genus within the *Orthomyxoviridae*. J. Virol. **73:**2136–2142.
19. **Krossoy, B., F. Nilsen, K. Falk, C. Endresen, and A. Nylund.** 2001. Phylogenetic analysis of infectious salmon anaemia virus isolates from Norway, Canada and Scotland. Dis. Aquat. Org. **44:**1–6.
20. **Laemmli, U. K.** 1970. Cleavage of structural proteins during the assembly of the head of bacteriophage T4. Nature **227:**680–685.
21. **Lamb, R. A., and R. M. Krug.** 2001. *Orthomyxoviridae*: the viruses and their replication, p. 1487–1579. *In* B. N. Fields, D. M. Knipe, P. M. V. Howley, and D. E. Griffin (ed.), Field's virology, 4th ed. Lippincott Williams & Wilkins, New York, N.Y.
22. **Martin, K., and A. Helenius.** 1991. Nuclear transport of influenza virus ribonucleoproteins: the viral matrix protein (M1) promotes export and inhibits import. Cell **67:**117–130.
23. **Martin, K., and A. Helenius.** 1991. Transport of incoming influenza virus nucleocapsids into the nucleus. J. Virol. **65:**232–244.
24. **Mjaaland, S., E. Rimstad, K. Falk, and B. H. Dannevig.** 1997. Genomic characterization of the virus causing infectious salmon anemia in Atlantic salmon (*Salmo salar* L.): An orthomyxo-like virus in a teleost. J. Virol. **71:**7681–7686.
25. **Muchmore, E. A., and A. Varki.** 1987. Selective inactivation of influenza C esterase: a probe for detecting 9-O-acetylated sialic acids. Science **236:**1293–1295.
26. **Mullins, J., D. Groman, and D. Wadowska.** 1998. Infectious salmon anemia in salt water Atlantic salmon (*Salmo salar* L.) in New Brunswick, Canada. Bull. Eur. Assoc. Fish Pathol **18:**110–114.
27. **Neumann, G., M. R. Castrucci, and Y. Kawaoka.** 1997. Nuclear import and export of influenza virus nucleoprotein. J. Virol. **71:**9700.
28. **Rimstad, E., S. Mjaaland, M. Snow, A. B. Mikalsen, and C. O. Cunningham.** 2001. Characterization of the infectious salmon anemia virus genomic segment that encodes the putative hemagglutinin. J. Virol. **75:**5352–5356.
29. **Ritchie, R. J., J. Heppell, M. B. Cook, S. Jones, and S. G. Griffiths.** 2001. Identification and characterization of segments 3 and 4 of the ISAV genome. Virus Genes **22:**289–297.
30. **Rodger, H. D., T. Turnbull, F. Muir, S. Millar, and R. H. Richards.** 1998. Infectious salmon anaemia (ISA) in the United Kingdom. Bull. Eur. Assoc. Fish Pathol. **18:**115–116.
31. **Rosenthal, P. B., X. Zhang, F. Formanowski, W. Fitz, C. H. Wong, H. Meier-Ewert, J. J. Skehel, and D. C. Wiley.** 1998. Structure of the haemagglutinin-esterase-fusion glycoprotein of influenza C virus. Nature **396:**92–96.
32. **Sandvik, T., E. Rimstad, and S. Mjaaland.** 2000. The viral RNA 3′- and 5′-end structure and mRNA transcription of infectious salmon anaemia virus resemble those of influenza viruses. Arch. Virol. **145:**1659–1669.
33. **Snow, M., R. Ritchie, O. Arnaud, S. Villoing, V. Aspehaug, and C. O. Cunningham.** 2003. Isolation and characterisation of segment 1 of the infectious salmon anaemia virus genome. Virus Res. **92:**99–105.
34. **Thorud, K. E., and H. O. Djupvik.** 1988. Infectious anaemia in Atlantic salmon (*Salmo salar* L.). Bull. Eur. Assoc. Fish Pathol. **8:**109–111.
35. **Vlasak, R., M. Krystal, M. Nacht, and P. Palese.** 1987. The influenza-C virus glycoprotein (He) exhibits receptor-binding (hemagglutinin) and receptor-destroying (esterase) activities. Virology **160:**419–425.
36. **Vlasak, R., W. Luytjes, J. Leider, W. Spaan, and P. Palese.** 1988. The E3 protein of bovine coronavirus is a receptor-destroying enzyme with acetylesterase activity. J. Virol. **62:**4686–4690.
37. **Vlasak, R., T. Muster, A. M. Lauro, J. C. Powers, and P. Palese.** 1989. Influenza C virus esterase: analysis of catalytic site, inhibition, and possible function. J. Virol. **63:**2056–2062.
38. **Wurzer, W. J., K. Obojes, and R. Vlasak.** 2002. The sialate-4-O-acetylesterases of coronaviruses related to mouse hepatitis virus: a proposal to reorganize group 2 Coronaviridae. J. Gen. Virol. **83:**395–402.
39. **Zhirnov, O. P., and V. B. Grigoriev.** 1994. Disassembly of influenza C viruses, distinct from that of influenza A and B viruses requires neutral-alkaline pH. Virology **200:**291.

Paper II

Available online at www.sciencedirect.com
SCIENCE DIRECT®
Virus Research 106 (2004) 51–60
Virus Research
www.elsevier.com/locate/virusres

Infectious salmon anemia virus (ISAV) genomic segment 3 encodes the viral nucleoprotein (NP), an RNA-binding protein with two monopartite nuclear localization signals (NLS)☆

Vidar Aspehaug[a,b], Knut Falk[b], Bjørn Krossøy[c], Jegatheswaran Thevarajan[c], Lisette Sanders[d], Lindsey Moore[e], Curt Endresen[a], Eirik Biering[c,*]

[a] *Department of Biology, University of Bergen, Bergen, Norway*
[b] *Section for Fish Health, National Veterinary Institute, Oslo, Norway*
[c] *Intervet Norbio, Thormohlensgt. 55 Bergen, 5020 Norway*
[d] *Intervet International BV, Boxmeer, The Netherlands*
[e] *Department of Microbiology and Immunology, Centre for Research in Virology, The Gade Institute, Bergen, Norway*

Received 11 February 2004; received in revised form 4 June 2004; accepted 4 June 2004
Available online 5 August 2004

Abstract

Infectious salmon anemia virus (ISAV) is the type species of the genus *Isavirus* belonging to the Orthomyxoviridae, and causes serious disease in Atlantic salmon (*Salmo salar*). This study presents the expression and functional analysis of the ISAV genome segment 3, and provides further evidence that it encodes the viral nucleoprotein (NP). The encoded protein was expressed in a baculovirus system, and Western blot analysis showed that it corresponds to the 66–71 kDa structural protein previously found in purified ISAV preparations. RNA-binding activity was established by the interaction of viral and recombinant NP with single-stranded RNA transcribed in vitro. Immunofluorescence studies of infected cells showed the ISAV NP to be an early protein. It locates to the nucleus of infected cells before it is transported to the cytoplasm prior to virus assembly. A similar localization pattern was observed in cells transfected with the NP gene, confirming that the encoded protein has an intrinsic ability to be imported into the nucleus. Two monopartite nuclear localization signals (NLS) at amino acids ^{230}RPKR^{233} and ^{473}KPKK^{476} were identified by computer analysis, and validated by site-directed mutagenesis. In contrast to other orthomyxovirus-NPs, that have several NLSs that function independent of each other, both NLSs had to be present for the ISAV NP protein to be transported into the nucleus, indicating that these motifs cooperate to target the protein to the nucleus.

Keywords: ISAV; Isavirus; Orthomyxoviridae; Nucleoprotein; NP

1. Introduction

Infectious salmon anemia virus (ISAV) is a pathogen of Atlantic salmon (*Salmo salar*) in Norway, Scotland, the Faeroe Islands, Canada, and the United States (Lovely et al., 1999; Mullins et al., 1998; Rodger and Richards, 1998; Schyth et al., 2003; Thorud and Djupvik, 1988). The virus has also been isolated from Coho salmon (*Oncorhynchus kisutch)* in Chile (Kibenge et al., 2001). ISAV is the type species of the genus *Isavirus* belonging to the Orthomyxoviridae (ICTV index of viruses, http://www.ncbi.nlm.nih.gov/ICTVdb/Ictv/index.htm), and shares several properties with the influenza viruses, including genetic as well as biochemical, physiochemical, and morphological properties (Eliassen et al., 2000; Falk et al., 1997; Koren and Nylund, 1997; Krossøy et al., 2001a, 1999; Mjaaland et al., 1997; Sandvik et al., 2000). The ISAV genome is composed of eight negative sense, single stranded

☆ Note: GenBank accession number: AX137949.
* Corresponding author. Tel.: +47 55 54 37 63; fax: +47 55 96 01 35.
E-mail address: eirik.biering@intervet.com (E. Biering).

0168-1702/$ – see front matter © 2004 Elsevier B.V. All rights reserved.
doi:10.1016/j.virusres.2004.06.001

(ss) RNA segments, and nucleotide sequences of all segments have been published (Biering et al., 2002; Clouthier et al., 2002; Krossøy et al., 2001a, 1999; Mjaaland et al., 1997; Rimstad et al., 2001; Ritchie et al., 2001; Snow and Cunningham, 2001; Snow et al., 2003). Segment 2 encodes the polymerase basic protein 1 (PB1) as evident by the presence of polymerase motifs characteristic to all viral RNA-dependent RNA-polymerases. The coding assignments of the remaining genomic segments needs to be elucidated by functional studies, since they do not show significant sequence homology to other known genes, neither at the nucleotide nor at the amino acid (aa) level.

Four major structural proteins with estimated molecular weights (MW) of 22–24, 42–43, 50–53, and 66–71 kDa have been detected in purified ISAV particles (Falk et al., 2004, 1997; Kibenge et al., 2000). The estimated molecular masses of these proteins differ slightly in the literature, probably due to differences in experimental conditions, but 22, 42, 50, and 66 kDa will be used in the following.

The 22 kDa protein has been linked to one of the two open reading frames (ORF) of segment 8 (Biering et al., 2002), and was recently suggested to represent the matrix protein (Falk et al., 2004). Several studies has established that the 42 kDa protein is encoded by segment 6, and that it is a viral hemagglutinin-esterase (HE) (Clouthier et al., 2002; Falk et al., 2004, 1998; Griffiths et al., 2001; Hellebø et al., 2004; Krossøy et al., 2001a; Rimstad et al., 2001), and Clouthier et al. (2002) determined the 50 kDa protein to be encoded by segment 5, but the function of this protein remains to be elucidated.

Three separate studies have reported the cloning of a cDNA sequence corresponding to genomic segment 3 of the ISAV (Clouthier et al., 2002; Ritchie et al., 2001; Snow and Cunningham, 2001), and they suggest that this sequence encodes the NP. These studies also suggested an RNA-binding domain in the putative protein, based on computer simulations of the physicochemical nature of the aa residues in the region, and on aa alignments with the RNA-binding domain of the NP from influenza A and B. The region is however not well conserved between influenza and ISAV. All viruses with negative sense RNA genomes encode a NP which binds ss RNA. In orthomyxoviruses, the NP is the major structural protein that interacts with the RNA segments (Lamb and Krug, 1996), and its primary function is to encapsidate the virus genome to facilitate RNA transcription, replication, and packaging (Portela and Digard, 2002). Along with the polymerase proteins (PB1, PB2, and PA) and viral RNA, the NP forms viral ribonucleoprotein (RNP) complexes that represent the minimal components required for transcription and replication of viral RNA (Huang et al., 1990; Lamb and Krug, 1996; Lee et al., 2002). Similar RNP-like particles appearing as right-handed double helices have been observed in electron microscopy studies of purified, lysed ISAV preparations (Falk et al., 1997). Also, immunofluorescence staining of ISAV infected cells using a polyclonal antibody prepared against purified whole virus indicates that the ISAV pursue a nuclear replication strategy similar to the influenza viruses (Falk et al., 1997), and nuclear localization signals (NLS) have been suggested in the putative NP (Rimstad and Mjaaland, 2002). Recently, we demonstrated that the 66 kDa protein is a phosphorylated protein associated with the internal structures of the virus particle (Falk et al., 2004), supporting that it represents the viral NP. The present study was undertaken to verify that the ISAV genomic segment 3 encodes the 66 kDa protein, and to provide further evidence that this is the viral NP. We have shown experimentally that the encoded protein exhibit the general characteristics described for NPs of the influenza viruses. Transfection experiments showed that the NP localized to the nucleus in the absence of other viral proteins, indicating the presence of at least one functional NLS within the protein. This was substantiated by mutation studies, and two cooperating monopartite NLSs were identified.

2. Materials and methods

2.1. Virus and cells

Two virus isolates were used in this study. The cloning was performed using a virus strain isolated by Krossøy et al. (2001b), designated Bremnes/98. Unless otherwise is stated, other assays were performed using the ISAV strain isolated by Dannevig et al. (1995), designated Glesvær/2/90. Virus stocks were prepared in salmon head kidney (SHK-1) cells (Dannevig et al., 1995), and all assays were performed with fourth or fifth passages of the virus. Functional assays were performed using Atlantic salmon kidney (ASK) cells (Devold et al., 2000). Infections were performed as reported by Falk et al. (1997). Chinook salmon embryo cells (CHSE-214) (Lannan et al., 1984), plated on glass coverslips at 50–70% confluency 12–24 h (h) earlier, were used for transfection. All cell types were grown as previously described. Cell lysates were prepared 4 days post infection (p.i.) in TNE buffer (10 mM Tris–HCl [pH 7.4], 100 mM NaCl, 1 mM EDTA) with 1% NP-40 (lysis buffer). Insoluble debris was removed by centrifugation at 20,000 × *g* for 20 min at 4 °C. Lysates were stored at −80 °C until used.

Sf9 cells grown in suspension culture were infected with baculovirus at 28 °C and harvested 5 days p.i. by centrifugation at 750 × *g* for 20 min at 4 °C. The cell pellet was resuspended in lysis buffer, and used for immunization and functional assays.

Radiolabelled cell lysates of ISAV- or mock-infected ASK cells were prepared by incubating cells grown in 25 cm^2 tissue culture flasks with 350 μCi of [^{35}S]methionine (Amersham Biosciences) in 2.5 ml methionine free DMEM. At 4 days p.i., the cells were washed twice with 10 mM phosphate buffered saline [pH 7.4] (PBS) and lysed on ice for 15 min in lysis buffer. Radiolabelled cell lysates of Sf9 cells were prepared by adding 350 μCi of [^{35}S]methionine (Pro-Mix; Amersham Biosciences) directly to a 10 ml suspension culture at 48 h

p.i., followed by incubation another 48 h at 28 °C. The cells were washed twice with PBS by centrifugation at 750 × *g* for 10 min at 4 °C, and lysed on ice for 15 min in lysis buffer. Insoluble debris was removed by centrifugation at 20,000 × *g* for 20 min at 4 °C. Lysates were stored at −80 °C until used.

Purified ISAV preparations were made by sucrose gradient centrifugation as described previously (Falk et al., 1997). ISAV infectivity was determined by endpoint titration in 96-well culture plates, using an immunofluorescence assay as published by Falk et al. (1997).

2.2. Cloning, sequencing, and sequence analysis

A unidirectional cDNA library from ISAV infected ASK cells was constructed in bacteriophage Lambda as previously described (Krossøy et al., 2001a), and a clone designated 1H was identified by immunoscreening with a polyclonal anti-ISAV rabbit serum (ISAV-PAb2, see below) using the picoBlue immunoscreening kit (Stratagene). The pBlueScript plasmid containing the 1H sequence was excised by use of the ExAssist helper phage and the SOLR strain of *Escherichia coli* (Stratagene). Complete sequencing was performed on the isolated plasmid. To obtain a full-length cDNA sequence, 5′ RACE was performed with the 5′ RACE system, version 2.0 (Life Technologies). RACE products were cloned into the pCR 2.1-TOPO vector using the TOPO TA cloning kit (Invitrogen) and sequenced. For sequencing, the BigDye terminator sequencing kit (PE Biosystems) and an ABI 377 DNA analyzer (PE Biosystems) were used. Sequences were assembled with the Sequencher software (Gene Codes Corporation), and GeneBank searches were performed with BLAST (http://www.ncbi.nlm.nih.gov/BLAST/). ProtParam tool (http://us.expasy.org/tools/protparam.html) was used to calculate the p*I* and theoretical MW of the full length protein and the C-terminal 30 residues. The predicted aa sequence was analyzed for NLSs using PSORT (http://psort.nibb.ac.jp/).

2.3. Baculovirus expression of 1H cDNA

1H cDNA was amplified using primers 5′-cgggatccatggccgataaaggtatgac-3′ and 5′-ggggtacctgcagtttcaaatgtcagtgtc-3′ and cloned into the pFastBac1 vector (Life Technologies) using the *Bam*HI and *Kpn*I restriction enzymes (Promega). The construct was transformed into TOP 10 cells (Invitrogen) and the isolated plasmids were used to transform DH10Bac competent cells (Life Technologies). Recombinant baculovirus was constructed according to Life Technologies' recommendations.

2.4. Antisera

Antiserum against peptides derived from the 1H sequence (anti-pep1H) were prepared by Eurogentec (Belgium) using the peptides SRPKRSDYRKGQGSKC and CIEFDEDDQEEEDTDI coupled to keyhole limpet haemocyanin. The conjugated peptides were pooled and injected in two rabbits according to Eurogentec's procedures. An antiserum against the baculovirus expressed 1H protein (anti-1H) was prepared by immunizing a rabbit four times with four weeks intervals using approximately 200 μg protein from a crude lysate of Sf9 cells infected with 1H-recombinant baculovirus.

Two polyclonal antisera prepared against whole ISAV, ISAV-PAb1 (Falk and Dannevig, 1995), and ISAV-PAb2 (Krossøy et al., 2001a), and a monoclonal antiserum directed against the ISAV HE, anti-HE MAb (Falk et al., 1998), were also used in this study. All polyclonal antisera were adsorbed by incubation on monolayers of acetone fixed ASK cells prior to use.

2.5. SDS–PAGE and Western blot (WB) analysis

Purified ISAV and lysates of Sf9 cells were resolved by SDS–PAGE and transferred to a nitrocellulose membrane as previously described (Krossøy et al., 2001a). The membrane was treated with blocking solution (PBS, 0.1% Tween-20, 5% non-fat dry milk, 0.01% anti-foam A (Sigma)) overnight at 4 °C followed by a 1 h incubation with the primary rabbit immune serum. The membrane was then washed three times in blocking solution and incubated with goat anti-rabbit horseradish peroxidase (HRP) conjugate (AMDEX: Amersham Biosciences) for 1 h at room temperature (RT). Diaminobenzidine was used as a color reagent for detection of bound HRP-conjugate (Sigma).

2.6. Affinity purification/radioimmune precipitation assay (RIPA)

Anti-rabbit IgG-conjugated immunomagnetic beads (Dynabeads M-280; Dynal, Norway) were incubated with rabbit immune serum in PBS for 1 h, followed by washing with RIPA-buffer (PBS, 1% Triton X-100, 1 mg/mL BSA, 1% sodium deoxycholate, 0.5 M lithium chloride, 0.1% SDS). Coated beads were incubated with the cell lysates for 1 h in RIPA-buffer, and washed two times in RIPA-buffer followed by washing in PBS and 50 mM Tris–HCl [pH 6.8]. Beads were then either analyzed by SDS–PAGE followed by autoradiography to confirm the purity of the protein preparations, or used in the RNA-binding assay described below.

2.7. RNA-binding assay

^{32}P-labeled RNA was made by using a full length clone of the ISAV HE gene in the pVAX1 vector (Invitrogen), which was linearized using *Bam*HI (Promega). One μg linearized DNA template was transcribed into RNA with T7 RNA polymerase using an RNA transcription kit (Stratagene). The RNA was transcribed in the presence of 50 μCi ^{32}P-rUTP (Amersham Biosciences), giving a labeled product of 294 bases of positive sense, of which approximately 100 bases originated from the vector sequence. Dynabeads

with bound protein were washed three times in RNAse-free PBS, and incubated with the ^{32}P-labeled RNA for 15 min at rt. Unbound RNA was removed by washing three times in RNAse-free 10 mM Tris–HCl [pH 8.0]. The Dynabeads were dotted onto nitrocellulose membranes which were dried and exposed to a Kodak BioMax MS film for 7 days at −80 °C.

2.8. Immunofluorescence

Coverslips with attached cells were washed in PBS and fixed with 3.7% formaldehyde in PBS for 20 min, rinsed in PBS, and subsequently permeabilized with 0.2% Triton X-100 in PBS for 30 min followed by blocking in 5% non-fat dry milk in PBS for 30 min. The cells were incubated with the primary antibodies diluted in 2.5% non-fat dry milk in PBS for 1 h and washed in PBS. Bound antibodies were detected using goat anti-mouse FITC or goat anti-rabbit FITC (Southern Biotechnology Associates Inc.). In double labeling experiments, rabbit antibodies were detected using goat anti-rabbit biotin (VECTOR) visualized by a Neutralite Avidin-Texas red (Southern Biotechnology Associates Inc.). After washing, the cells were mounted with SlowFade antifade kit (Molecular Probes) and examined in a confocal microscope (Leica, TCS-SP).

2.9. NLS mutation and transfection

The ORF of the 1H-gene was amplified by PCR using primers 5′-ggggtaccatggccgataaaggtatgac-3′ and 5′-ccgctcgagtgcagtttcaaatgtcagtgtc-3′, and cloned into the *Kpn*I and *Xho*I sites of the pVAX1 vector (Invitrogen). The construct was designated 1H-pVAX1. Two putative NLSs (designated NLS1 and NLS2) were subjected to mutagenesis. The ^{230}RPKR^{233} motif in NLS1 was mutated to AAAA by use of primers 5′-gctttcagacagagcgcagccgcagcgtcagactacaggaaag-3′ and 5′-ctttcctgtagtctgacgctgcggctgcgctctgtctgaaagc-3′, and the ^{473}KPKK^{476} motif in NLS2 was mutated to AAAA by use of primers 5′-caaggcaaacacaaccgcagccgcggcggactcaacatacac-3′ and 5′-gtgtatgttgagtccgccgcggctgcggttgtgtttgccttg-3′. Both mutations were performed with the QuickChange XL site-directed mutagenesis kit (Stratagene), and the resulting constructs were designated 1H-pVAX1-ΔNLS1 and 1H-pVAX1-ΔNLS2, respectively. In order to generate the double mutant 1H-pVAX1-ΔNLS1ΔNLS2, the ^{230}RPKR^{233} motif in the NLS1 region

Fig. 1. Alignment of three isolates of the ISAV segment 3 indicating the putative RNA-binding region (underlined) and the NLSs (shaded gray). The acid region in the C-terminal is framed. The isolates are Bremnes/98 (accession no. AX137949), Scotland (accession no. AJ276858) and Canada (accession no. AF306549).

of 1H-pVAX1-ΔNLS2 was mutated to AAAA by use of primers 5′-gctttcagacagagcgcagccgcagcgtcagactacaggaaag-3′ and 5′-ctttcctgtagtctgacgctgcggctgcgctctgtctgaaagc-3′. All constructs were sequenced. Transfections were performed in 24-well plates on CHSE-214 cells using the FuGENE 6 transfection reagent (Roche Diagnostics). Transfected cells were analyzed by immunofluorescence using the anti-1H antisera. ASK and SHK-1 cells were also transfected with the above mentioned constructs to confirm that the localization did not vary with cell type, and although transfected cells were observed, the transfection efficacy proved very low. This is a very common problem with some fish cell systems.

3. Results

3.1. ISAV segment 3 shows identity to previously published ISAV sequences and has two putative NLSs

Immunoscreening of the bacteriophage Lambda cDNA library with the ISAV-PAb2 identified an ISAV clone designated 1H with one ORF of 1851 bases, theoretically encoding a protein of 616 aa with an estimated MW of 68 kDa and a p*I* of 8.2. The C-terminal 30 aa residues of the theoretical protein were markedly rich in acidic amino acid residues, with a p*I* of 3.3 (Fig. 1). The cDNA contained the conserved nucleotide sequence 5′-agcaaaga-3′ at the 5′ end as earlier reported for ISAV genomic segments (Krossøy et al., 1999; Ritchie et al., 2001; Sandvik et al., 2000; Snow and Cunningham, 2001). Database searches showed that at the nucleotide level the 1H sequence shared 99% and 85% identity with the Scottish and the Canadian segment 3 sequences, respectively (Clouthier et al., 2002; Ritchie et al., 2001; Snow and Cunningham, 2001). At the aa level, only two substitutions were found compared to the Scottish sequence, whereas the similarity to the Canadian sequences was 96% (Fig. 1). No significant similarity to other sequences was found. Using PSORT (http://psort.nibb.ac.jp/), two theoretical NLS were predicted at aa ^{230}RPKR^{233} and ^{473}KPKK^{476} (Fig. 1). These NLSs were conserved in all ISAV segment 3 sequences published, and were designated NLS1 and NLS2, respectively.

3.2. The 1H sequence encodes the 66 kDa structural protein of ISAV

WB analysis of lysates of Sf9 cells expressing the 1H gene using the ISAV-PAb1 showed one major band of 66 kDa, and two minor bands of approximately 58 and 43 kDa (Fig. 2a, lane 1). Similar results were obtained using the anti-pep1H antiserum (Fig. 2a, lane 3). The antibodies did not react with lysates of Sf9 cells infected with non-recombinant baculovirus (Fig. 2a, lanes 2 and 4). Furthermore, the anti-pep1H antiserum bound exclusively to the 66 kDa protein of purified virus preparations (Fig. 2b, lane 1), whereas the anti-1H antiserum gave a minor band of approximately 43 kDa in addition to the major band of 66 kDa (Fig. 2b, lane 2). ISAV-PAb1 which is prepared against whole virus reacted with the four major structural proteins in WB analysis of purified virus (Fig. 2b, lane 3), which is in agreement with previous reports (Falk et al., 2004, 1997; Krossøy et al., 2001a).

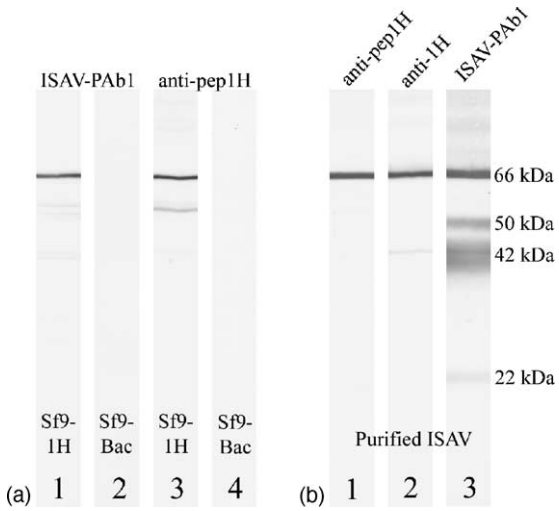

Fig. 2. WB analyses of recombinant proteins (a) and purified ISAV (b). Antibodies are indicated on the top, antigens in each lane, and molecular sizes are indicated on the right. (a) A polyclonal antiserum prepared against purified virus preparations (ISAV-PAb1) (lanes 1 and 2), and an antiserum prepared against peptides derived from the 1H-sequence (anti-pep1H) (lanes 3 and 4) both reacted with the 66 kDa gene product of segment 3 expressed in SF9 cells (lanes 1 and 3). Lysates of Sf9 cells infected with non-recombinant baculovirus was negative (lanes 2 and 4). (b) The anti-pep1H and an antiserum prepared against lysates of Sf9 cells expressing 1H (anti-1H) reacted with a 66 kDa protein in purified ISA-virus (lanes 1 and 2). The ISAV-PAb1 reacted with four major ISAV structural proteins of indicated sizes (lane 3).

3.3. The 66 kDa protein has RNA-binding activity

The 1H protein and the viral 66 kDa protein were affinity purified from Sf9 cells infected with recombinant 1H-baculovirus using ISAV-PAb1, and from ISAV-infected ASK cells using anti-1H antiserum, respectively. Both the recombinant and the viral protein exhibited RNA-binding activity as demonstrated in Fig. 3a (boxes 1 and 3). The corresponding controls were negative (Fig. 3a (boxes 2 and 4)). The purity of the protein preparations prepared by affinity purification were demonstrated by SDS–PAGE analysis on preparations prepared likewise from corresponding cell lysates labeled by [^{35}*S*]methionine (Fig. 3b).

3.4. The putative NP is an early protein shuttling between the nuclei and cytoplasm

ISAV- and mock-infected ASK cells fixed every fourth hour from 4 to 24 h p.i., at 36 and at 48 h p.i. were analyzed by immunofluorescence using the anti-1H rabbit immune serum and the anti-HE MAb. No staining was observed in ISAV-infected cells until 8 h p.i. Faint nuclear staining with the anti-1H was detected at 8 h p.i. (Fig. 4a and b), increasing in intensity until the HE was detected at 20 h p.i. using the anti-

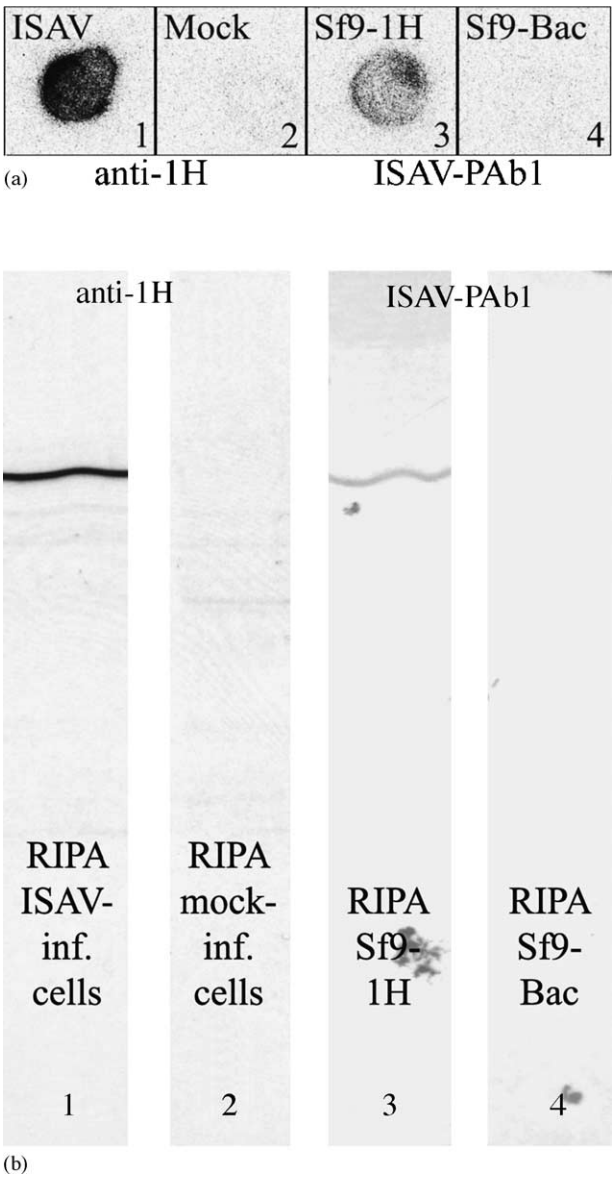

Fig. 3. RNA-binding assay. (a) Affinity purified viral and recombinant protein were allowed to react with radioactively labeled RNA, washed, and applied to a nitrocellulose membrane. The dried membrane was exposed to an autoradiographic film. Protein purified from lysates of ISAV-infected ASK cells using the anti-1H (NP) gave a clear reaction with the labeled RNA (box 1), while the corresponding extract from mock-infected cells gave no reaction (box 2). Similarly, protein extracted from lysates of Sf9 cells expressing 1H gave a weaker but still clear reaction with the RNA (box 3), while the Sf9 cells infected with non-recombinant baculovirus (Bac) did not (box 4). (b) The purity of the protein preparations prepared by affinity purification were demonstrated by SDS–PAGE analysis on preparations prepared likewise as the ones used for the RNA-binding assay, from the corresponding cell lysates labeled by [35S]methionine. Autoradiography revealed one unique band of 66 kDa from both the ISAV-infected ASK cells (lane 1), and from Sf9 cells expressing 1H (lane 3), while mock infected ASK-cells and Sf9 cells infected with non-recombinant baculovirus gave no such band. Boxes and lanes holding the same numbers in (a) and (b) have the corresponding protein preparations.

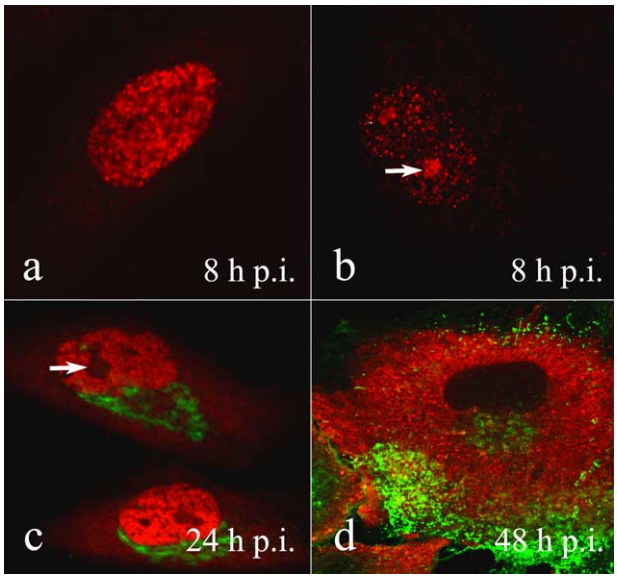

Fig. 4. Kinetics of cellular localization of NP (red) and HA (green) in ISAV infected ASK-cells. Immunofluorescence analysis are shown from 8 (a and b), 20 (c) and 48 (d) h p.i. using the Glesvær/2/90 isolate. The NP can be detected in the nucleus at 8 h p.i. (a and b), while the HA appears at about 20 h p.i. (c). At 48 h p.i., the NP has been exported to the cytoplasm (d). Using the Glesvær/2/90 isolate, the NP was observed sporadically in the nucleolus, seemingly very early after the onset of NP detection (b, indicated by arrows), while the nucleolus appeared devoid of NP during the remaining of the infectious cycle (c and d).

HE MAb, indicating that the 1H is an early protein. Weak anti-1H staining was observed in the nucleolus in a few cells at the onset of 1H detection (Fig. 4b). Preceding the onset of HE detection, the anti-1H staining had only been observed in the nucleus. At 20 h p.i., most cells showed strong nuclear staining using the anti-1H, whereas a more limited and dispersed fluorescence was found in the cytoplasm (Fig. 4c). Thus, it seemed that the initiation of the export of the protein detected by the anti-1H to the cytoplasm coincided with the first detection of the HE. At 36 and 48 h p.i., anti-1H staining exhibited increasing cytoplasmic fluorescence with little if any nuclear fluorescence at 48 h p.i. (Fig. 4d). At this time point, the HE was located to the cell membrane of most cells. Mock-infected cells did not show any staining at any time.

3.5. *The putative NP contains two NLSs*

Following transfection of CHSE-214 cells with 1H-pVAX1, approximately 5% of the cells expressed 1H 5 days post transfection (p.t.). Twenty-four hours p.t. (Fig. 5a) immunofluorescence staining with the ISAV-PAb1 revealed a distinct staining in the nucleolus, and a more evident nucleoplasmic staining escalating in cells expressing more protein. At 48 h p.t. (Fig. 5b), the number of cells expressing the protein in the nucleoplasm increased, but still a distinct staining was observed in the nucleolus of transfected cells. At 70 h p.t. (Fig. 5c), staining was still observed predominantly in the nucleus, but also dispersed throughout the cy-

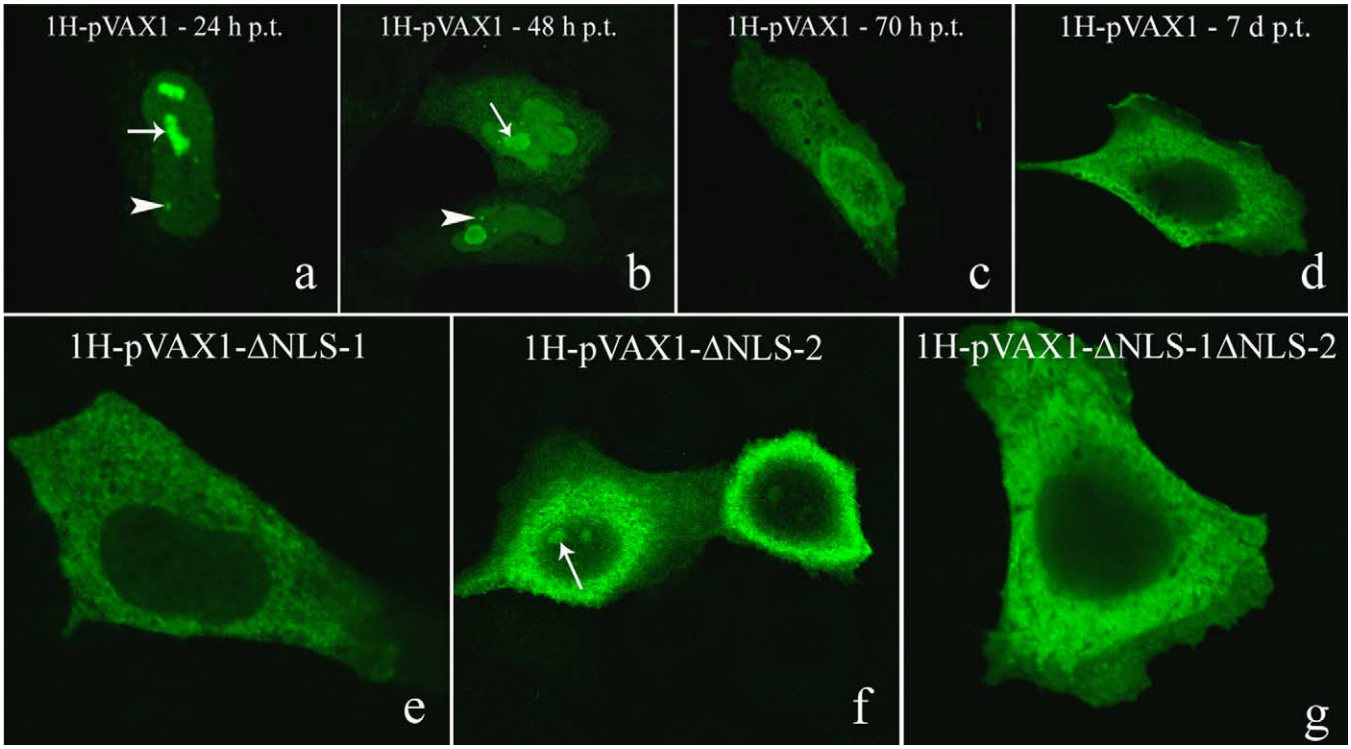

Fig. 5. Cellular localization of the NP in CHSE-214 cells transfected with constructs of the Bremnes/98 segment 3. The full length clone encoded a protein that initially was detected in the nucleoli (indicated by stretched arrows) followed by the detection in the nucleoplasm (a and b). Localization to structures resembling Cajal bodies were also observed in transfected cells (a and b, indicated by arrowheads). The nucleoli staining became less prominent as the protein was exported to the cytoplasm (c), and at 7 days p.t. most of the staining was observed in the cytoplasm (d). The mutant lacking NLS-1 located exclusively to the cytoplasm (e) while the mutant lacking NLS-2 located to the nucleoli and the cytoplasm (f). The double mutant encoded a protein that located exclusively to the cytosol (g).

toplasma, whereas the nucleolus staining was less prominent. Cells were also inspected at day 7 p.t., and at that time most of the staining was located to the cytoplasm (Fig. 5d). The distinct nucleolus staining observed in the transfected cells using the Bremnes/98 segment 3 genome sequence was observed a few times in infected cells whether the Glesvær/2/90 or the Bremnes/98 isolate was used (Fig. 4b, showing Glesvær/2/90).

Cells transfected with the NLS-mutants were fixed 48 h p.t. The NLS mutant 1H-pVAX1-ΔNLS1 showed a clear cytoplasmic localization with no staining of the nucleus (Fig. 5e). The 1H-pVAX1-ΔNLS2 showed a similar staining pattern as 1H-pVAX1-ΔNLS1, except that some of the cells showed a distinct staining in the nucleolus (Fig. 5f). The same staining pattern as 1H-pVAX1-ΔNLS1 was observed for the double mutant 1H-pVAX1-ΔNLS1ΔNLS2 (Fig. 5g).

4. Discussion

In this report, we describe the expression and functional analysis of the gene product of ISAV genomic segment 3. WB analysis revealed that the expressed protein was equivalent to the 66 kDa protein previously detected in purified ISAV preparations (Falk et al., 2004, 1997), documenting that this protein is encoded by segment 3. We demonstrate that the protein share several properties with the influenza NP, including RNA-binding activity. It is an early protein initially detected in the nuclei which is transported out of the nuclei at the onset of the production of the late proteins, represented here by the HE. Transfection studies confirmed that the nucleoprotein has intrinsic ability to be imported into the nucleus, and two monopartite NLSs at aa ^{230}RPKR^{233} and ^{473}KPKK^{476} were identified by computer analysis, and confirmed by site-directed mutagenesis. Segment 3 seemed to be conserved between known ISAV isolates, like the NP-gene of the influenza viruses. In addition to the previously reported sequence analysis data (Clouthier et al., 2002; Ritchie et al., 2001; Snow and Cunningham, 2001), it was found that the C-terminal 30 aa residues of the predicted ISAV segment 3 protein were markedly rich in acidic amino acid residues, with a p*I* of 3.3, comparable to the equivalent aa residues in the influenza NP (Portela and Digard, 2002).

WB analysis of lysates of Sf9 cells expressing the 1H gene using the ISAV-PAb1 and the anti-pep1H antibody showed one major band of 66 kDa. In addition, some minor bands in the range of approximately 43–58 kDa were detected, possibly representing incomplete proteins or breakdown products of the 66 kDa protein. No reaction was detected with lysates of Sf9 cells infected with non-recombinant baculovirus. The

anti-pep1H antiserum bound exclusively to the 66 kDa protein of purified virus preparations, whereas the anti-1H antiserum also gave a minor band of approximately 43 kDa substantiating that this band may represent an incomplete protein or breakdown product of the 66 kDa protein.

The primary function of the NP in orthomyxoviruses is to encapsidate the virus genome to facilitate RNA transcription, replication, and packaging (Portela and Digard, 2002). Several studies have demonstrated the non-specific binding of ssRNA to the influenza NP (Albo et al., 1995; Galarza et al., 1992; Harley et al., 1990; Kingsbury et al., 1987; Scholtissek and Becht, 1971). The RNA-binding properties of the ISAV NP was confirmed by the interaction of purified viral and recombinant protein with ssRNA transcribed in vitro, demonstrating that this protein has one of the key features of a NP.

Time-course immunofluorescence studies of ISAV infected ASK cells using the anti-1H antiserum gave a localization pattern comparable to that of the influenza NP. The ISAV putative NP was first detected 8 h p.i., and was located exclusively in the nucleus until the onset of HE detection 12 h later. This is in agreement with reports on the NP of influenza virus which is an early protein detectable 2.5–3 h p.i., as opposed to the matrix (M1) and haemagglutinine (HA) which are late proteins that become detectable 1–4 h after the NP, depending on the infectious dose (Inglis et al., 1976; Maeno and Kilbourne, 1970; Martin and Helenius, 1991; Skehel, 1973; Sugawara et al., 1991). Time-course studies have demonstrated that the production of influenza M1 and HA in infected cells coincide, and that this event again coincides with the appearance of NP in the cytoplasm (Martin and Helenius, 1991). Since the anti-HE MAb is the only characterized ISAV monoclonal antibody (Falk et al., 1998), the ISAV-HE was used as a representative of the late proteins in the present study. Thus, the appearance of the HE was used as an indicator to determine the relative time of appearance as compared to the protein detected by the anti-1H antiserum in ISAV infected cells. The initiation of nuclear export of the ISAV putative NP coincided with the first appearance of HE, and continued until the nuclei appeared devoid of detectable protein, approximately 48 h p.i. Thus the protein detected with the anti-1H antiserum shares several properties with the influenza NP, including it being an early protein, initially detected in the nuclei, followed by transport out of the nuclei at the onset of the production of the late proteins represented here by the HE. The optimal replication temperature for the ISAV is 15 °C (Falk et al., 1997), thus as expected, the ISAV replication is slower than that of the influenza viruses. However, the relative time of appearance of the different proteins should be correlated to the replication control systems used by the virus in the cells. It is assumed that a significant part of the replication control system established by influenza virus in infected cells is directed at the early synthesis of NP, while delaying the synthesis of the M1 protein. The NP is synthesized early, presumably because it is needed for the synthesis of template RNAs and viral RNAs. The synthesis of the M1 is delayed, probably because this protein stops the transcription of viral RNA into viral mRNA, and because it is a major regulator of nuclear export of viral RNP (Bui et al., 2000; Lamb and Krug, 1996; Martin and Helenius, 1991). Given that the ISAV uses a similar replication control system as influenza viruses, these observations, together with the RNA-binding properties of the protein, support that the protein encoded by ISAV segment 3 corresponds to the NP. This is also supported by studies showing that this protein is one of the major structural proteins of the ISAV (Falk et al., 1997), and a major structural component of the RNP-complex (Falk et al., 2004).

Transfections using the 1H-pVAX1, corresponding to the ORF of segment 3, confirmed that the encoded protein has an intrinsic ability to be imported into the nucleus, and to be exported from the nucleus to the cytoplasm later on. These results are in agreement with previous reports on the NP of influenza viruses (Bullido et al., 2000; Neumann et al., 1997). However, the expressed protein initially located to the nucleolus in the transfected cells, whereas a more evident nucleoplasmic staining escalated in cells expressing more protein. A similar nucleolus localization of the NP was observed in ISAV-infected cells, but to a much lesser extent. The localization of the NP to the nucleolus is a feature that has been described in the influenza literature (Davey et al., 1985; Hiscox, 2002; Stevens and Barclay, 1998), but many studies also report that the NP is absent from the nucleolus (Bucher et al., 1989; Martin and Helenius, 1991). Observations done in this study indicate that the ISAV NP enters the nucleolus initially in the replication process, but seems to be absent from the nucleolus in the remaining of the infection cycle. In transfected cells however, the nucleolus was distinctly positive for at least 48 h p.t., and the export of NP to the cytoplasm was initiated much later than during a viral infection. This could indicate the need for another viral protein to facilitate the transport of the NP, even from the nucleolus to the nucleoplasm.

Proteins less than 30–40 kDa can be transported through the nuclear pore complex by diffusion (Gant and Wilson, 1997), while larger molecules generally require a specific NLS. NLSs have been identified for a number of viral and cellular proteins which have been classified as either monopartite or bipartite, depending on whether or not stretches of basic residues are interrupted by a 10 aa space region (Silver and Ferrigno, 2000). The ISAV NP is 66 kDa, and almost certainly relies on an active transport into the nucleus by one or several NLSs, similar to the influenza A NP. Here, we identified two monopartite NLSs at aa ^{230}RPKR^{233} and ^{473}KPKK^{476} designated NLS1 and NLS2, respectively, by computer analysis and site-directed mutagenesis. Transfection studies demonstrated that both NLSs were required for the transport of NP into the nuclei. However, some of the cells transfected using the mutant lacking NLS2 showed a distinct nucleolus staining in addition to the cytoplasmic staining, while no mutants lacking NLS1 localized to the nucleolus. This might indicate that the region around NLS1 is involved in the nucleolus targeting of the protein in addition to the nuclear import. Since both NLSs had to be present for the

protein to localize in the nucleus, it is concluded that these NLSs cooperate to target the protein to the nucleus, and that no independent NLSs can be present in the ISAV NP. This is in contrast to previous findings that suggest that the NP of orthomyxoviruses have independent NLSs (Neumann et al., 1997; Weber et al., 1998).

In conclusion, the data presented provide further evidence that the ISAV segment 3 encodes the NP, and that the ISAV NP shows several characteristics similar to the NP of the influenza virus. These include intracellular localization and migration, time of expression and detection in cell culture, and RNA-binding activity. Two NLSs have been identified, but in contrast to other orthomyxoviruses that have independent NLSs, these seem to cooperate in the nuclear import of the ISAV NP. The distinct nucleolus staining observed in the transfected cells indicate that there is a nucleolus localization sequence in the NP, and mutagenesis studies indicate that the region around NLS1 may be involved in this nucleolus targeting of the protein, however, further studies are needed to confirm this nucleolus localization signal.

Acknowledgements

The authors would like to thank A.M. Szilvay and A. Hellebø for helpful comments on the manuscript. This study was funded by Intervet International and by grant 128044/103 from the Norwegian Research Council.

References

Albo, C., Valencia, A., Portela, A., 1995. Identification of an RNA binding region within the N-terminal third of the influenza A virus nucleoprotein. J. Virol. 69 (6), 3799–3806.

Biering, E., Falk, K., Hoel, E., Thevarajan, J., Joerink, M., Nylund, A., Endresen, C., Krossøy, B., 2002. Segment 8 encodes a structural protein of infectious salmon anaemia virus (ISAV); the co-linear transcript from segment 7 probably encodes a non-structural or minor structural protein. Dis. Aquat. Organ. 49 (2), 117–122.

Bucher, D., Popple, S., Baer, M., Mikhail, A., Gong, Y.F., Whitaker, C., Paoletti, E., 1989. M protein (M1) of influenza virus: antigenic analysis and intracellular localization with monoclonal antibodies. J. Virol. 63 (9), 3622–3633.

Bui, M., Wills, E.G., Helenius, A., Whittaker, G.R., 2000. Role of the influenza virus M1 protein in nuclear export of viral ribonucleoproteins. J. Virol. 74 (4), 1781–1786.

Bullido, R., Gomez-Puertas, P., Albo, C., Portela, A., 2000. Several protein regions contribute to determine the nuclear and cytoplasmic localization of the influenza A virus nucleoprotein. J. Gen. Virol. 81 (Pt 1), 135–142.

Clouthier, S.C., Rector, T., Brown, N.E., Anderson, E.D., 2002. Genomic organization of infectious salmon anaemia virus. J. Gen. Virol. 83 (Pt 2), 421–428.

Dannevig, B.H., Falk, K., Namork, E., 1995. Isolation of the causal virus of infectious salmon anemia (ISA) in a long-term cell-line from Atlantic salmon head kidney. J. Gen. Virol. 76, 1353–1359.

Davey, J., Colman, A., Dimmock, N.J., 1985. Location of influenza virus M, NP and NS1 proteins in microinjected cells. J. Gen. Virol. 66 (Pt 11), 2319–2334.

Devold, M., Krossoy, B., Aspehaug, V., Nylund, A., 2000. Use of RT-PCR for diagnosis of infectious salmon anaemia virus (ISAV) in carrier sea trout *Salmo trutta* after experimental infection. Dis. Aquat. Organ. 40 (1), 9–18.

Eliassen, T.M., Froystad, M.K., Dannevig, B.H., Jankowska, M., Brech, A., Falk, K., Romoren, K., Gjoen, T., 2000. Initial events in infectious salmon anemia virus infection: evidence for the requirement of a low-pH step. J. Virol. 74 (1), 218–227.

Falk, K., Aspehaug, V., Vlasak, R., Endresen, C., 2004. Identification and partial characterisation of viral structural proteins of infectious salmon anaemia (ISA) virus. J. Virol. 78 (6), 3063–3071.

Falk, K., Dannevig, B.H., 1995. Demonstration of infectious salmon anaemia (ISA) viral antigens in cell cultures and tissue sections. Vet. Res. 26 (5–6), 499–504.

Falk, K., Namork, E., Dannevig, B.H., 1998. Characterization and applications of a monoclonal antibody against infectious salmon anaemia virus. Dis. Aquat. Organ. 34 (2), 77–85.

Falk, K., Namork, E., Rimstad, E., Mjaaland, S., Dannevig, B.H., 1997. Characterization of infectious salmon anemia virus, an orthomyxo-like virus isolated from Atlantic salmon (*Salmo salar* L.). J. Virol., 9016–9023.

Galarza, J.M., Sowa, A., Hill, V.M., Skorko, R., Summers, D.F., 1992. Influenza A virus NP protein expressed in insect cells by a recombinant baculovirus is associated with a protein kinase activity and possesses single-stranded RNA binding activity. Virus Res. 24 (1), 91–106.

Gant, T.M., Wilson, K.L., 1997. Nuclear assembly. Annu. Rev. Cell Dev. Biol. 13, 669–695.

Griffiths, S., Cook, M., Mallory, B., Ritchie, R., 2001. Characterisation of ISAV proteins from cell culture. Dis. Aquat. Organ. 45, 19–24.

Harley, V.R., Mather, K.A., Power, B.E., McKimm-Breschkin, J.L., Hudson, P.J., 1990. Characterisation of an avian influenza virus nucleoprotein expressed in *E. coli* and in insect cells. Arch. Virol. 113 (3–4), 267–277.

Hellebø, A., Vilas, U., Falk, K., Vlasak, R., 2004. Infectious salmon anemia virus specifically binds to and hydrolyzes 4-*O*-acetylated sialic acids. J. Virol. 78 (6), 3055–3062.

Hiscox, J.A., 2002. The nucleolus—a gateway to viral infection? Arch. Virol. 147, 1077–1089.

Huang, T.-S., Palese, P., Krystal, M., 1990. Determination of influenza virus proteins required for genome replication. J. Virol. 64 (11), 5669–5673.

Inglis, S.C., Carroll, A.R., Lamb, R.A., Mahy, B.W., 1976. Polypeptides specified by the influenza virus genome I. Evidence for eight distinct gene products specified by fowl plague virus. Virology 74 (2), 489–503.

Kibenge, F.S., Garate, O.N., Johnson, G., Arriagada, R., Kibenge, M.J., Wadowska, D., 2001. Isolation and identification of infectious salmon anaemia virus (ISAV) from Coho salmon in Chile. Dis. Aquat. Organ. 45 (1), 9–18.

Kibenge, F.S., Lyaku, J.R., Rainnie, D., Hammell, K.L., 2000. Growth of infectious salmon anaemia virus in CHSE-214 cells and evidence for phenotypic differences between virus strains. J. Gen. Virol. 81 (1), 143–150.

Kingsbury, D.W., Jones, I.M., Murti, K.G., 1987. Assembly of influenza ribonucleoprotein in vitro using recombinant nucleoprotein. Virology 156 (2), 396–403.

Koren, C.W.R., Nylund, A., 1997. Morphology and morphogenesis of infectious salmon anaemia virus replicating in the endothelium of Atlantic salmon *Salmo salar*. Dis. Aquat. Organ. 29, 99–109.

Krossøy, B., Devold, M., Sanders, L., Knappskog, P.M., Aspehaug, V., Falk, K., Nylund, A., Koumans, S., Endresen, C., Biering, E., 2001a. Cloning and identification of the infectious salmon anaemia virus haemagglutinin. J. Gen. Virol. 82 (Pt 7), 1757–1765.

Krossøy, B., Hordvik, I., Nilsen, F., Nylund, A., Endresen, C., 1999. The putative polymerase sequence of infectious salmon anemia virus suggests a new genus within the Orthomyxoviridae. J. Virol. 73 (3), 2136–2142.

Krossøy, B., Nilsen, F., Falk, K., Endresen, C., Nylund, A., 2001b. Phylogenetic analysis of infectious salmon anaemia virus isolates from Norway, Canada and Scotland. Dis. Aquat. Organ. 44 (1), 1–6.

Lamb, R.A., Krug, R.M., 1996. Orthomyxoviridae: the viruses and their replication. In: Fields, B.M., Knipe, D.M., Howley, P.M., Chanock, R.M., Melnick, J.L., Monath, T.P., Roizman, B., Straus, S.E. (Eds.), Fields Virology. Lippincott-Raven, Philadelphia, PA, pp. 1353–1395.

Lannan, C.N., Winton, J.R., Fryer, J.L., 1984. Fish cell lines: establishment and characterization of nine cell lines from salmonids. In Vitro 20 (9), 671–676.

Lee, M.T., Bishop, K., Medcalf, L., Elton, D., Digard, P., Tiley, L., 2002. Definition of the minimal viral components required for the initiation of unprimed RNA synthesis by influenza virus RNA polymerase. Nucleic Acids Res. 30 (2), 429–438.

Lovely, J.E., Dannevig, B.H., Falk, K., Hutchin, L., MacKinnon, A.M., Melville, K.J., Rimstad, E., Griffiths, S.G., 1999. First identification of infectious salmon anaemia virus in North America with haemorrhagic kidney syndrome. Dis. Aquat. Organ. 35 (2), 145–148.

Maeno, K., Kilbourne, E.D., 1970. Developmental sequence and intracellular sites of syntehsis of three structural protein antigens of influenza A2 virus. J. Virol. 5 (2), 153–164.

Martin, K., Helenius, A., 1991. Nuclear transport of influenza virus ribonucleoproteins: the viral matrix protein (M1) promotes export and inhibits import. Cell 67 (1), 117–130.

Mjaaland, S., Rimstad, E., Falk, K., Dannevig, B.H., 1997. Genomic characterization of the virus causing infectious salmon anemia in Atlantic salmon (*Salmo salar* L.): an orthomyxo-like virus in a teleost. J. Virol. 71 (10), 7681–7686.

Mullins, J.E., Groman, D., Wadowska, D., 1998. Infectious salmon anaemia in salt water Atlantic salmon (*Salmo salar* L.) in New Brunswick, Canada. Bull. Eur. Assoc. Fish Pathol. 18 (4), 110–114.

Neumann, G., Castrucci, M.R., Kawaoka, Y., 1997. Nuclear import and export of influenza virus nucleoprotein. J. Virol. 71 (12), 9690–9700.

Portela, A., Digard, P., 2002. The influenza virus nucleoprotein: a multifunctional RNA-binding protein pivotal to virus replication. J. Gen. Virol. 83 (Pt 4), 723–734.

Rimstad, E., Mjaaland, S., 2002. Infectious salmon anaemia virus. Apmis 110 (4), 273–282.

Rimstad, E., Mjaaland, S., Snow, M., Mikalsen, A.B., Cunningham, C.O., 2001. Characterization of the infectious salmon anemia virus genomic segment that encodes the putative hemagglutinin. J. Virol. 75 (11), 5352–5356.

Ritchie, R.J., Heppell, J., Cook, M.B., Jones, S., Griffiths, S.G., 2001. Identification and characterization of segments 3 and 4 of the ISAV genome. Virus Genes 22 (3), 289–297.

Rodger, H.D., Richards, R.H., 1998. Haemorrhagic smolt syndrome: a severe anaemic condition in farmed salmon in Scotland. Vet. Rec., 538–541.

Sandvik, T., Rimstad, E., Mjaaland, S., 2000. The viral RNA 3′- and 5′-end structure and mRNA transcription of infectious salmon anaemia virus resemble those of influenza viruses. Arch. Virol. 145 (8), 1659–1669.

Scholtissek, C., Becht, H., 1971. Binding of ribonucleic acids to the RNP-antigen protein of influenza viruses. J. Gen. Virol. 10 (1), 11–16.

Schyth, B.D., Olesen, N.J., Østergård, P., Falk, K., 2003. Laboratory diagnosis of infectious salmon anemia (ISA): experience gained from the outbreaks on the Faroe Islands 2000–2003. In: Diseases of Fish and Shellfish, 11th International Conference of the EAFP, vol. 11, p. O-79.

Silver, P.A., Ferrigno, P., 2000. Nuclear–cytoplasmic transport. In: Nature Encyclopedia of Life Sciences. Nature Publishing Group. http://www.els.net/ [doi:10.1038/npg.els.0001351].

Skehel, J.J., 1973. Early polypeptide synthesis in influenza virus-infected cells. Virology 56 (1), 394–399.

Snow, M., Cunningham, C.O., 2001. Characterisation of the putative nucleoprotein gene of infectious salmon anaemia virus (ISAV). Virus Res. 74 (1–2), 111–118.

Snow, M., Ritchie, R., Arnaud, O., Villoing, S., Aspehaug, V., Cunningham, C.O., 2003. Isolation and characterisation of segment 1 of the infectious salmon anaemia virus genome. Virus Res. 92 (1), 99–105.

Stevens, M.P., Barclay, W.S., 1998. The N-terminal extension of the influenza B virus nucleoprotein is not required for nuclear accumulation or the expression and replication of a model RNA. J. Virol. 72 (6), 5307–5312.

Sugawara, K., Nishimura, H., Hongo, S., Kitame, F., Nakamura, K., 1991. Antigenic characterization of the nucleoprotein and matrix protein of influenza C virus with monoclonal antibodies. J. Gen. Virol. 72 (Pt 1), 103–109.

Thorud, K., Djupvik, H.O., 1988. Infectious salmon anaemia in Atlantic salmon (*Salmo salar* L.). Bull. Eur. Assoc. Fish Pathol. 8, 109–111.

Weber, F., Kochs, G., Gruber, S., Haller, O., 1998. A classical bipartite nuclear localization signal on Thogoto and influenza A virus nucleoproteins. Virology 250 (1), 9–18.

Paper III

First Characterization of the Infectious Salmon Anemia Virus Fusion Protein

Vidar Aspehaug[1*], Aase B. Mikalsen[2], Mike Snow[3], Eirik Biering[4†] and Stephane Villoing[4]

[1] Department of Biology, University of Bergen, Bergen, Norway

[2] Norwegian School of Veterinary Science, Oslo, Norway

[3] FRS Marine Laboratory, Aberdeen, UK

[4] Intervet Norbio, Bergen, Norway

[†] Current address: Institute of Marine Research, Bergen, Norway

*Corresponding author:

Vidar Aspehaug, Department of Biology, University of Bergen, Thormøhlensgate 55, 5020 Bergen, Norway

e-mail: Vidar.Aspehaug@bio.uib.no

Tlf: +47 55 58 44 06

Fax: +47 55 58 44 50

Word count summary: 257

Word count main text: 6537

Running title: First Characterization of the ISAV Fusion Protein

Key words: orthomyxovirus, ISAV, fusion protein, coiled-coil, fusion peptide, metastable, F_0, F_1, F_2, proteolytic activation, proteolytic cleavage, structural proteins.

The GenBank accession numbers of the sequences reported in this study are CAD99169 (protein sequence) and AX752070 (nucleotide sequence).

Summary

Infectious salmon anemia virus (ISAV) is an orthomyxovirus causing serious disease in Atlantic salmon (*Salmo salar* L.). This study presents the characterization of the ISAV 50 kDa glycoprotein encoded by segment 5, and we propose that it should be termed the viral membrane fusion protein (F). This is the first description of a separate orthomyxovirus F protein, and to our knowledge, the first pH dependent separate viral F protein described. Our data demonstrate that the F protein is synthesized as a precursor protein F_0 which is proteolytically cleaved to F_1 and F_2, held together by disulfide bridges. The cleaved protein is in a metastable, fusion activated state that can be triggered by low pH, high temperature, or a high concentration of urea. Cell-cell fusion in ISAV infected and transfected cells can be initiated by treatment with trypsin and low pH. Fusion is initiated at pH 5.4-5.6, and the fusion process is coincident with the trimerization of the F protein, or a stabilization of the trimer, providing strong evidence that it represents the formation of the fusogenic structure. Exposure to trypsin and low pH prior to infection inactivated the virus, demonstrating the non-reversibility of this conformational change. Sequence analyses indicate that the protein carries a coiled-coil and a fusion peptide. Size estimates of F_1 and F_2 and the localization of the putative fusion peptide and theoretical trypsin cleavage sites suggest that the proteolytic cleavage site is after residue K^{276} in the protein sequence. The cleavage site structure is probably not a major determinant of pathogenicity in the ISAV.

Introduction

Infectious salmon anemia virus (ISAV) is an enveloped virus belonging to the family *Orthomyxoviridae,* genus *Isavirus*, causing serious disease in Atlantic salmon (*Salmo salar* L.) aquaculture (53, 59, 69, 72, 81). The ISAV genome is composed of eight negative-sense, single-stranded RNA segments, and whilst nucleotide sequences of all segments have been published (9, 45, 46, 57, 67, 68, 75, 76), much remains to be elucidated with respect to protein identification and characterization. A total of 12 proteins have been detected by immunoprecipitation of lysates from radiolabeled infected cells (42), while four major structural proteins have been recognized in purified ISAV particles, including the matrix (M1; 22–24 kDa) (7, 24), the nucleoprotein (NP; 66-71 kDa) (3, 24), and two membrane glycoproteins (24). The receptor-binding and receptor-destroying activities are associated with the 42 kDa glycoprotein encoded by segment 6, termed the hemagglutinin-esterase (HE) (24, 25, 36, 44, 45, 67), while the activities of the second glycoprotein, glycoprotein 50 (Gp50) encoded by segment 5 (9), have not been described previously.

ISAV pursues a nuclear replication strategy similar to the influenza viruses (3, 26), which is initiated by receptor-binding and internalization into cellular endosomes where the viral and cellular membranes fuse in response to low pH (21). The addition of trypsin to the culture medium during ISAV replication has been demonstrated to have a beneficial effect on the production of infective virus particles (26), suggesting that ISAV replication depends on proteolytic activation to exert infectivity.

Fusion between viral and cellular membranes is mediated by viral membrane fusion glycoproteins, which are usually divided into two distinct categories. Type I fusion proteins are activated by proteolytic cleavage, and include the fusion proteins of orthomyxo-, paramyxo-,

retro-, and filoviruses (19). Type II fusion proteins comprise the fusion proteins of flaviviruses, alphaviruses, and bunyaviruses, and these do not depend on proteolytic cleavage for activation, but are associated with a second protein whose cleavage is essential for establishing fusion competence (30, 34, 35).

Type I fusion proteins are synthesized as single-chain precursors which assemble into homotrimers (13). An essential step in rendering the proteins fusion competent, is the cleavage of the protein by host proteases to generate two subunits bound together by disulfide bridges (50). This cleaved form of the protein is in a metastable state, trapped from achieving its lower energy state by a kinetic barrier, and is readily activated by destabilization such as receptor-binding or low pH (50). Once activated, the protein refolds into a highly stable conformation (12). Type I fusion proteins contain a hydrophobic sequence, known as the fusion peptide (FP), at or near the new amino-terminal region created by the cleavage event (58, 63, 77), and their final (post-fusion) state contains a characteristic α-helical coiled-coil core structure corresponding to a heptad-repeat motif (12, 58). In recent years, these structures have been the target for development of new anti-viral drugs, including fusion inhibiting peptides and antibodies (20, 52, 83), suggesting that fusion proteins might be important candidates both for vaccination and as therapeutic targets.

Fusion of influenza A viruses to the cell membrane is mediated through the hemagglutinin (HA), and although the pathogenicity of influenza viruses is polygenic, numerous studies have established that the cleavage site structure of the HA precursor is the most significant determinant of pathogenicity (reviewed in 65, 78). Generally, HAs of avirulent strains are cleaved by a restricted number of host proteases. More virulent strains convey enhanced HA-cleavability due to basic residues within the cleavage site, and can be cleaved by a wide range of host proteases, leading to systemic infection and a higher pathogenicity. A similar correlation

between F protein cleavage site structure and pathogenicity has been observed in paramyxoviruses (32, 79, 82), and may also be important in the pathogenicity of ISAV. Thus, the identification of the F protein and its proteolytic cleavage site might be key factors in establishing the virulence factors of the ISAV.

The present study was undertaken to verify that the ISAV genomic segment 5 encodes the 50 kDa glycoprotein, and to demonstrate that it is the viral F protein. We have shown experimentally that the encoded protein exhibits the general characteristics described for type I viral fusion proteins.

Materials and methods

Virus and cells

The ISAV isolates used in the experiments were Bremnes/98 (47) or Glesvaer/2/90 (15) as indicated. The virus isolates were propagated in Salmon Head Kidney (SHK-1) cells as previously described (14). Functional assays were performed using SHK-1, Atlantic Salmon Kidney (ASK) cells (18), and Chinook Salmon Embryo (CHSE-214) cells (51). Infections were performed as described by Falk et al. (26).

Sf9 cells were grown in suspension culture, infected with baculovirus at 28°C and harvested 5 days post infection (p.i.) by centrifugation at 750 x g for 20 min at 4°C. The cell pellet was resuspended in 10 mM phosphate buffered saline (PBS) [pH 7.4] with 0.2% Triton X-100 (Amersham Biosciences), and used for immunization.

Purified ISAV preparations were prepared by sucrose gradient centrifugation using the Bremnes/98 isolate, and infectivity titrations of ISAV and virus neutralization assays were performed by endpoint titration in 96-well culture plates, using an immunofluorescence assay, all as described previously (25, 26).

Cloning and sequencing

A unidirectional cDNA library from ASK cells infected with ISAV Bremnes/98 isolate was constructed in bacteriophage Lambda, as previously described (45). A clone, designated EB5, was identified by immunoscreening with a polyclonal anti-ISAV rabbit serum (ISAV-PAb) using the picoBlue immunoscreening kit (Stratagene). The EB5 cDNA insert was excised as described previously (45), and sequenced. Full-length cDNA sequence was obtained by 5' RACE (5'

RACE system version 2.0, Invitrogen). RACE products were cloned in the pCR2.1-TOPO vector using the TOPO TA cloning kit (Invitrogen) and sequenced.

To amplify the coding region of the EB5 cDNA insert, the primer set EB5-EcoRI: 5'-GAGCTAACAGAGAGGAATTCATGGCTTTTCTAAC-3' and EB5-XhoI: 5'-CCAGCAGAAACTCGAGTTATCTCCTAATGC-3' were used. The PCR product was subsequently cloned into pFastBac1 and pVAX1 vectors (Invitrogen), using the EcoRI and XhoI restriction enzymes (Promega). These vectors were named pFastBac1/EB5 and pVAX1/EB5, respectively.

For expression of the ISAV-HE in fish cells, the vector pVAX1/HE was constructed. ISAV Bremnes/98 HE-gene (45) was amplified by PCR using primers HE-KpnI-f (5'-GGGTACCGCAAAGATGGCACGATTC-3') and HE-XhoI-r (5'-CCGCTCGAGGTTGTCTTTCTTTCATAATC-3'), and cloned into the restriction sites KpnI and XhoI of the pVAX1 vector.

The pFastBac1/EB5, pVAX1/EB5 and pVAX1/HE were all used in transformations of *E.coli* TOP10 cells (Invitrogen), purified using endofree plasmid Midi kit (Qiagen), and sequenced using the BigDye terminator sequencing kit (PE Biosystems) and an ABI 377 DNA analyzer (PE Biosystems). Sequences were assembled and analyzed as previously described (45).

Computer-based Protein Sequence Analysis

Sequence database searches were performed using BLAST (1). Pair-wise sequence alignments were performed using ClustalX (80) and viewed using GeneDoc (60). Primary and secondary structure predictions were performed using the Expasy tools, including Compute pI/MW and PeptideCutter (31). DISULFIND was used to predict disulfide bridges (85). Post-translational

modifications were predicted using SignalP (5), NetOglyc 2.0 (33), and Motif Scan (61), while topology predictions were done by TopPred2 (84), SPLIT (41), and TMPred (38). Learncoil-VMF, a program specialized in the prediction of viral coiled-coil membrane fusion domains (74), was used to search for sequences with the probability of forming α-helical coiled-coils using a probability of 0.5 as the cut-off value. The program COILS, which estimate the probability that a sequence will adopt a coiled-coil conformation, was also used (54). Structure homology searches were done by FUGUE (73) and PDB-BLAST (2). Tertiary structure predictions based on structural homology were done by TITO/MODELLER 4.0 (27, 55, 71), using a PDB structure from Visna virus Env coiled-coil (1jek) to perform 3D-modeling. Genbank sequence accession numbers reported in this study are CAD99169 (protein sequence) and AX752070 (nucleotide sequence) for segment 5 of the Norwegian ISAV isolate Bremnes/98.

Expression of EB5 cDNA in Sf9 cells

Purified pFastBac1/EB5 was transformed into *E.coli* TOP10 cells (Invitrogen), and the isolated plasmid used to transform *E.coli* DH10Bac competent cells (Invitrogen). Recombinant bacmid was obtained from the transformed DH10Bac cells and used to recover recombinant baculovirus (BacEB5) after transfection of Sf9 cells according to the method described in the Bac-to-bac kit (Invitrogen). BacEB5 was used to express the EB5 protein in Sf9 cells according to the recommendations of the manufacturer. The expression level and specificity of the recombinant EB5 protein expressed in Sf9 cells was verified using the ISAV-PAb (see below) in immunoblot and immune staining of EB5 expressing cells (results not shown).

Antisera

An antisera against two synthetic peptides derived from the EB5 sequence were prepared by Eurogentec using the peptides [HWTTSRSRLEDSTWQGG]-NH2 and [HFTTERIKTGKVDLDSC]-NH2 (indicated in Fig. 1.a.) coupled to keyhole limpet

haemocyanin. The conjugated peptides were pooled and injected into a rabbit according to Eurogentec's procedures, resulting in the antiserum termed anti-pepEB5.

A synthetic peptide [GAASAEDVKEKLNGIIDQINKVNLLLEGEIEAVRRIAYMN]-NH2 corresponding to the predicted EB5 coiled-coil sequence (see results section) was synthesized by Sigma-Genosys Ltd, purified to >95% purity by HPLC, and coupled to keyhole limpet haemocyanin. The conjugated peptide was injected into a rabbit according to Sigma-Genosys Ltd's procedures, resulting in the antiserum named anti-pepcoilEB5.

An antiserum against the baculovirus expressed EB5 protein (anti-EB5Bac) was prepared by immunizing a rabbit four times with four weeks intervals, using approximately 150 µg protein from a crude lysate of Sf9 cells infected with BacEB5.

A polyclonal antiserum prepared against whole ISAV, ISAV-PAb (45), a monoclonal antiserum directed against the ISAV NP, anti-NP MAb (Aquaculture Diagnostics Limited), and a monoclonal antiserum directed against the ISAV HE, anti-HE MAb (3H6F8) (25), were also used in this study.

Transfections

Transfections performed for immunofluorescence analysis were done on CHSE-214 cells grown on coverslips in 24-well plates using the FuGENE 6 Transfection reagent (Roche Diagnostics) according to the manufacturer's recommendations.

For fusion assays, single and combined transfections of SHK-1 cells were performed with the plasmid pVAX1/EB5 and/or pVAX1/HE using the Amaxa Nucleofector™ Technology (Amaxa

GmbH). A procedure optimized according to the manufacturer's protocol for the fish cell line TO, by E. García-Rosado and coworkers (personal communication) was used. The pVAX1/EB5 and pVAX1/HE plasmids were used in 1:2, 1:1, and 2:1 ratio, transfecting 5x 10^6 cells using a total of 9 μg DNA in transfections using both plasmids, and 7.5 μg DNA in single transfections. The transfected cells were transferred into two parallel wells in a 6-well plate and incubated as recommended for SHK-1.

Fusion assay

A syncytium fusion assay was established using SHK-1 cells infected with the ISAV Glesvaer/2/90 isolate. The cells were treated with 0, 2.5, 5, 10, 20, 40, and 60 μg/ml trypsin (Sigma) in Leibovitz L-15 (L-15; Gibco BRL) medium for 15 minutes at room temperature (RT), followed by incubation at pH 3.5-8.5 for 15 minutes at RT. After initial experiments, the syncytium assay was standardized to using 20 μg/ml trypsin in L-15 and pH 4.5. Trypsin was inactivated by 10% fetal calf serum in L-15, and between incubations the cells were washed in L-15. Finally, the cells were incubated in L-15 at RT for 2 h and kept at 4°C overnight prior to fixation by incubation in 80% acetone for 20 min and immune staining as described below.

Immunofluorescence

Cells attached to cover slips were fixed with cold 3.7% formaldehyde in PBS for 10 min on ice, rinsed in PBS, and permeabilized with 0.2% Triton-X 100 (Amersham Biosciences) in PBS for 30 min at RT, followed by blocking in 5% non-fat dry milk (Sigma) in PBS for 30 min. The cells were incubated with primary antibodies diluted in 2.5% non-fat dry milk in PBS for 1 h and washed in PBS. Bound antibodies were detected using Alexa dye 488-labeled anti-rabbit IgG (Molecular probes) and/or Alexa dye 594-labeled anti-mouse IgG (Molecular probes). For staining in fusion assays, cell nuclei were stained by incubation with 10 μg/ml propidium iodide

(Sigma) in PBS for 1 min prior to the last wash in the staining procedure. After washing, the cells were mounted with SlowFade Antifade (Molecular Probes) or Vectashield antifade medium containing DAPI (Vector Laboratories) and examined in a confocal microscope (Leica, TCS SP2 AOBS) or a standard inverted microscope (Olympus, IX81). Polyclonal antisera (including secondary antisera) were adsorbed by incubation on monolayers of formaldehyde fixed and permeabilized ASK cells prior to use in immunofluorescence.

SDS-PAGE and Western blot (WB) analysis

Samples were treated with dissociation buffer (50 mM Tris-HCl [pH 6.8], 1% SDS, 50 mM dithiothreitol, 8 mM EDTA, 0.01% bromophenol blue) and heated for 5 min at 95°C. In non-reduced samples, dithiothreitol was omitted and samples were incubated for 30 min at RT. Proteins were separated by SDS-PAGE with the discontinuous system devised by Laemmli (48) using 0.5 mm-thick precast 12.5%, or 8-18% gradient, polyacrylamide gels (ExcelGel SDS; Amersham Biosciences), and transferred to a PVDF membrane (Hybond™-P: Amersham Biosciences) as previously described (45). The membrane was treated with blocking solution (PBS, 0.1% Tween-20, 5% non-fat dry milk) overnight at 4°C followed by 1 h incubation at RT with the primary rabbit immune serum. The membrane was then washed 3 times in blocking solution and incubated with goat anti-rabbit horseradish peroxidase (HRP) conjugate (AMDEX: Amersham Biosciences) for 1 h at RT. Bound HRP-conjugate was detected using ECL Plus™ (Amersham Biosciences) and exposure on Hyperfilm™ ECL™ (Amersham Biosciences). The blots were scanned in a desktop scanner (CanoScan 3000F, Canon) and analyzed using Quantity One 1D-gel analysis software (Version 4.5.2. BioRad).

A 2D-electrophoresis was performed by using non-reducing SDS-PAGE in the first dimension. A lane excised from the polyacrylamide gel was immersed in dissociation buffer and heated for 5

min at 95°C before it was run in the second dimension on reducing SDS-PAGE and blotted as described.

Trypsin digestion assay and Gp50 homotrimer formation/stabilization

Samples were incubated with trypsin (Sigma) to a final concentration of 20 μg/ml in PBS for 10 min at 37°C. The digestion was stopped by addition of trypsin inhibitor from bovine pancreas (type I-P; Sigma) to a final concentration of 20 μg/ml. After digestion, the pH of the samples was adjusted by diluting the samples 1:1 in 0.2 M citrate buffer (pH in the range 4.5 - 7.3 ± 0.1), or the samples were exposed to 60°C or 4.5 M urea (final concentration), incubated 1 h at RT and analyzed under non-reducing conditions on SDS-PAGE and WB as described above.

Chemical Cross-Linking

Chemical cross-linking of purified virus was attempted by incubation with ethylene glycol bis(sulfosuccinimidyl succinate) (EGS) (Sigma) for 1 h either on ice or at RT, at concentrations of 0.1, 0.5, 2.0, and 5.0 mM EGS. Crosslinked products were analyzed under reducing conditions on SDS-PAGE and WB as described above.

Results

EB5 sequence shares a high identity with previously published segment 5 sequences

Immunoscreening of the bacteriophage Lambda cDNA library identified an ISAV clone designated EB5 (1468 nucleotides). The EB5 cDNA insert contained one ORF of 1332 nucleotides, theoretically encoding a protein of 444 amino acids with an estimated MW of ~48.6 kDa and a p*I* of 7.76. The EB5 nucleotide sequence shared 99%, 98%, and 81% identity with the previously published Scottish, Norwegian, and Canadian segment 5 sequences, respectively (9). At the amino acid level, EB5 shared 93% identity with the Scottish isolate, and 78% and 91% identity with the Canadian and a Norwegian isolate, respectively (Fig. 1.) (9). No significant similarity to any other sequences was found.

TMPred predicted residues M^{1}-C^{17}, F^{274}-Y^{292}, and V^{417}-W^{439} to be potential transmembrane regions (Fig. 1.), and these were confirmed by TopPred2 and SPLIT. Residues V^{417}-W^{439} were predicted as the primary transmembrane region, whereas residues M^{1}-C^{17} were predicted to be a signal sequence by SignalP. Two N-glycosylation and two O-glycosylation sites were predicted by Motif Scan and NetOglyc 2.0, respectively. A total of 46 potential trypsin cleavage sites were identified by PeptideCutter and 20 cysteine residues putatively involved in disulfide bonds were predicted using DISULFIND (all indicated in Fig. 1).

The segment 5 protein contains a putative coiled-coil motif

Learncoil-VMF predicted a coiled-coil domain typical of viral membrane fusion proteins at residues G^{301}-N^{340} in the segment 5 protein sequence with an average probability of 87% (Fig. 1). This region was also predicted as forming a coiled-coil with the program COILS with an average probability higher than 80% (window of 28 residues). Also, FUGUE predicted a structural homology between residues V^{297}-K^{367} in the segment 5 protein sequence and the PDB

structure 1jek corresponding to the Visna virus Env transmembrane core structure, with the highest Z-score (4.15) with a 95% confidence. This structure is composed of two coiled-coil motifs in the Env polyprotein of Visna virus, located between residues S^{694}-E^{731} and Q^{776}-A^{807} of this protein. The structural homology to these Visna virus motifs was localized to V^{297}-R^{334} and R^{335}-K^{367} in the segment 5 protein sequence, spanning through the putative coiled-coil (Fig. 1). Other PDB structures giving high scores were leucine zipper domains, which also form coiled-coil structures enabling oligomerization, and coiled-coil domains of the HIV and SIV Gp41 protein (data not shown).

Using the structural homology found with the PDB structure 1jek, the computation of a 3D model for the putative coiled-coil motif present in the segment 5 protein sequence was performed using MODELLER 4.0. This software, which performs homology modeling of protein structures by satisfaction of spatial restraints, predicted the structurally homologous regions of the ISAV predicted coiled-coil motif to adopt an α-helix conformation. Such a helix is typically formed by a coiled-coil domain enabling oligomerization and assembly of the fusion protein in a trimer-of-hairpin structure.

Using PDB-BLAST, a significant structural and sequence homology was also found between residues A^{379}-M^{427} in the influenza A HA2 (accession # AF194991), corresponding to the coiled-coil region (8), and residues G^{301}-N^{340} in the ISAV segment 5, predicted as the coiled-coil (Fig. 2).

The segment 5 protein contains a putative FP

Multiple sequence alignments of the ISAV segment 5 protein sequence and viral FPs from several paramyxoviruses, orthomyxoviruses, and retroviruses suggested a putative ISAV FP (pFP) at residues C^{277}-Y^{292} (Table 1). Residue G^{279} in the pFP was conserved amongst all the

included viruses, whereas F^{280} was common to ISAV, pneumoviruses, retroviruses, and orthomyxoviruses, and G^{285} was conserved in ISAV, pneumoviruses, and retroviruses (Table 1). The highest level of conservation was found between the Canadian ISAV pFP (9) and the FP from Bovine Respiratory Syncytial Virus (BRSV), and between the Norwegian pFP and the Human Respiratory Syncytial Virus subgroup A (HRSV) FP. These revealed a 43.8 % identity (7 out of 16 residues in the pFP are identical) (Table 1). It was noteworthy that identical amino acids corresponded to residues conserved in several pneumoviruses (11). The potential transmembrane region predicted at residues F^{274}-Y^{292} overlaps the pFP.

Antibodies towards recombinant segment 5 protein and synthetic peptides react with Gp50

The antisera anti-pepEB5, anti-pepcoilEB5, and anti-EB5bac all reacted specifically with a protein of 50 kDa (Gp50) in WB analysis of purified ISAV run at reducing conditions in SDS-PAGE (Fig. 3a, lane 1, 3, and 5). The anti-pepEB5 and anti-EB5bac also reacted with two weaker bands of approximately 30 and 100 kDa. The two latter antibodies also reacted with infected cells, giving identical immune staining (described below).

Trypsin and low pH is required for cell-cell fusion of ISAV infected fish cells and red blood cells

The syncytium fusion assay demonstrated that trypsin treatment combined with subsequent lowering of the pH to 5.5 or below is a prerequisite for fusion between ISAV-infected SHK-1 cells (Fig. 4a). No fusion was seen when omitting either the trypsin treatment or the acidification (Fig. 4c). Increasing the concentration of trypsin resulted in both an increase in the total number of cells involved in syncytium formation, and an increase in the number of cells involved in each syncytium (seen as number of nuclei). The optimal conditions for fusion were at the highest concentration of trypsin possible without causing detachment of a large proportion of the cells

(20 µg/ml) combined with pH 4.5. This resulted in syncytia containing up to 40 nuclei in some repetitions (results not shown).

These optimal conditions for fusion were confirmed using a lipid mixing assay based on the fusion between ISAV infected cells and Octadecyl rhodamine B (R18) (Molecular Probes) membrane-labeled Atlantic salmon erythrocytes (4), which resulted in transfer of R18 from the erythrocyte membrane to the cell membrane after induction of fusion (Fig 4e).

Cell-cell fusion in transfected cells

The optimal conditions for the syncytium fusion assay (20 µg/ml trypsin and pH 4.5) were used for testing the fusion activity in SHK-1 cells after transfection with pVAX1/EB5 and/or pVAX1/HE. Fused cells resulting in syncytia with up to 9 nuclei were observed in wells transfected with both constructs (Fig. 4b). Syncytium formations were most abundant in wells transfected with pVAX1/EB5 and pVAX1/HE in 2:1 ratio. No syncytia were observed in wells transfected with only one of the constructs, thus this experiment did not produce enough evidence to conclude that the segment 5 protein alone is responsible for the fusion activity. This was probably due to the generally low transfection efficacy which is a very common problem with fish cell systems. Transfected cells incubated with 20 µg/ml trypsin, followed by incubation at pH 7.4 served as negative controls (Fig. 4d), and no signs of syncytium formation was observed in these cells expressing either protein, separately or combined.

Gp50 is a late protein locating to the ER, golgi and the cell membrane

ISAV-infected and mock-infected ASK cells fixed every fourth hour from 4 to 24 h p.i., at 36 and 48 h p.i. were analyzed by immunofluorescence using the anti-EB5bac rabbit immune serum in combination with the anti-HE MAb or the anti-NP MAb. No staining was observed in ISAV-infected cells until 8 h p.i. when the NP was detected in the nucleus, representing an early

protein as previously described (3). At 20 h p.i. the NP was detected in the nucleus and cytoplasm and the HE was detected in the endoplasmatic reticulum (ER) or golgi, representing a late protein, also as previously described (3). At 24 h p.i. the anti-EB5bac revealed a distinct staining in the ER or golgi of infected cells (Fig. 5a), and at 36 and 48 h p.i., the anti-EB5bac staining was also located to the cell membrane of infected cells (Fig. 5b). The immune staining using anti-EB5bac differed from what has been observed for the HE by appearing a little later, and by appearing in the membrane of vacuole-like structures of different sizes in infected cells (Fig 5b.). Only limited co-localization was observed between the HE and the segment 5 protein (Fig. 5c.) Mock-infected cells did not show any staining at any time.

Following transfection of CHSE-214 cells with pVAX1/EB5 using FuGENE 6, approximately 3-5% of the cells expressed the segment 5 protein 5 days post transfection (p.t.). Transfected cells were immune stained with the anti-EB5bac, and cells expressing the protein revealed a similar immune staining as infected cells (Fig. 5d).

Gp50 can be cleaved by trypsin into two disulphide linked fragments

As described, the new antibodies presented in this study are specific for Gp50, and in addition anti-pepEB5 and anti-EB5bac recognize two bands of 30 and 100 kDa in WB analysis of purified ISAV run in reducing conditions on SDS-PAGE. Trypsin treatment of purified virus resulted in a reduction in the amount of Gp50 detected by all antibodies, while the intensity of the 30 kDa protein band increased when using anti-pepEB5 and anti-EB5bac (Fig 3a, lane 2 and 4). Concurrently, a band of approximately 20 kDa was detected by anti-pepcoilEB5 only (Fig. 3a, lane 6). Lowering the pH in the samples did not affect the results in reducing SDS-PAGE (results not shown). When the trypsin treated and untreated virus were run at non-reducing conditions in SDS-PAGE all antibodies detected only the 50 and 100 kDa proteins indicating that the 30 and 20 kDa fragments are the cleavage products of Gp50, and that these are bound

together by disulphide bridges (results shown for anti-pepEB5) (Fig. 3b, lane 1 and 2). A slight change in mobility of the 100 kDa band was observed in samples treated with trypsin, possibly representing a configuration change due to the trypsin cleavage.

Trimers of Gp50 are detected after trypsin cleavage and exposure to low pH, 60°C or urea

No difference was observed when trypsin treated, purified virus was incubated at pH 4.5 compared to pH 7.3 when analyzed by WB run in reducing conditions on SDS-PAGE (results not shown). On non-reducing SDS-PAGE however, a strong band of 150 kDa suggestive of a trimer, was observed in the pH 4.5 treated virus in addition to the 50 and 100 kDa proteins (Fig. 3b, lane 3). The 150 kDa band was not detected in trypsin untreated virus after incubating in pH 4.5 (Fig. 3b, lane 4). The anti-pepcoilEB5 had a slightly reduced affinity to the 150 kDa band as compared to anti-pepEB5 (results not shown).

Trimer formation was also observed in trypsin cleaved virus treated with 60°C or urea (Fig. 3b, lanes 6 and 8**),** indicating that the cleaved form of this protein is in a metastable configuration, and that treatment with either low pH, 60°C or urea induces a conformational change. Virus that had not been treated with trypsin was not susceptible to these conformational changes (Fig. 3b, lanes 5 and 7).

Chemical Cross-Linking using various concentrations of EGS incubated on ice or at RT did not result in any increased polymerization, and was not considered as successful. However, 2D-electrophoresis using non-reducing SDS-PAGE in the first dimension and reducing SDS-PAGE in the second verified that the non-reduced 50, 100 and 150 kDa proteins contain the reduced 50 and 30 kDa proteins (Fig. 6a). The 150 kDa protein consisted mainly of cleaved fragments, indicating that a proteolytic cleavage of Gp50 is a prerequisite for trimerization.

Trimerization of the Gp50 protein treated with trypsin began at pH 5.4 - 5.6 (Fig. 6b), indicating that fusion is initiated in multi-vesicular carrier bodies in the cell where the pH is about 5.5. Exposing the PVDF membrane for an extended time to the Hyperfilm™ ECL™, revealed two additional bands at pH values between pH 4.0 and 7.3, of approximately 75 and 125 kDa (Fig. 6b). These bands probably represent intermediates of the monomer, dimmer, and trimer variants of this protein.

Trypsin treated ISAV is almost completely inactivated by exposure to low pH

Incubating ISAV with 0, 20 or 40 µg/mL trypsin followed by exposure to pH 7.3 or 5.0 prior to infecting cells had little effect on the virus titer recovered (Table 2). Lowering the pH to 4.0 however, reduced the titer by more that one log. Combining the pH 4.0 with a treatment of 40 µg/mL trypsin almost completely inactivated the virus, reducing the virus titer by about three additional log units (Table 2).

Discussion

Previous studies have localized the ISAV receptor-binding and -destroying activities (24, 45, 67), representing important foundations for ISAV pathogenicity studies. In this study we present the characterization of the ISAV 50 kDa glycoprotein (Gp50) (24) as the membrane fusion protein (F), adding essential information to further understand the mechanisms of ISAV pathogenicity. Cloned sequences showed identity to previously published ISAV genomic segment 5 sequences, and expression and WB analysis verified that this genome segment encodes Gp50 as previously reported (9).

Type I fusion proteins require a proteolytic cleavage to induce fusion competence (12), and the beneficial effect of trypsin on the replication of ISAV implies the classification of its fusion protein (26, 43). In the present study the requirement for proteolytic activation was linked to the fusion activity. Cell-cell fusion assays of infected cells demonstrated the requirement for trypsin and low pH to induce fusion, and cell-cell fusion was observed in cells co-transfected with the HE and F. Previous studies have suggested the ISAV HE as an unlikely target of this proteolytic activation as indicated by the lack of disulfide binding of its cleaved products (24, 45).

Computational analysis of the protein sequence revealed a potential coiled-coil at residues G^{301}-N^{340} with an average probability of 87% and structural homologies to the coiled-coils of Influenza A HA2 and Visna virus Env. Coiled-coils have been reported from a number of viral membrane fusion proteins, and the presence of coiled-coil motifs based on heptad repeats are amongst the general characteristics of type I fusion proteins (recently reviewed by 6, 22, 58, 64, 74). A structural homology to the Visna virus Env coiled-coil enabled the construction of a 3D-model of the putative ISAV F coiled-coil, and suggests common mechanisms for the viral fusion in these viruses. It also supports the hypothesis that Gp50 is the viral fusion protein, and that it

can form trimers as suggested in this study. The putative ISAV F coiled-coil represents a possible target for antiviral peptides which potentially inhibit viral fusion by hindering the formation of the fusogenic structure, as described for retroviruses (20, 52).

Sequence alignments of the ISAV F protein sequence with several known viral FP sequences identified an ISAV pFP at residues C^{277}-Y^{292}. One of the most important characteristics of membrane fusion proteins is the presence of a FP, generally a stretch of hydrophobic residues capable of interacting with and destabilizing a lipid bilayer (63). These hydrophobic domains are the most highly conserved regions of type I fusion-mediating glycoproteins (70), and have been found to be homologous amongst several enveloped viruses (28). FPs are rich in glycine and alanine residues, and their sequences are usually conserved within but not between virus families (63). The ISAV pFP share 43.8 % identity with the FPs of pneumoviruses, and conserved amino acids reflect the conservation amongst several pneumoviruses (11), providing a strong indication that this represents the ISAV FP. Additionally, residues F^{274}-Y^{292} corresponding to the pFP gave high scores in transmembrane predictions, reflecting the hydrophobicity of this peptide.

Two additional regions, M^{1}-C^{17} and V^{417}-W^{439} also gave high scores in transmembrane predictions. The first corresponded to a signal sequence predicted by SignalP which has also been identified by N-terminal sequencing (9). The second was predicted as the primary transmembrane region of F.

The expected size of F as determined from the segment 5 protein sequence is 48.7 kDa, while a slightly larger size is observed in SDS-PAGE probably owing to the glycosylated nature of this protein (24). The ISAV Gp50 was shown to be synthesized as a precursor termed F_0, cleavable by trypsin to the disulfide linked fragments termed F_1 and F_2 of 30 and 20 kDa respectively. Eight cysteine residues were predicted to be available for disulfide linkages. Two peptide anti-

sera defined F_1 and F_2 as the N-terminal and C-terminal cleavage products of Gp50 respectively and two theoretical trypsin cleavage sites (after residue K^{276} or after residue R^{266}) match with the size estimates of F_1 and F_2 in WB. However, type I fusion proteins generally have their FP localized to the N-terminal of F_2, generated by the cleavage event (12), thus we consider the trypsin cleavage site located next to the pFP as the best candidate for being the proteolytic cleavage site (after residue K^{276}). According to the protein sequence, this trypsin cleavage site should produce cleaved fragments F_1 and F_2 of 28.2 and 18.5 kDa respectively. Glycosylation sites are predicted on both fragments, thus the putative proteolytic cleavage site is in accordance with the results obtained in WB. Although a predicted cleavage site after residue R^{267} also matches the results obtained in WB, it would imply a longer FP than expected as well as altered hydrophobic properties of the FP. Additionally, no homology to other FPs was found for this region.

The pre-fusion polymerization status of the ISAV F_0 was not established, although monomers and dimers were observed in WB. However, incubating trypsin treated purified virus with low pH induced a conformational change in the protein, revealing a band suggestive of a trimer in WB, indicating a trimerization as part of the fusion process, or more likely, a stabilization of the trimer. This conformational change was coincident with induction of membrane-fusion activity, providing strong evidence that it represents the formation of the fusogenic structure. Both cell-cell fusion and the conformational change required pretreatment with trypsin, and was initiated at pH 5.4-5.6. Additionally, an SDS-PAGE run in two dimensions combining non-reducing and reducing conditions and blotted verified that the 100 and 150 kDa proteins suggestive of dimers and trimers can be reduced into 50 and 30 kDa proteins, corresponding to the F_0 and F_1 (F_2 was not detected by the antibody used). The trimer consisted mainly of cleaved F, probably reflecting the requirement of proteolytic cleavage for trimerization. Additionally, the computationally predicted 3D-structure of the putative ISAV coiled-coil motif supports the formation of a F

trimer. The same conformational change could also be induced by high temperature and by urea, suggesting that the cleaved form of the protein is in a metastable state, in accordance with the characteristics of type I viral membrane F proteins (12). This also supports that the conformational change represents the formation of the fusogenic structure. Acidification of proteolytically activated virions prior to incubation on cell monolayers lead to a drastic reduction in virus titer, probably reflecting the non-reversible nature of the conformational change upon acidification, known to inactivate type I fusion proteins (12). Some inactivation was also observed from the acidification process alone, possibly representing a fraction of the virus population already cleaved by available proteases.

A multiple sequence alignment of the ISAV pFP with FPs from several paramyxoviruses, orthomyxoviruses, and retroviruses revealed one residue that was conserved amongst all (G^{279}), and two that were conserved amongst several (F^{280} and G^{285}), corresponding to residues G^{3}, F^{4}, and G^{9} in the ISAV pFP, respectively. Additionally, a glycine corresponding to residue G^{7} (representing G^{283} in the protein) in the pFP was conserved amongst the RSV and ISAV. Interestingly, a study of the conserved residues of the paramyxovirus FPs revealed that mutations of G^{3} and G^{7} destabilize the native fusion protein, contributing to increased membrane fusion (39). The invariant amino acids in the FPs were suggested to preserve a balance between high fusion activity and successful viral replication, as high fusion activity is deleterious to cell viability. Additionally, in some paramyxoviruses these mutations influence the regulatory activity of hemagglutinin-neuraminidase (HN) on the fusion activity (70). Studies on the conserved glycine residues of the FP in HIV-1 have revealed that G^{10}, corresponding to G^{3} in the ISAV pFP, seemingly the most highly conserved residue in PFs in general, is critical for both cell-cell and virus-cell fusion, while the less conserved glycine residues are less critical (17).

The cleavability of the viral F proteins by intracellular proteases like furin present in the golgi network is a critical determinant of pathogenicity in orthomyxo- and paramyxoviruses (reviewed by 49, 50, 78). F proteins that have multiple basic residues at the cleavage site are cleavable by ubiquitous intracellular proteases, enabling a systemic spread of the virus, thereby increasing virulence. Viruses that have a single basic residue at the F protein cleavage site need an extracellular protease for proteolytic activation, and they only cause localized infections. In the present study, ISAV F protein sequences from two distantly related virulent strains causing major mortalities in Atlantic salmon were shown to contain single basic residues at their putative cleavage sites, indicating that the ISAV depend on an extracellular cleavage for fusion activation. This is supported by results in this study showing that purified virus run under reducing conditions in SDS-PAGE revealed mainly the uncleaved F protein. Also, the requirement for trypsin to induce syncytia in cells could be an indication that the F protein is not cleaved intracellularly prior to virus assembly/budding. However, ISAV does not depend on the addition of trypsin to replicate efficiently in cell cultures (16, 43), and it infects most organs in Atlantic salmon (*S. salar* L.) (56, 66) causing major pathological and histopathological changes (23, 81). Thus, in contrast to other orthomyxo- and paramyxoviruses, the efficient cleavage of the ISAV F protein is not restricted by the single basic residue at the cleavage site, indicating a disparate proteolytic cleavage mechanism. Additionally, the lack of variation in the protein sequence at the cleavage site of the distantly related ISAV isolates published suggests that the cleavage site structure is not as important in determining the pathogenicity of the ISAV as in other orthomyxoviruses and in paramyxoviruses (reviewed by 10, 78, 79).

The present study is the first description of an orthomyxovirus with its fusion activity localized on a separate protein. Influenza A and B viruses contain two glycoproteins, namely the HA which is responsible for virus-cell attachment and membrane fusion activity, and the neuraminidase (NA) holding the receptor-destroying activity. In influenza C, thogoto and dhori

viruses these activities are contained in a single surface glycoprotein (50). Paramyxoviruses have a HN and a separate F protein which is different from the orthomyxovirus fusion proteins because of its pH independence and because most members of this family require a second protein to induce fusion efficiently (49). Thus to our knowledge, the ISAV F protein represents the first pH dependent separate viral membrane F protein described. Whether the ISAV F protein requires the HE protein for fusion was not determined in the present study, although several studies confirm the importance of HN in influencing the fusion activity in paramyxoviruses (4, 37, 40, 49, 62). Also, as mentioned above, the FP residues G^3 and G^7, which have been found to influence the regulatory effect that the paramyxovirus HN has on the fusion activity, is conserved in the ISAV (70).

In conclusion, the ISAV segment 5 encodes a protein that shares several biochemical properties with viral type I membrane F-proteins. It is a glycoprotein (24) synthesized as a precursor termed F_0 that is proteolytically processed into two disulfide linked subunits F_1 and F_2. The F_2 subunit contains a relatively hydrophobic N-terminal sequence that fulfills the criteria of a FP. Furthermore, the conformational change in F was coincident with induction of membrane-fusion activity, strongly suggesting that it represents the formation of the fusogenic structure.

Acknowledgments

The authors thank Maike Joerink for her contribution during the cloning phase, Endy Spire at the Molecular Imaging Center in Bergen for superb assistance on the confocal microscope, and Audny Hellebø and Lindsey Moore for proofreading. This work was supported by grant no. 150091/120 and 134426/140 from the Norwegian Research Council, and by Intervet International.

Table 1.

An overview and a multiple sequence alignment of the ISAV pFP (C^{277}-Y^{292}) with known FPs of type I fusion proteins belonging to several viral families including paramyxoviruses (HRSV, BRSV, SV5, Sendai, NDV, Measles, Mumps), retroviruses (HIV, SIV) and orthomyxoviruses (Influenza A and B). Fusion peptide length, sequences accession numbers and references where each FP has been described are indicated. This alignment was generated with ClustalX (80).

Virus isolate	Fusion peptide [a]	Length (aa)	Accession #	References
ISAV Norway	----------CCGFTLGIGGAWFQAY--------	16	CAD99169	Current paper
ISAV Canada	----------CCGFTLGVGGAWFQAY--------	16	AF404343	(9)
HRSV	----------FLGFLLGVGSAIASGIAVS----	19	P13843	(86)
BRSV	----------FLGFLLGIGSAIASGVAVS----	19	AAB28458	(86)
SV5	FAGVVIGLAALGVATAAQVTAAVAL--------	25	AF05275	(70)
Sendai	FFGAVIGTIALGVATSAQIT------------	20	P04856	(39)
NDV	FIGAIIGSVALGVATAAQITAASAL--------	25	M21881	(70)
Measles	FAGVVLAGAALGVATAAQITAGIAL--------	25	U03655	(70)
Mumps	FAGIAIGIAALGVATAAQVTAAVSL--------	25	AAS93903	(39)
HIV-1 NL4-3	--AVGIGALFLGFLGAAGSTMGAAS--------	23	VCLJBR	(17)
HIV-2 Rod	---GVFVLGFLGFLATAGSAMGAAS--------	22	ENV_HV2RO	(17)
SIV tyo-1	---VPFVLGFLGFLGAAGTAMGAAA--------	22	ENV_SIVAT	(17)
SIV K6W	---GVFVLGFLGFLATAGSAMGAAS--------	22	ENV_SIVMK	(17)
InfA HA	----GLFGAIAGFIENGWEGMIDGWYGF----	24	HEMA_INAAI	(17)
InfB HA	----GFFGAIAGFLEGGWEGMIDGWHGY----	24	HEMA_INBBO	(17)

[a] Black shading: residues 100% conserved; dark gray shading: residues at least 50% conserved; light gray shading: residues at least 20% conserved.

Table 2.

ISAV titer after combined exposure to different concentrations of trypsin and various pHs prior to infecting cells. Trypsin and low pH had an additive effect on the inactivation of the ISAV.

pH	Virus titer (TCID50/mL) after exposure to the indicated concentrations of trypsin and pHs:		
	0µg/mL	20µg/mL	40µg/mL
pH 7.5	6.9×10^5	6.9×10^5	3.1×10^5
pH 5.0	6.9×10^5	3.1×10^5	6.9×10^5
pH 4.0	1.3×10^4	2.8×10^4	2.0×10^1

Figure legends

Fig. 1.

Pair-wise sequence alignment of the genomic segment 5 encoded proteins of the Norwegian ISAV isolate Bremnes/98 (Norway) (accession # CAD99169) and the Canadian isolate ME/01 (Canada) (accession # AAN57720) (9). Predicted transmembrane α-helix regions are framed (residues M^{1}-C^{17} (putative signal peptide); residues I^{275}-Y^{292} (internal transmembrane region); residues V^{417}-W^{439} (putative C-terminal anchor)). Potentially O-glycosylated threonins T^{52} and T^{62}, and N-glycosylation sites are underlined with plain and dashed lines, respectively, and are shown in bold. The putative fusion peptide region C^{277}-Y^{292} is shown in italics. The putative coiled-coil domain (residues G^{301}-N^{340}) is underlined. Potential trypsin cleavage sites are shown with grey shading, while the ones at positions R^{267} and K^{276}, considered the most likely proteolytic cleavage sites, are shaded in black. Cysteine residues putatively supporting disulfide bridges are shown in bold. The regions corresponding to the synthetic peptides used in immunizations to make the anti-pepEB5 antibody are shown with dashed frames.

Fig. 2.

Alignment of amino acid residues from the Influenza A HA2 sequence (accession # AF194991) predicted to have structural and sequence homology to residues G^{283}-Q^{341} of the ISAV Bremnes/98 genomic segment 5 sequence, representing the putative coiled-coil predicted by learncoil-VMF. Conserved residues are shown in black shading.

Fig. 3.

WB analyses showing the specificity of antibodies towards the Gp50, and the effect of trypsin and a kinetically destabilizing stimulus. a) Trypsin treated and untreated purified ISAV run at

reducing conditions in SDS-PAGE. Antibodies are indicated at the bottom and molecular sizes are indicated on the right. All antibodies were specific for the 50 kDa protein band corresponding to Gp50 in purified virus untreated with trypsin. In addition, two weaker bands of 30 and 100 kDa were detected by the anti-EB5bac and anti-pepEB5. After trypsin treatment of the virus the 30 kDa band is much stronger using anti-EB5bac and anti-pepEB5, while the anti-pepcoilEB5 detected a 20 kDa band in addition to Gp50. b) When run at non-reducing conditions in SDS-PAGE the antibodies detected only the 50 and 100 kDa proteins in both trypsin treated and untreated virus (lanes 1 and 2). Purified virus treated with trypsin and pH 4.5 revealed an additional band of 150 kDa suggestive of a trimer (lane 3). The trimer was also detected in trypsinated virus treated with 4.5M urea or incubated at 60°C (lanes 6 and 8), indicating that the trypsinated Gp50 is in a metastable state. The trimer was not detected in untrypsinated virus (lanes 1, 4, 5 and 7). The antibodies used in (a) gave comparable results in this experiment, and only the results for anti-pepEB5 are presented.

Fig. 4.

Fusion of infected and transfected cells after syncytium fusion assay. The cells are visualized by immune staining using the anti-HE MAb (green), and nuclei are red. The nuclei are approximately 20µm wide. a) Trypsin treated ISAV infected cells incubated at pH 4.5 showing fused cells with at least 4 and 9 nuclei. b) Trypsin treated pVAX1/HE and pVAX1/EB5 transfected cells incubated at pH 4.5 showing fused cells with at least 8 nuclei. c) Trypsin treated ISAV infected cells incubated at neutral pH showing no fused cells. d) Trypsin treated pVAX1/HE and pVAX1/EB5 transfected cells incubated at neutral pH showing no fused cells. e) Trypsin treated ISAV infected cells incubated at pH 4.5 fused with Atlantic salmon erythrocytes. Red fluorescent R18 is transferred from erythrocytes to cell membrane.

Fig. 5.

Immunofluorescent staining of ISAV infected and transfected cells showing the appearance and localization of the F protein. In a) and b) the NP is visualized in red, the F-protein in green and the nuclei are blue. In c) and d) the HE is visualized in red, the F-protein in green and the nuclei are blue. The nuclei are approximately 20µm wide. a) The first detection of the F protein using the anti-EB5bac was at 24 h p.i., and the staining was localized to the ER or Golgi of infected cells. b) At 36 and 48 h p.i. the F-protein localized to the membrane of vesicle like structures in the cytoplasm, and to the plasma membrane (the picture is taken at 36 h p.i.). c) Infected cells immune stained using the MAb anti-HE and the anti-EB5bac demonstrates that the ISAV glycoproteins is not co-localized in infected cells until they are both present in the plasma membrane (see also fig 4). d) The F-protein had the same localization pattern in transfected cells as in infected cells, and was not affected by the HE.

Fig. 6.

a) Trypsin treated purified ISAV incubated at pH 4.0 was analyzed by a 2D-electrophoresis run at non-reducing SDS-PAGE in the first dimension and reducing SDS-PAGE in the second dimension. The WB was immune stained with the anti-pepEB5 antisera, confirming that the 50, 100 and 150 kDa protein bands could be reduced to 30 and 50 kDa proteins. b) WB analysis of trypsin treated purified ISAV incubated at various pHs as indicated at the bottom. The trimerization of Gp50 is initiated at pH5.6 seen as a rather weak 150 kDa protein band, increasing in intensity at lower pHs.

Fig. 1.

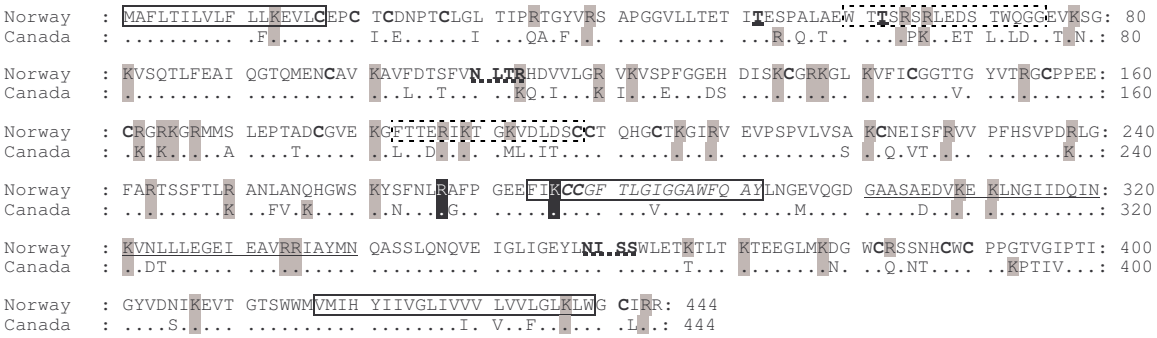
Norway : MAFLTILVLF LLKEVLCEPC TCDNPTCLGL TIPRTGYVRS APGGVLLTET ITESPALAEW TTSRSRLEDS TWQGGEVKSG: 80
Canada : .... .F..... I.E.....I ...QA.F.. ....R.Q.T.. ...PK..ET L.LD..T.N.: 80
Norway : KVSQTLFEAI QGTQMENCAV KAVFDTSFVN LTRHDVVLGR VKVSPFGGEH DISKCGRKGL KVFICGGTTG YVTRGCPPEE: 160
Canada : ....L..T... ..KQ.I...K I...E...DS ...V.....V. ...V.....V. ...V.....: 160
Norway : CRGRKGRMMS LEPTADCGVE KGFTTERIKT GKVDLDSCCT QHGCTKGIRV EVPSPVLVSA KCNEISFRVV PFHSVPDRLG: 240
Canada : .K.K....A ....T..... .L..D..... .ML.IT.... .....V...V. ....S .Q.VT..... .....K..: 240
Norway : FARTSSFTLR ANLANQHGWS KYSFNLRAFP GEEFIKCCGF TLGIGGAWFQ AYLNGEVQGD GAASAEDVKE KLNGIIDQIN: 320
Canada : ..V.....K ..FV.K.... .N...G.. .....V.... ...V..... .....M.... .....D..V. .V.....: 320
Norway : KVNLLLEGEI EAVRRIAYMN QASSLQNQVE IGLIGEYLNI SSWLETKTLT KTEEGLMKDG WCRSSNHCWC PPGTVGIPTI: 400
Canada : .DT..... ...V..... ....T... .....V..N. ..Q.NT.... ..KPTIV...: 400
Norway : GYVDNIKEVT GTSWWMVMIH YIIVGLIVVV LVVLGLKLWG CIRR: 444
Canada : ....S..... ....I. V..F..V... .L..: 444

Fig. 2.


290
300
310
320
330
340
ISAV Seg5 : GIGGAWFQAYLNGEVQGDGAASAEDVKEKLNGIIDQINKVNLLLEGEIEAV--------RRIAYMNQ
InfA HA2 : GMVDGWYG-YHHSNEQGSGAADKESTQKAIDGITNKVNSIIDKMNTQFEAVGKEFNNLERRIENLNK
Coiled coil domains

Fig. 3.

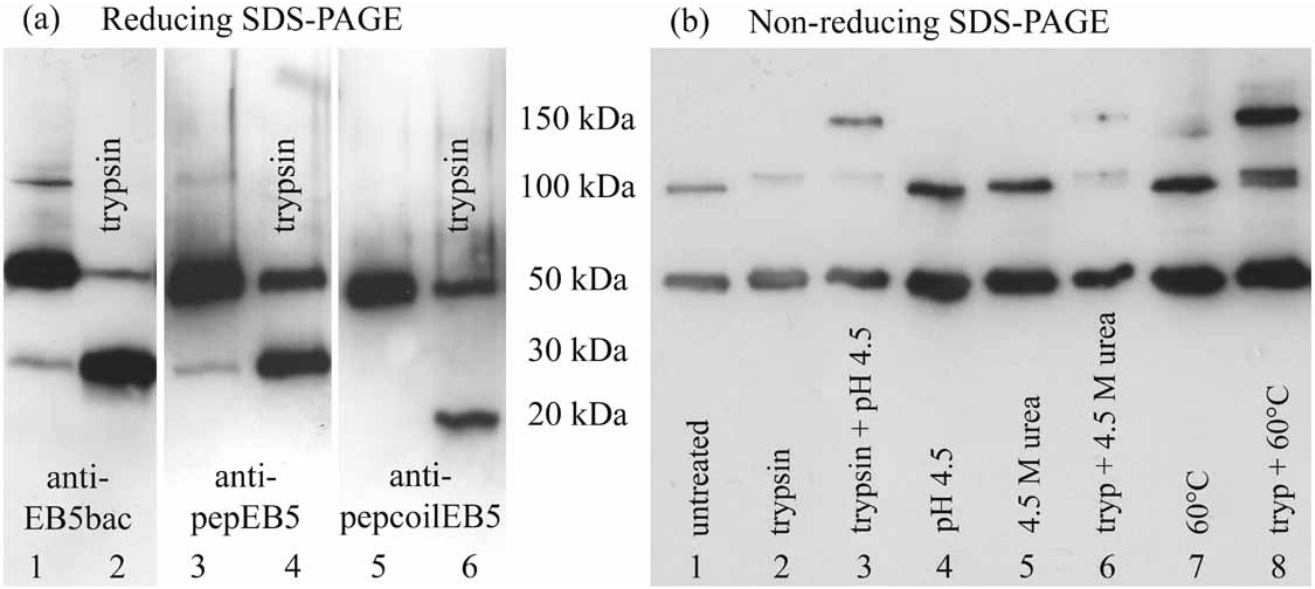
(a) Reducing SDS-PAGE
trypsin
trypsin
trypsin
anti-EB5bac
anti-pepEB5
anti-pepcoilEB5
1 2 3 4 5 6
150 kDa
100 kDa
50 kDa
30 kDa
20 kDa
(b) Non-reducing SDS-PAGE
untreated
trypsin
trypsin + pH 4.5
pH 4.5
4.5 M urea
tryp + 4.5 M urea
60°C
tryp + 60°C
1 2 3 4 5 6 7 8

Fig. 4.

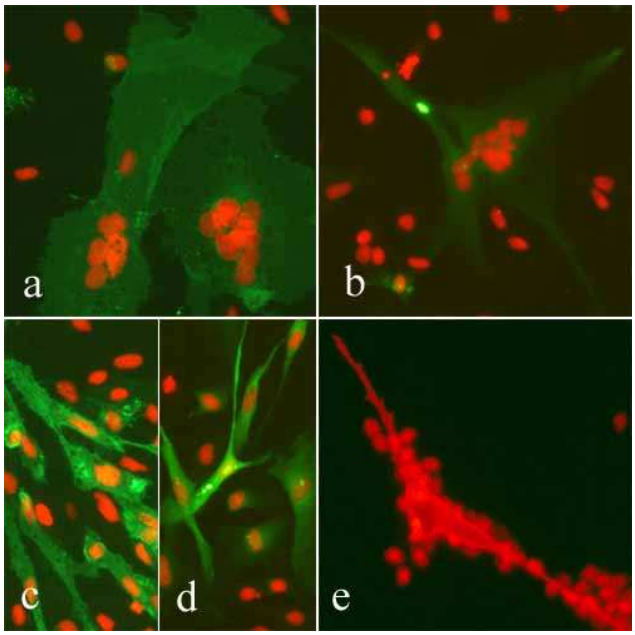

Fig. 5.

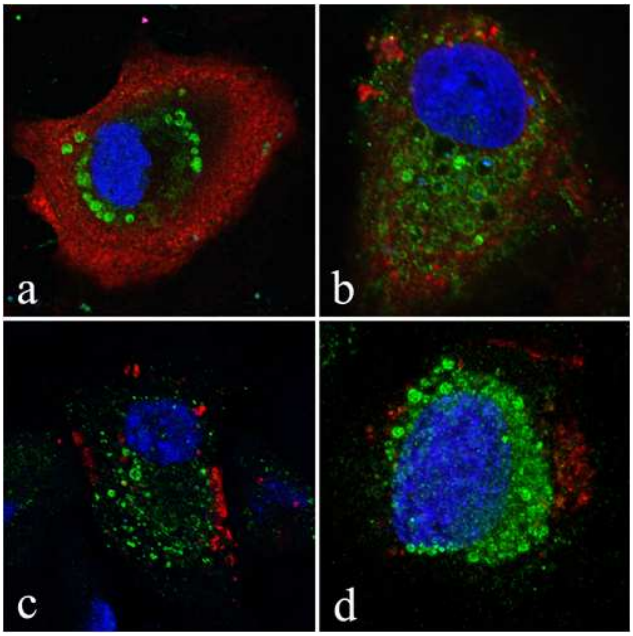

Fig. 6.

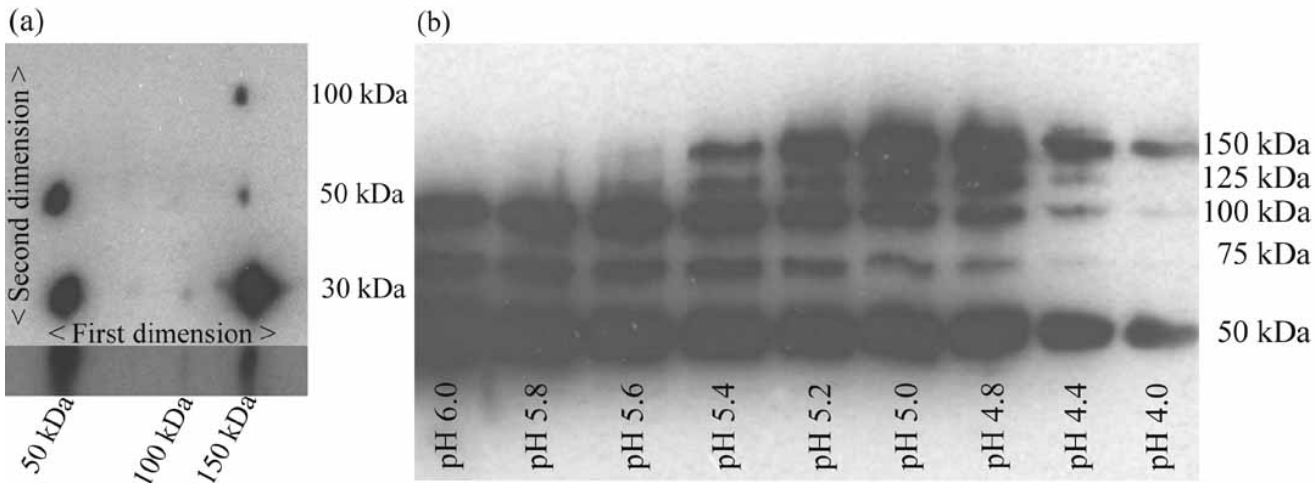
(a)
< Second dimension >
< First dimension >
100 kDa
50 kDa
30 kDa
50 kDa
100 kDa
150 kDa
(b)
pH 6.0
pH 5.8
pH 5.6
pH 5.4
pH 5.2
pH 5.0
pH 4.8
pH 4.4
pH 4.0
150 kDa
125 kDa
100 kDa
75 kDa
50 kDa

References

1. **Altschul, S. F., W. Gish, W. Miller, E. W. Myers, and D. J. Lipman.** 1990. Basic local alignment search tool. J Mol Biol **215:**403-10.
2. **Altschul, S. F., T. L. Madden, A. A. Schaffer, J. Zhang, Z. Zhang, W. Miller, and D. J. Lipman.** 1997. Gapped BLAST and PSI-BLAST: a new generation of protein database search programs. Nucleic Acids Res **25:**3389-402.
3. **Aspehaug, V., K. Falk, B. Krossoy, J. Thevarajan, L. Sanders, L. Moore, C. Endresen, and E. Biering.** 2004. Infectious salmon anemia virus (ISAV) genomic segment 3 encodes the viral nucleoprotein (NP), an RNA-binding protein with two monopartite nuclear localization signals (NLS). Virus Res **106:**51-60.
4. **Bagai, S., and R. A. Lamb.** 1995. Quantitative measurement of paramyxovirus fusion: differences in requirements of glycoproteins between simian virus 5 and human parainfluenza virus 3 or Newcastle disease virus. J Virol **69:**6712-9.
5. **Bendtsen, J. D., H. Nielsen, G. von Heijne, and S. Brunak.** 2004. Improved prediction of signal peptides: SignalP 3.0. J Mol Biol **340:**783-95.
6. **Bentz, J., and A. Mittal.** 2003. Architecture of the influenza hemagglutinin membrane fusion site. Biochim Biophys Acta **1614:**24-35.
7. **Biering, E., K. Falk, E. Hoel, J. Thevarajan, M. Joerink, A. Nylund, C. Endresen, and B. Krossøy.** 2002. Segment 8 encodes a structural protein of infectious salmon anaemia virus (ISAV); the co-linear transcript from Segment 7 probably encodes a non-structural or minor structural protein. Dis Aquat Organ **49:**117-22.
8. **Bullough, P. A., F. M. Hughson, J. J. Skehel, and D. C. Wiley.** 1994. Structure of influenza haemagglutinin at the pH of membrane fusion. Nature **371:**37-43.
9. **Clouthier, S. C., T. Rector, N. E. Brown, and E. D. Anderson.** 2002. Genomic organization of infectious salmon anaemia virus. J Gen Virol **83:**421-8.

10. **Collins, M. S., J. B. Bashiruddin, and D. J. Alexander.** 1993. Deduced amino acid sequences at the fusion protein cleavage site of Newcastle disease viruses showing variation in antigenicity and pathogenicity. Arch Virol **128:**363-70.

11. **Collins, P. L., R. M. Chanock, and B. R. Murphy.** 2001. Respiratory Syncytial Virus, p. 1443-1485. *In* D. M. Knipe, P. M. Howley, and B. N. Fields (ed.), Fields Virology, 4th ed. Lippincott Williams & Wilkins, Philadelphia.

12. **Colman, P. M., and M. C. Lawrence.** 2003. The structural biology of type I viral membrane fusion. Nat Rev Mol Cell Biol **4:**309-19.

13. **Copeland, C. S., R. W. Doms, E. M. Bolzau, R. G. Webster, and A. Helenius.** 1986. Assembly of influenza hemagglutinin trimers and its role in intracellular transport. J Cell Biol **103:**1179-91.

14. **Dannevig, B. H., B. E. Brudeseth, T. Gjoen, M. Rode, H. I. Wergeland, O. Evensen, and C. M. Press.** 1997. Characterisation of a long-term cell line (SHK-1) developed from the head kidney of Atlantic salmon (*Salmo salar L*). **7:**213-226.

15. **Dannevig, B. H., K. Falk, and E. Namork.** 1995. Isolation of the causal virus of infectious salmon anemia (ISA) in a long-term cell-line from Atlantic salmon head kidney. J Gen Virol **76:**1353-1359.

16. **Dannevig, B. H., K. Falk, and C. M. Press.** 1995. Propagation of infectious salmon anemia (ISA) virus in cell culture. Vet Res **26:**438-442.

17. **Delahunty, M. D., I. Rhee, E. O. Freed, and J. S. Bonifacino.** 1996. Mutational analysis of the fusion peptide of the human immunodeficiency virus type 1: identification of critical glycine residues. Virology **218:**94-102.

18. **Devold, M., B. Krossoy, V. Aspehaug, and A. Nylund.** 2000. Use of RT-PCR for diagnosis of infectious salmon anaemia virus (ISAV) in carrier sea trout (*Salmo trutta*) after experimental infection. Dis Aquat Organ **40:**9-18.

19. **Dutch, R. E., T. S. Jardetzky, and R. A. Lamb.** 2000. Virus membrane fusion proteins: biological machines that undergo a metamorphosis. Biosci Rep **20:**597-612.

20. **Eckert, D. M., and P. S. Kim.** 2001. Mechanisms of viral membrane fusion and its inhibition. Annu Rev Biochem **70:**777-810.

21. **Eliassen, T. M., M. K. Froystad, B. H. Dannevig, M. Jankowska, A. Brech, K. Falk, K. Romoren, and T. Gjoen.** 2000. Initial events in infectious salmon anemia virus infection: evidence for the requirement of a low-pH step. J Virol **74:**218-227.

22. **Epand, R. M.** 2003. Fusion peptides and the mechanism of viral fusion. Biochim Biophys Acta **1614:**116-21.

23. **Evensen, O., K. E. Thorud, and Y. A. Olsen.** 1991. A morphological study of the gross and light microscopic lesions of infectious anaemia in Atlantic salmon (*Salmo salar*). Res Vet Sci **51:**215-22.

24. **Falk, K., V. Aspehaug, R. Vlasak, and C. Endresen.** 2004. Identification and partial characterisation of viral structural proteins of infectious salmon anaemia (ISA) virus. J Virol **78:**3063-71.

25. **Falk, K., E. Namork, and B. H. Dannevig.** 1998. Characterization and applications of a monoclonal antibody against infectious salmon anaemia virus. Dis Aquat Org **34:**77-85.

26. **Falk, K., E. Namork, E. Rimstad, S. Mjaaland, and B. H. Dannevig.** 1997. Characterization of infectious salmon anemia virus, an orthomyxo-like virus isolated from Atlantic salmon (*Salmo salar* L.). J Virol **Dec:**9016-9023.

27. **Fiser, A., R. K. Do, and A. Sali.** 2000. Modeling of loops in protein structures. Protein Sci **9:**1753-73.

28. **Gallaher, W. R.** 1987. Detection of a fusion peptide sequence in the transmembrane protein of human immunodeficiency virus. Cell **50:**327-8.

29. **García-Rosado, E., S. Mjaaland, and E. Rimstad.** (Submitted). Infectious salmon anemia virus (ISAV) genomic segment 7 protein antagonizes type I interferon response.

30. **Garry, C. E., and R. F. Garry.** 2004. Proteomics computational analyses suggest that the carboxyl terminal glycoproteins of Bunyaviruses are class II viral fusion proteins (beta-penetrenes). Theor Biol Med Model **1:**10.

31. **Gasteiger, E., A. Gattiker, C. Hoogland, I. Ivanyi, R. D. Appel, and A. Bairoch.** 2003. ExPASy: The proteomics server for in-depth protein knowledge and analysis. Nucleic Acids Res **31:**3784-8.

32. **Glickman, R. L., R. J. Syddall, R. M. Iorio, J. P. Sheehan, and M. A. Bratt.** 1988. Quantitative basic residue requirements in the cleavage-activation site of the fusion glycoprotein as a determinant of virulence for Newcastle disease virus. J Virol **62:**354-6.

33. **Hansen, J. E., O. Lund, N. Tolstrup, A. A. Gooley, K. L. Williams, and S. Brunak.** 1998. NetOglyc: prediction of mucin type O-glycosylation sites based on sequence context and surface accessibility. Glycoconj J **15:**115-30.

34. **Heinz, F. X., and S. L. Allison.** 2003. Flavivirus structure and membrane fusion. Adv Virus Res **59:**63-97.

35. **Heinz, F. X., K. Stiasny, and S. L. Allison.** 2004. The entry machinery of flaviviruses. Arch Virol Suppl**:**133-7.

36. **Hellebø, A., U. Vilas, K. Falk, and R. Vlasak.** 2004. Infectious salmon anemia virus specifically binds to and hydrolyzes 4-O-acetylated sialic acids. J Virol **78:**3055-62.

37. **Heminway, B. R., Y. Yu, and M. S. Galinski.** 1994. Paramyxovirus mediated cell fusion requires co-expression of both the fusion and hemagglutinin-neuraminidase glycoproteins. Virus Res **31:**1-16.

38. **Hofmann, K., and W. Stoffel.** 1993. TMbase - A database of membrane spanning proteins segments, vol. 374.

39. **Horvath, C. M., and R. A. Lamb.** 1992. Studies on the fusion peptide of a paramyxovirus fusion glycoprotein: roles of conserved residues in cell fusion. J Virol **66:**2443-55.

40. **Hu, X. L., R. Ray, and R. W. Compans.** 1992. Functional interactions between the fusion protein and hemagglutinin-neuraminidase of human parainfluenza viruses. J Virol **66:**1528-1534.

41. **Juretic, D., B. Lee, N. Trinajstic, and R. W. Williams.** 1993. Conformational preference functions for predicting helices in membrane proteins. Biopolymers **33:**255-73.

42. **Kibenge, F. S., O. N. Garate, G. Johnson, R. Arriagada, M. J. Kibenge, and D. Wadowska.** 2001. Isolation and identification of infectious salmon anaemia virus (ISAV) from Coho salmon in Chile. Dis Aquat Organ **45:**9-18.

43. **Kibenge, F. S., J. R. Lyaku, D. Rainnie, and K. L. Hammell.** 2000. Growth of infectious salmon anaemia virus in CHSE-214 cells and evidence for phenotypic differences between virus strains. J Gen Virol **81:**143-150.

44. **Kristiansen, M., M. K. Froystad, A. L. Rishovd, and T. Gjoen.** 2002. Characterization of the receptor-destroying enzyme activity from infectious salmon anaemia virus. J Gen Virol **83:**2693-7.

45. **Krossøy, B., M. Devold, L. Sanders, P. M. Knappskog, V. Aspehaug, K. Falk, A. Nylund, S. Koumans, C. Endresen, and E. Biering.** 2001. Cloning and identification of the infectious salmon anaemia virus haemagglutinin. J Gen Virol **82:**1757-65.

46. **Krossøy, B., I. Hordvik, F. Nilsen, A. Nylund, and C. Endresen.** 1999. The putative polymerase sequence of infectious salmon anemia virus suggests a new genus within the *Orthomyxoviridae*. J Virol **73:**2136-42.

47. **Krossøy, B., F. Nilsen, K. Falk, C. Endresen, and A. Nylund.** 2001. Phylogenetic analysis of infectious salmon anaemia virus isolates from Norway, Canada and Scotland. Dis Aquat Organ **44:**1-6.

48. **Laemmli, U. K.** 1970. Cleavage of structural proteins during the assembly of the head of bacteriophage T4. Nature **227:**680-5.

49. **Lamb, R. A., and D. Kolakofsky.** 2001. *Paramyxoviridae*: The Viruses and Their Replication, p. 1305-1340. *In* D. M. Knipe, P. M. Howley, G. D. E., M. M. A., L. R. A., R. B., and S. E. Straus (ed.), Fields virology. Lippincott-Raven, Philadelphia, Pa.

50. **Lamb, R. A., and R. M. Krug.** 2001. *Orthomyxoviridae*: The Viruses and Their Replication, p. 1487-1579. *In* D. M. Knipe, P. M. Howley, G. D. E., M. M. A., L. R. A., R. B., and S. E. Straus (ed.), Fields virology. Lippincott-Raven, Philadelphia, Pa.

51. **Lannan, C. N., J. R. Winton, and J. L. Fryer.** 1984. Fish cell lines: establishment and characterization of nine cell lines from salmonids. In Vitro **20:**671-6.

52. **Louis, J. M., I. Nesheiwat, L. Chang, G. M. Clore, and C. A. Bewley.** 2003. Covalent trimers of the internal N-terminal trimeric coiled-coil of gp41 and antibodies directed against them are potent inhibitors of HIV envelope-mediated cell fusion. J Biol Chem **278:**20278-85.

53. **Lovely, J. E., B. H. Dannevig, K. Falk, L. Hutchin, A. M. MacKinnon, K. J. Melville, E. Rimstad, and S. G. Griffiths.** 1999. First identification of infectious salmon anaemia virus in North America with haemorrhagic kidney syndrome. Dis Aquat Organ **35:**145-8.

54. **Lupas, A., M. Van Dyke, and J. Stock.** 1991. Predicting coiled coils from protein sequences. Science **252:**1162-4.

55. **Marti-Renom, M. A., A. C. Stuart, A. Fiser, R. Sanchez, F. Melo, and A. Sali.** 2000. Comparative protein structure modeling of genes and genomes. Annu Rev Biophys Biomol Struct **29:**291-325.

56. **Mikalsen, A. B., A. Teig, A. L. Helleman, S. Mjaaland, and E. Rimstad.** 2001. Detection of infectious salmon anaemia virus (ISAV) by RT-PCR after cohabitant exposure in Atlantic salmon (*Salmo salar*). Dis Aquat Organ **47:**175-81.

57. **Mjaaland, S., E. Rimstad, K. Falk, and B. H. Dannevig.** 1997. Genomic characterization of the virus causing infectious salmon anemia in Atlantic salmon (*Salmo salar* L.): an orthomyxo-like virus in a teleost. J Virol **71:**7681-7686.

58. **Morrison, T. G.** 2003. Structure and function of a paramyxovirus fusion protein. Biochim Biophys Acta **1614:**73-84.

59. **Mullins, J. E., D. Groman, and D. Wadowska.** 1998. Infectious salmon anaemia in salt water Atlantic salmon (*Salmo salar* L.) in New Brunswick, Canada. Bull Eur Assic Fish Pathol **18:**110-114.

60. **Nicholas, K. B., N. H. B. Jr., and D. W. Deerfield.** 1997. GeneDoc: Analysis and Visualization of Genetic Variation. EMBNEW.NEWS **4**.

61. **Pagni, M., V. Ioannidis, L. Cerutti, M. Zahn-Zabal, C. V. Jongeneel, and L. Falquet.** 2004. MyHits: a new interactive resource for protein annotation and domain identification. Nucleic Acids Res **32:**W332-5.

62. **Paterson, R. G., M. A. Shaughnessy, and R. A. Lamb.** 1989. Analysis of the relationship between cleavability of a paramyxovirus fusion protein and length of the connecting peptide. J Virol **63:**1293-301.

63. **Pecheur, E. I., J. Sainte-Marie, A. Bienven e, and D. Hoekstra.** 1999. Peptides and membrane fusion: towards an understanding of the molecular mechanism of protein-induced fusion. J Membr Biol **167:**1-17.

64. **Peisajovich, S. G., and Y. Shai.** 2003. Viral fusion proteins: multiple regions contribute to membrane fusion. Biochim Biophys Acta **1614:**122-9.

65. **Perdue, M. L., and D. L. Suarez.** 2000. Structural features of the avian influenza virus hemagglutinin that influence virulence. Vet Microbiol **74:**77-86.

66. **Rimstad, E., K. Falk, A. B. Mikalsen, and A. Teig.** 1999. Time course tissue distribution of infectious salmon anaemia virus in experimentally infected Atlantic salmon (*Salmo salar*). Dis Aquat Organ **36:**107-112.

67. **Rimstad, E., S. Mjaaland, M. Snow, A. B. Mikalsen, and C. O. Cunningham.** 2001. Characterization of the infectious salmon anemia virus genomic segment that encodes the putative hemagglutinin. J Virol **75:**5352-6.

68. **Ritchie, R. J., J. Heppell, M. B. Cook, S. Jones, and S. G. Griffiths.** 2001. Identification and characterization of segments 3 and 4 of the ISAV genome. Virus Genes **22:**289-97.

69. **Rodger, H. D., T. Turnbull, F. Muir, S. Millar, and R. H. Richards.** 1998. Infectious salmon anaemia (ISA) in the United Kingdom. Bulletin of the European Association of Fish Pathology **18:**115-116.

70. **Russell, C. J., T. S. Jardetzky, and R. A. Lamb.** 2004. Conserved glycine residues in the fusion peptide of the paramyxovirus fusion protein regulate activation of the native state. J Virol **78:**13727-42.

71. **Sali, A., and T. L. Blundell.** 1993. Comparative protein modelling by satisfaction of spatial restraints. J Mol Biol **234:**779-815.

72. **Schyth, B. D., N. J. Olesen, P. Østergård, and K. Falk.** 2003. Presented at the Diseases of Fish and Shellfish, 11 th International Conference of the EAFP, Malta.

73. **Shi, J., T. L. Blundell, and K. Mizuguchi.** 2001. FUGUE: sequence-structure homology recognition using environment-specific substitution tables and structure-dependent gap penalties. J Mol Biol **310:**243-57.

74. **Singh, M., B. Berger, and P. S. Kim.** 1999. LearnCoil-VMF: computational evidence for coiled-coil-like motifs in many viral membrane-fusion proteins. J Mol Biol **290:**1031-41.

75. **Snow, M., and C. O. Cunningham.** 2001. Characterisation of the putative nucleoprotein gene of infectious salmon anaemia virus (ISAV). Virus Res **74:**111-118.

76. **Snow, M., R. Ritchie, O. Arnaud, S. Villoing, V. Aspehaug, and C. O. Cunningham.** 2003. Isolation and characterisation of segment 1 of the infectious salmon anaemia virus genome. Virus Res **92:**99-105.

77. **Stegmann, T.** 2000. Membrane fusion mechanisms: the influenza hemagglutinin paradigm and its implications for intracellular fusion. Traffic **1:**598-604.

78. **Steinhauer, D. A.** 1999. Role of hemagglutinin cleavage for the pathogenicity of influenza virus. Virology **258:**1-20.

79. **Tashiro, M., N. L. McQueen, and J. T. Seto.** 1999. Determinants of organ tropism of sendai virus. Front Biosci **4:**D642-5.

80. **Thompson, J. D., T. J. Gibson, F. Plewniak, F. Jeanmougin, and D. G. Higgins.** 1997. The CLUSTAL_X windows interface: flexible strategies for multiple sequence alignment aided by quality analysis tools. Nucleic Acids Res **25:**4876-82.

81. **Thorud, K., and H. O. Djupvik.** 1988. Infectious salmon anaemia in Atlantic salmon (*Salmo salar* L.). Bull Eur Assoc Fish Pathol **8:**109-111.

82. **Toyoda, T., T. Sakaguchi, K. Imai, N. M. Inocencio, B. Gotoh, M. Hamaguchi, and Y. Nagai.** 1987. Structural comparison of the cleavage-activation site of the fusion glycoprotein between virulent and avirulent strains of Newcastle disease virus. Virology **158:**242-7.

83. **Vareckova, E., V. Mucha, S. A. Wharton, and F. Kostolansky.** 2003. Inhibition of fusion activity of influenza A haemagglutinin mediated by HA2-specific monoclonal antibodies. Arch Virol **148:**469-86.

84. **von Heijne, G.** 1992. Membrane protein structure prediction. Hydrophobicity analysis and the positive-inside rule. J Mol Biol **225:**487-94.

85. **Vullo, A., and P. Frasconi.** 2004. Disulfide connectivity prediction using recursive neural networks and evolutionary information. Bioinformatics **20:**653-9.

86. **Zimmer, G., L. Budz, and G. Herrler.** 2001. Proteolytic activation of respiratory syncytial virus fusion protein. Cleavage at two furin consensus sequences. J Biol Chem **276:**31642-50.